The biodistribution of ^{14}C in the digestive organs of rats fed [^{14}C]CD14 protein

Laura D. R. Davis

Thesis submitted to the Faculty of Graduate and Postdoctoral Studies
In partial fulfillment of the requirements
for the Master of Science degree in Biochemistry

Department of Biochemistry, Microbiology and Immunology
Faculty of Medicine
University of Ottawa

Salvador Dalí. 1937. Untitled (Woman with Flower Head)

Abstract

Human milk contains ~ 25 µg/mL of soluble cluster of differentiation 14 (sCD14) protein, a pattern recognition receptor (PRR) that triggers the innate immune system to respond to bacterial lipopolysaccharide (LPS). To date, the role of CD14 in the digestive tract of breast fed infants has not been well characterized and is the subject of this thesis.

To investigate the biodistribution of proteins such as CD14 *in vivo*, a novel method for ^{14}C radiolabeling of proteins to high specific radioactivity was developed using *in vacuo* methylation. Bovine serum albumin (BSA) and casein were used as test proteins to determine the following: 1) The efficacy of the *in vacuo* radiolabeling procedure; 2) The extent of incorporation of the ^{14}C-label into the organs of oro-gastric gavaged 10 day old Sprague Dawley rats. [^{14}C]BSA, [^{14}C]casein and [^{14}C]CD14 were prepared with specific radioactivities of 10 400, 10 800 and 163 000 dpm/µg, respectively. After feeding 6.25 µg of ^{14}C-labeled proteins, quantifiable levels of ^{14}C were found in the stomach, jejunum, duodenum, ileum, large intestine, intestinal luminal flushes, blood, liver, spleen and kidneys of rats. The accumulation of radiolabel in the organs of [^{14}C]CD14 fed rats was temporally and spatially distinct from [^{14}C]BSA and [^{14}C]casein. Most notably, the label persisted in the stomach 480 min post-gavage.

To design a neonate animal model for biodistribution, the segmental and total gastrointestinal transit times (GItt) were measured in two litters of 10 and 15 day old Sprague Dawley rat pups using barium sulfate. Ten day old rat pups that remained with and without the dam had a total gastrointestinal transit time of 13.8 ± 0.9 hr and 9.3 ± 0.7 hr,

respectively. This decrease ($p<0.05$) in total gastrointestinal transit time in the absence of the dam was age-dependent, as it was not observed ($p>0.05$) in the 15 day old rat pup litter.

The immunological impact of an exogenous sCD14 source was examined in human peripheral blood mononuclear cells (PBMC). Pre-treatment of $CD14^{+}$ monocytes with sCD14 had a protective effect, one of reducing the production of proinflammatory cytokines (TNF-α, IL-6, IL-8, IL-1β) when challenged with LPS.

^{14}C was absorbed by neonate rats upon ingestion of [^{14}C]CD14 and exposure to relatively high concentrations of rCD14 led to a reduction in inflammation. This may be beneficial to initial gut colonization in breast-fed newborns.

Acknowledgements

I would like to express appreciation to my supervisor, Prof. Illimar Altosaar, for constantly challenging my ideas and for provoking new thought. I am thankful to the members of my thesis advisory committee, Dr. David Blais, Prof. Anthony Krantis, Dr. Kylie Scoggan, and co-supervisor Dr. David Mack, Chief of Gastroenterology, Hepatology and Nutrition at the Children's Hospital of Eastern Ontario, for their guidance and counsel. Special thanks to Dr. William Spencer, Postdoctoral Fellow, and to Prof. Harvey Kaplan for their patience, revisions and help through my graduate studies. Also to Kimberly Yates, Animal Care and Veterinary Services staff, for her animal expertise. Finally, I am grateful to the wonderful graduate students and postdoctoral fellows in the Altosaar lab, specially Dr. Van Thong Pham, Tonya Ward and Adam Koziol, for providing experimental ideas and creating a productive work environment.

My graduate work has allowed me to perform research in Tokyo, Japan. For this, I would like to thank the Japan Society for the Promotion of Science and Prof. Toshifumi Hibi and Prof. Tadakazu Hisamatsu for hosting my research at Keio University Hospital. Thanks also to Mina T. Kitazume and Jon Chang for their experimental guidance. I have also been fortunate to volunteer for Science Travels at the University of Ottawa where I traveled to Nunavut, Sudbury and North Bay to teach science and nutrition. These opportunities have enriched my graduate studies immensely and have enhanced my self-development.

Finally, I would like to express gratitude to my family and friends for their continual support and encouragement. I am extremely grateful to have such wonderful people in my life.

Table of Contents

Abstract ……iii

Acknowledgements ……v

Table of Contents ……..vi

List of Abbreviations ……...vii

List of Figures ……...ix

List of Tables ……xi

Chapter 1 Introduction ……1
1-1 Gastrointestinal development ……1
1-2 Gastrointestinal diseases ……8
1-3 Tracking bioactives in the gut ……12
1-4 Objectives & rationale ……16

Chapter 2 Gastrointestinal transit in Sprague Dawley rat ……17
2-1 Summary ……..17
2-2 Materials and methods ……18
2-3 Results ……22
2-4 Discussion ……25

Chapter 3 Pharmacokinetic studies using radiolabeled ^{14}C protein ……29
3-1 Summary ……..29
3-2 Materials and methods ……30
3-3 Results ……32
3-4 Discussion ……41

Chapter 4 Stimulation of human blood $CD14^{+}$ monocytes ……,…….46
4-1 Summary ……..46
4-2 Materials and methods ……..……...47
4-3 Results ……....49
4-4 Discussion ……52

Chapter 5 Conclusions and future research ……..55

References ……58

Contributions of Collaborators ……68

Appendices ……..69

Curriculum Vitae ……90

List of Abbreviations

^{14}C	Carbon 14
^{125}I	Iodine 125
^{131}I	Iodine 131
ADME	Absorption, distribution, metabolism, excretion
BLP	Bacterial lipoprotein
BSA	Bovine serum albumin
CBA	Cytokine bead array
CD	Crohn's disease
CD14	Cluster of differentiation 14 protein
cpm	Counts per minute
DC	Dendritic cell
dpm	Disintegrations per minute
EDTA	Ethylenediaminetetraacetic acid
GI	Gastrointestinal
GPI	Glycosylphosphatidylinositol
GItt	Gastrointestinal transit time
IBD	Inflammatory bowel disease
IEC	Intestinal epithelial cell
IgA	Immunoglobulin A
IL-1β/6/8/10	Interleukin 1β/6/8/10
IRAK1/4	Interleukin-1/4 receptor-associated kinase
LAM	Lipoarabinomannan
LBP	Lipopolysaccharide binding protein
LI	Large intestine
LPS	Lipopolysaccharide
LTA	Lipoteichoic acid
MAMP	Microbe-associated molecular patterns molecules
MAP kinase	Mitogen-activated protein kinase
mCD14	Membrane-bound CD14
MD-2	Myeloid differentiation protein 2
MLN	Mesenteric lymph nodes
MyD88	Myeloid differentiation factor 88
NF-κB	Nuclear factor κB
NMR	Nuclear magnetic resonance
NT	No treatment
PAMP	Pathogen-associated molecular patterns molecules
PBMC	Peripheral blood mononuclear cells
PBS	Phosphate buffered saline
PGN	Peptidoglycan
PMN	Polymorphonuclear neutrophil
PRR	Pattern recognition receptor
rbosCD14	Recombinant bovine CD14

rpm	Revolutions per minute
RT-PCR	Real-time polymerase chain reaction
sCD14	Soluble CD14
SDS	Sodium dodecyl sulfate
SEM	Standard error of mean
SI	Small intestine
SQPI	Spectral quench parameter of the isotope
TLR	Toll-like receptor
TNF	Tumor necrosis factor
UC	Ulcerative colitis

List of Figures

Chapter 1

Figure 1. Signaling pathway of CD14 protein ……....3

Figure 2. Secondary structure and crystal structure of mouse CD14 ……. 5

Figure 3. Reductive methylation reaction of amino groups in proteins using [^{14}C]formaldehyde …….....15

Figure 4. Trimethylation of amino groups on proteins using methyl iodide …….....15

Chapter 2

Figure 5. Barium sulfate radiocontrast imaging of the gastrointestinal tract in a 10 day old Sprague Dawley rat pup using x-radiography...……21

Figure 6. Gastrointestinal transit time in 10 and 15 day old rats in the presence (M^+) or absence (M^-) of their mothers ...……24

Chapter 3

Figure 7. Counting efficiency curve for liquid scintillation counting ……..35

Figure 8. Representative graph of rats fed [^{14}C]CD14 and euthanized 480 min post-gavage……. 36

Figure 9. Distribution of ^{14}C in the organs of rats fed [^{14}C]BSA, [^{14}C]casein or [^{14}C]CD14 …...……38

Figure 10. Distribution of percent dose fed in the intestinal lumen of rats fed [^{14}C]BSA, [^{14}C]casein or [^{14}C]CD14 ...……..40

Chapter 4

Figure 11. Influence of recombinant CD14 on cytokine production by LPS-stimulated $CD14^+$ monocytes……...50

Figure 12. Quantitative RT-PCR of cytokine mRNA expression levels in isolated $CD14^+$ monocytes……...51

List of Tables

Chapter 2

Table 1. Gastroduodenal, gastrocecal and total transit times in 10 and 15 day old rats……..23

Chapter 3

Table 2. Specific radioactivities (dpm/µg) of [^{14}C]BSA, [^{14}C]casein and [^{14}C]CD14……..33

Table 3. Detectability of ^{14}C in Sprague Dawley rats 480 min post-gavage with [^{14}C]CD14 (1 020 400 dpm).…….37

Chapter 1

Introduction

1-1 Gastrointestinal development

Gut immunology

Mammalians have a multilayer immune system necessary to protect the body from infection. The two arms of the immune system are the innate (nonspecific) and the adaptive (acquired, specific) systems. The innate immune system is the first form of defense against invading pathogens, viruses or parasites. The major components of this system are surface barriers (epithelial cells), dendritic cells (DCs), soluble factors and professional phagocytes (macrophages and granulocytes) [1]. Innate receptors recognize conserved structural features of microorganisms called pathogen-associated molecular patterns (PAMPs) and microbe-associated molecular patterns (MAMPs). Examples of these conserved structures include lipopolysaccharide (LPS), peptidoglycan (PGN), lipoarabinomannan (LAM), lipoteichoic acid (LTA) and lipoproteins [2-4]. These innate structures are recognized by pattern recognition receptors (PRRs) synthesized by host cells. Cluster of differentiation 14 (CD14) protein is a well characterized PRR capable of recognizing several pathogen-related molecules [5] and phospholipids [6-8].

CD14 is expressed on the surface of mature monocytes, macrophages and neutrophils [9-12]. There are two forms of CD14: membrane-bound (mCD14) and soluble CD14 (sCD14). mCD14 is a 55 kDa glycoprotein with a glycosylphosphatidylinositol (GPI)-linkage that anchors the protein to the outer surface of the plasma membrane. The

soluble form is secreted and present in the serum at concentrations of 2-6 µg/mL [13]. The primary CD14 ligand is LPS found on the surface of Gram negative bacteria. LPS has three domains that include the outer O-antigen, a hydrophilic polysaccharide inner core and hydrophobic lipid A (endotoxin).

Since CD14 does not contain an intracellular signaling domain, it requires Toll-like receptor 4 (TLR4) and myeloid differentiation protein 2 (MD-2) complexes to stimulate an intracellular signaling cascade. This has been experimentally determined using LPS hyporesponsive mice which show specific mutations in the TLR4 gene [14-16]. LPS-binding protein (LBP) enhances CD14 affinity for LPS by an order of magnitude and LBP's expression can be further enhanced during infection [17]. CD14 shuttles LPS to MD-2 and TLR4 with the aid of LBP to drive gene expression and the upregulation of proinflammatory cytokines [18-20] as seen in Figure 1 [21]. Upon binding, CD14/LPS complexes with TLR4 and/or TLR2 and the intracellular targets of MyD88 and IRAK1/IRAK4 are recruited. This leads to the activation of transcription factors such as AP-1 and NF-κB [18]. Cytokines such as IL-1β, IL-6, IL-8 and TNF-α are typically produced in an innate response.

CD14 heightens the responsiveness of the innate immune system during the invasion of pathogenic microorganisms [5, 11, 22-25]. Overstimulation of the CD14 pathways, especially in the presence of excess LPS can lead to the overproduction of cytokines (i.e. TNF-α) and septic shock. For example, transgenic mice expressing human CD14 are hypersensitive to LPS [26] because CD14 can detect LPS at concentrations as low as 0.01–1 ng/mL [27]. In contrast, CD14 knockout mice are insensitive to LPS and become resistant to septic shock [28, 29].

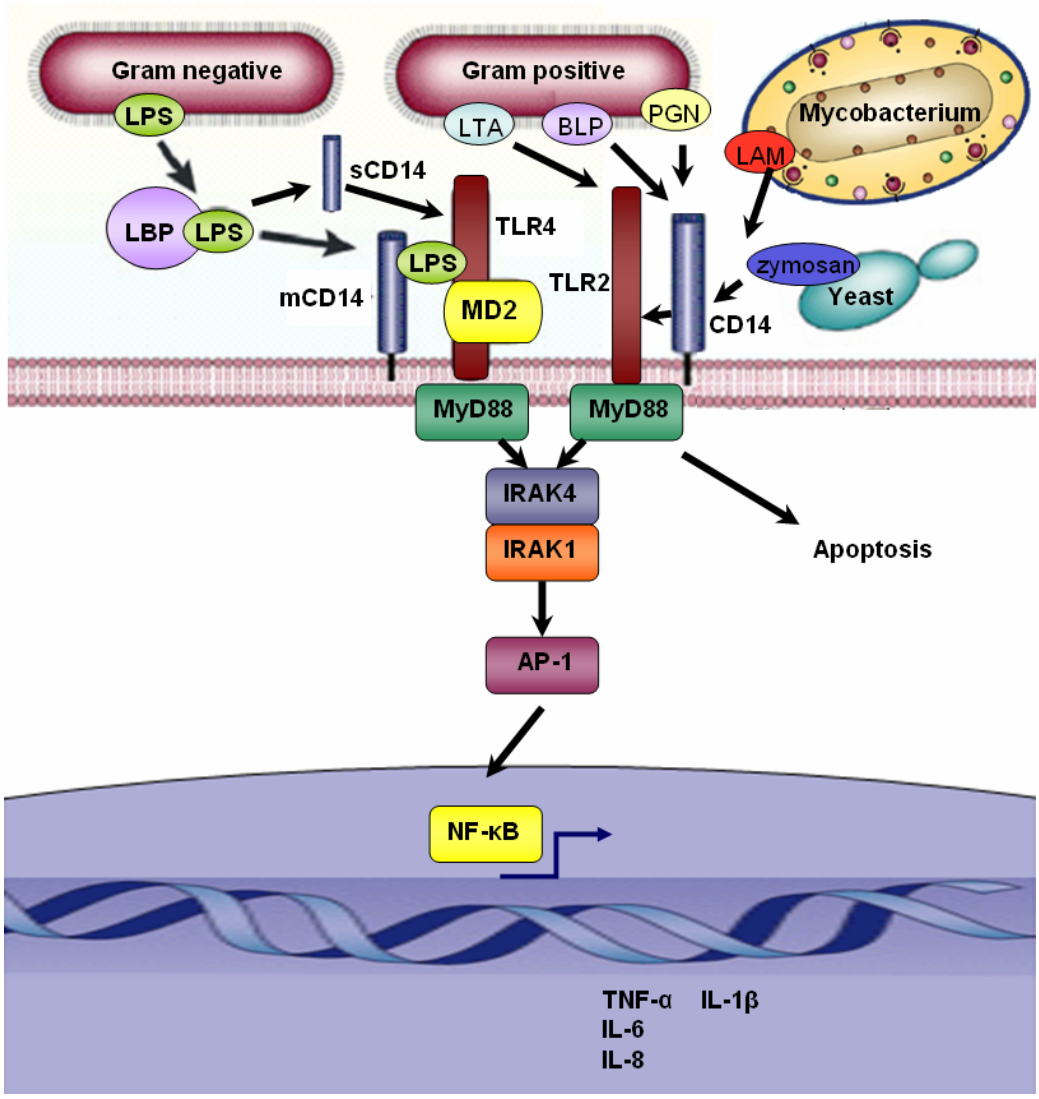

Figure 1. Signaling pathway of CD14 protein
CD14 recognizes Gram negative bacterial LPS, Gram positive PGN, LTA and BLP and mycobacterial LAM [2]. $CD14^{+}$ macrophages can remove apoptotic cells via the detection of yeast zymosan (a CD14-independent proinflammatory stimulus) [20, 30]. CD14 binds with TLR2, or CD14 can form a complex with TLR4 and MD-2, which recruits MyD88 and IRAK1/IRAK4. This activates the transcription factor AP-1 which results in the activation of NF-κB to elicit regulatory responses including the upregulation of proinflammatory cytokines, such as IL-1β, IL-6, IL-8, TNF-α. The figure was adapted from Finlay and Hancock [21].

Legend: CD14, cluster of differentiation 14; LPS, lipopolysaccharide; PGN, peptidoglycan; LTA, lipoteichoic acid; BLP, bacterial lipoprotein; LAM, lipoarabinomannan; TLR4, Toll-like receptor 4; MD-2, myeloid differentiation protein 2; MyD88, myeloid differentiation factor 88; IRAK1/4, interleukin-1/4 receptor-associated kinase; NF-κB, nuclear factor κB.

Mechanistically, CD14 transfers LPS to TLR4 and MD-2 found at the surface of receptor cells. Using surface plasmon resonance, the rates of association/dissociation of LPS binding to CD14, TLR4 and MD-2 have been estimated [30]. The association rate constant (K_{on}) for LPS to MD-2 was 5.61 x 10^3 $M^{-1}s^{-1}$, while their dissociation rate constant (K_{off}) was 1.28 x 10^{-2} s^{-1} [30]. It was suggested that LPS had a slow association and fast dissociation with MD-2. The dissociation constants for LPS to CD14 and MD-2 are 8.7 µM and 2.3 µM, respectively. It has been demonstrated *in vitro* and *in vivo* that low concentrations of LBP can enhance the response of LPS bioactivity, while high concentrations of LBP inhibit LPS activity [31].

The crystal structure of CD14 [32, 33] revealed a horseshoe shaped dimer that forms a large hydrophobic pocket at the N-terminal region of the protein (Figure 2) and is thought to be responsible for LPS binding. CD14 has broad ligand specificity for PAMPs [34]. This ligand binding diversity may be explained structurally by the large N-terminal pocket size, flexible pocket rim and multiple grooves available in the pocket for ligand binding [33].

Soluble CD14 (sCD14) is found at a concentration of 25 µg/mL in human milk compared with 5 µg/mL in human serum [35]. In *Bos taurus*, neutrophils increase the sCD14 concentration when the udders were injected with 100 µg of LPS [36]. For this reason, it has been speculated that sCD14 in breastmilk aids the innate immune system of the feeding infant from invading bacteria during early gastrointestinal colonization. However, due to the presence of proteolytic enzymes available in the human digestive system, it is believed that CD14 is completely degraded within the GI tract. It has been observed that breast fed newborns had trace quantities of CD14 in their feces and urine suggesting either complete digestion or tissue absorption [35].

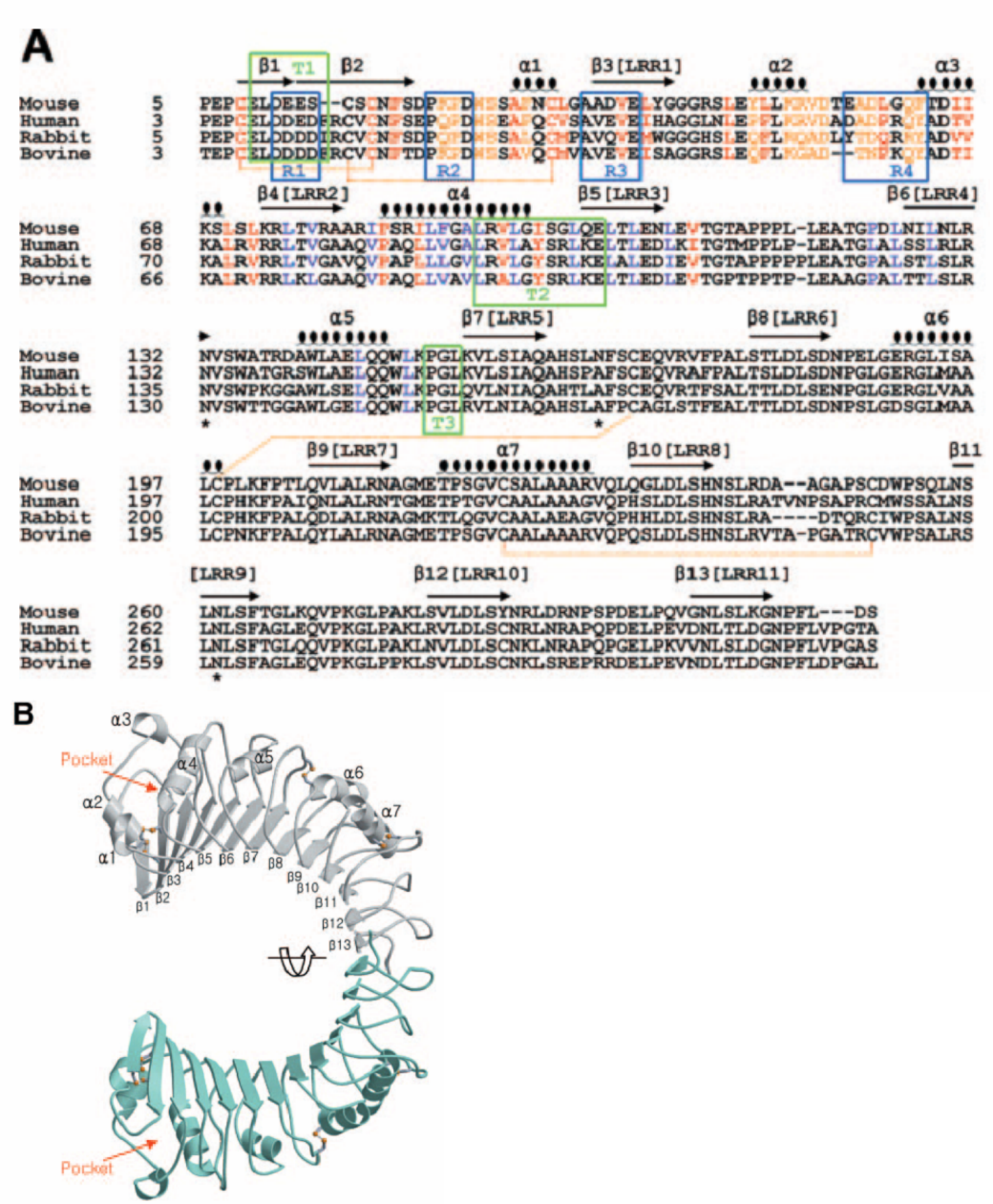

Figure 2. Secondary structure and crystal structure of mouse CD14

A) Alignment of mouse, human, rabbit, and bovine CD14. The assignment of secondary structure is shown above the sequences. * denotes N-glycosylation sites and yellow lines show the cysteines that form disulfide bridges. Orange writing shows the residues on the rim of the NH_2-terminal, red writing shows residues on the walls and base of the main pocket and purple writing shows residues on the sub-pocket. R1-R4 enclosed in blue boxes indicate LPS-binding regions. T1-T3 enclosed by green boxes show residues important for LPS signaling.

B) Crystal structure of mouse CD14 dimer (monomers shown in grey and cyan). Orange circles show disulfide bridges and the NH_2-terminal pockets are indicated by arrows [31].

Microbial colonization

The human gastrointestinal (GI) tract contains over 100 trillion bacteria, and the dynamics of this microbial ecology are believed to have a direct impact on long term health of the host [37]. Beneficial commensal microorganisms may positively influence metabolism, control obesity and help maintain homeostasis, while pathogenic species disrupt homeostasis and cause disease. The mechanisms for regulating a homeostatic population within the gut are relatively unknown. Since it has been shown that diet can manipulate the microflora in the GI tract, CD14-containing human milk may play a significant role in gut colonization of newborns.

The innate immune system helps control the colonization of bacteria in the GI tract. For instance, mucus secreting goblet cells are responsible for the production of mucins, which form a physical matrix barrier to limit the interaction of pathogenic microorganisms with the gut epithelium [38]. Paneth cells, found within the specialized stem cells at the base of the crypts of Lieberkühn in the small intestine, produce antimicrobial peptides and lysozyme. They have been shown to directly sense enteric bacteria through MyD88-dependent TLR activation [37]. Paneth cells can limit bacterial penetration in the intestinal epithelium by activating this pathway to produce antimicrobial factors such as lysozyme, Reg3γ, α-defensin and secretory phospholipase A_2 [39]. These substances aid in minimizing unwanted microbial colonization that may cause insult to the stem cells. This ability of Paneth cells helps to limit the number of bacteria that can localize on the epithelium and therefore inhibits the translocation of bacteria to the mesenteric lymph nodes (MLN) through the intervention of dendritic cells (DC).

Commensal microorganisms are capable of inhibiting pathogenic organisms from colonizing in the gastrointestinal tract through producing antimicrobial substances and creating undesirable environments for pathogenic growth. In conditions where pathogenic organisms reach sufficiently high populations, symptoms experienced by the host may include diarrhea and inflammation. To help maintain a symbiotic population, the gut's innate immune system integrates a number of pathways, cells and immunological factors to help maintain homeostasis. It has been suggested that intestinal microorganisms drive gene expression in the host epithelium by signaling to genetically predisposed cells [40]. There have been data to support the beneficial use of probiotics in the diet such as *Lactobacilli, Bifidobacterium* and *Saccharomyces boulardii* for conditions such as necrotizing enterocolitis (NEC), gastroenteritis, ulcerative colitis (UC) and Inflammatory Bowel Disease (IBD) [41]. Some probiotic bacteria have also been recognized in modulating GI health such as diarrhea and lactose intolerance [42].

Gut microbial populations established along the enteric system are actively involved in health and metabolism. In some segments, they are involved in the fermentation of nondigestible dietary fibers, resistant starches and oligosaccharides as well as anaerobically metabolizing peptides and proteins. Commensals can biotransform conjugated bile acids, degrade oxalate-based complexes and synthesize vitamins such as B12 and K [43]. Certain microbiomes are capable of modulating dietary health due to their anticarcinogenic nature and can lead to lower levels of cholesterol in the blood [42]. Therefore, some consider the gut microbiota to be an 'exteriorized organ' which aids in homeostasis in an *ex situ* mode rather than *in vivo* [43].

Intestinal microorganisms are also important in controlling body mass. Studies conducted using germ-free mice and mice homozygous for a mutation in the leptin gene, produced an obese phenotype. When the gut microflora were transplanted from obese mice to lean mice, the lean mice developed the obese phenotype. It was also observed that the obese intestinal microflora had an increased capacity to harvest energy from the diet [44]. Shotgun sequencing and metagenomic analysis revealed that lean mice showed an increase in gut bacteria from the phylum Bacteroidetes in comparison with Firmicutes. This ratio was attributed exclusively to weight loss and not to total caloric intake.

Since gut microflora play a role in maintaining homeostasis and health, it is important to understand how the GI tract is first colonized. It has been observed that the diet of newborns influences the microbial populations that colonize the GI tract. For infants that are both vaginally born and breast fed, *Bifidobacterium*, *Streptococcus* and *Lactobacilli* are characteristically found as early colonizers of the gut. Children who are delivered by Caesarean-section and who are formula fed have a higher commensal population of *Escherichia coli*, *Clostridia* and *Staphylococcus*, which are bacteria that can become pathogenic [45]. Therefore the presence of CD14 in human milk, which alerts the immune system to Gram negative bacteria, suggests a role in modulating the early events of gut colonization in infants.

1-2 Gastrointestinal diseases

Gastrointestinal diseases such as Crohn's disease (CD) and ulcerative colitis (UC), are classified as Inflammatory Bowel diseases (IBD). Studies conducted comparing CD, UC and

normal patients, showed that CD patients had a significant increase in their $CD14^+$ expressing macrophage population [46]. This subpopulation of macrophages was responsible for increased secretion of TNF-α, IL-6 and IL-23 in comparison to macrophages isolated from normal patients. Therefore, CD14 expressed on the surface of phagocytic cells in blood, suggests a broader role in the pathogenesis of IBD.

Necrotizing enterocolitis (NEC) is a form of IBD that afflicts very low birth weight neonates, especially infants that are born pre-term. NEC is a multi-factorial disease whose underlying etiology remains elusive, although bacterial colonization of the gut, formula feeding, and perinatal stress have been implicated as putative risk factors [47]. Symptoms include necrosis and chronic inflammation of the bowel and are associated with considerable mortality and morbidity. Prematurity in combination with prolonged inflammation are the primary risk factors in the pathogenesis of NEC. Premature infants are susceptible to NEC due to the incomplete development of the GI tract including decreased blood flow, reduced gastric acid and mucus production, poor intestinal motility, low levels of secretory immunoglobulin A and decreased proteolytic enzyme activity [47]. Under these limitations the infant is generally unable to respond appropriately to invading microorganisms.

It has been observed that 90% of NEC patients were fed infant formula without the accompaniment of breast milk [38]. This suggests that breast milk may have some protective factors that are presumed to reduce the incidence of NEC. These elements include lysozyme, lactoferrin, polymeric immunoglobulin A (IgA) and oligosaccharides as well as tumor necrosis factor (TNF) receptor, acetylhydrolase and IL-1 receptor antagonist [47]. Breast fed infants also show a microbiota that is rich in bifidobacteria and whose proliferative advantage in the infant gut may reduce the incidence of NEC [48].

Gastrointestinal transit

The mechanisms that control the development of the mammalian digestive system reveal a dynamic process. The course of early gut development underpins long-term health [49] and the role of maternal milk, with its multitude of bioactives, significantly influences this development [38]. Effects of environmental components such as diet are possible to study in offspring reared with the mother (maintenance models) and those reared in the absence of the mother (substitution model) [50]. For instance, maternal separation and social isolation experiments using rhesus monkeys, while causing significant physiological changes in the mother, also influence concomitant changes in the physical and behavioral development of the infants [51]. Infant monkeys (207-208 days) demonstrated a measurable increase in frustration and aggression when separated from their mothers. Furthermore, the infant monkeys displayed a decrease in play, indicative of distress [52].

In Wistar rats, psychological stress influenced the gastrointestinal transit time (GItt) by causing observable increases in stomach emptying when rats were exposed to the experimental stressor of water [53]. In addition, the use of a substitution model, where the pups were separated from the dam, artificially reared and fed milk substitutes, invoked abnormal growth in the gastrointestinal tract of rats [54-56]. This thesis, therefore, sets out to examine two variables, maternal deprivation and diet (maternal milk *versus* formula), to investigate their combined influence on GItt in young rats.

Total gastrointestinal transit time is the time required for newly ingested material to transit through the GI tract and be excreted from the anus. There is considerable interest in understanding the transit time of experimental animals, not only for nutritional research but also for the design of pharmacokinetic studies [57]. With increasing attention being given to

innate immune milk proteins, such as CD14, and the development of the neonatal gut, a suitable animal model is required to study the uptake of milk, dietary proteins and drugs [35, 58, 59]. This depends on measurement of transit time where the stage of gut development is largely age-dependent [60]. It is evident that the very early days of building the mother-baby dyad, one to ten days after birth, is critical for the establishment of gut health [48]. Administration protocols may become more 'informed' the more precise understanding of motility becomes.

Various methodologies for determining GI transit time have been devised. Radiocontrast tracers or markers fed to animals such as barium sulfate allow for segmental transit time determination by using timed x-rays [61-64]. Carmine red and Poly R-478 dyes [53, 65, 66], fluorescent compounds, radiotracers [67-69] and charcoal [70-76] facilitate the determination of total GItt. Additionally, hydrogen breath testing can measure the time that an orally ingested non-absorbable carbohydrate takes to reach the site of microbial concentration through measurement of gaseous products of fermentation, and thus, allow for determination of gastrocecal transit time [53].

Stress, gut development, age, diet and the use of anesthetics can influence GItt in experimental animals [53, 60, 76]. Anesthetics, such as isoflurane, permit surgical placement of catheters and enable easier gavage feeding. However, the use of isoflurane also causes a reduction in total transit time in rats fed a marker of activated charcoal [76]. Maternal deprivation may be an additional factor influencing GItt in young rats since her presence provides nutritional requirements, thermal regulation and tactile stimulation. Therefore, the consideration of maternal presence must be taken into account when studying GItt.

1-3 Tracking bioactives in the gut

The pharmaceutical industry routinely performs toxicity and absorption, distribution, metabolism, excretion (ADME) studies when developing new drugs. These studies use ^{14}C-labeled drugs to analyze transit, dissolution and uptake of the drug in the gastrointestinal tract. The preparation of ^{14}C-labeled proteins of sufficiently high specific radioactivity for ADME studies has not been economically feasible. For this reason, ^{125}I and ^{131}I labeling of proteins [77] has been used for tracing the biodistribution of fed proteins in the organs of animals. The major advantages of using ^{125}I or ^{131}I are its high specific radioactivity and ease of detection and quantification. Radioiodine as a high energy gamma emitter, however, increases the complexity of experimental procedures because added precautions are required [78]. Another disadvantage is the relatively short half-life of radioiodine (^{131}I - 8 days; ^{125}I - 60 days) which does not permit long-term storage of samples or the labeled protein for repetition of experiments.

The advantages of using ^{14}C-labeled proteins for ADME studies are the long half-life (5730 years), which would extend the experimental lifetime of a single labeled preparation of protein, and the negligible radiation hazard. However, very few ^{14}C-labeled proteins are available from commercial sources and the relatively high cost and low specific activity limit their use in biodistribution studies. The most common method for radiolabeling proteins with ^{14}C is by reductive methylation of amino groups using [^{14}C]formaldehyde [79]. Labeling of proteins with ^{14}C by reductive methylation is inefficient under aqueous conditions because the presence of water limits the amount of Schiff base that can be formed

by reaction with [^{14}C]formaldehyde, thus greatly decreasing the amount of ^{14}C-label incorporated into the protein [79]. This is especially true for the labeling of small amounts of protein where practicality requires the use of larger amounts of water relative to the amount of protein.

Taralp and Kaplan [80] developed a method for the methylation of lyophilized proteins *in vacuo* using methyl iodide. This anhydrous methylation reaction is performed in the absence of water and therefore improves the efficiency of protein methylation by limiting uncontrolled side reactions. [^{14}C]Methyl iodide is currently available with specific radioactivities of 40 - 60 mCi/mmol (Perkin Elmer, Waltham, USA) and the methylation reaction can be performed with undiluted [^{14}C]methyl iodide as delivered by the radiochemical supplier. The ability to methylate proteins using undiluted [^{14}C]methyl iodide makes it possible to prepare ^{14}C-labeled proteins of much higher specific radioactivity than currently available. There are generally more target amino acids and imidazole groups available for labeling with [^{14}C]methyl iodide than phenolic groups for labeling with radioiodine. The increased number of target amino acids for labeling makes it possible to partially compensate for the high specific radioactivity of the radioiodine.

Methyl iodide is an electrophile that can add one to three methyl groups onto amino groups on proteins, primarily the epsilon lysine amino group [80]. The low efficiency of the reductive methylation reaction using [^{14}C]formaldehyde is due to the presence of water which greatly reduces the amount of Schiff base formed (Figure 3) and therefore the number of ^{14}C-methyl groups incorporated into the protein. In contrast, *in vacuo* methylation (Figure 4) is performed in the absence of water where the losses of ^{14}C label due to side reactions under anhydrous conditions are minimized. Under vacuum, virtually all the

^{14}C-methyl label can be incorporated. Methyl esters can also be produced during the reaction due to the presence of carboxyl groups. However, these methyl esters are labile and are readily hydrolysed by resuspension in water at alkaline pH (see methods in Chapter 3).

NMR has demonstrated that *in vacuo* methylation of proteins produces trimethylated amino and dimethylated imidazole groups [80]. Most proteins contain a large number of free amino groups and since three methyl groups are incorporated into each amino group, a high specific radioactivity can be obtained with small quantities of ^{14}C reagent. The covalent bonds forming the trimethylamino and dimethylamino groups are highly stable to both chemical and enzymatic degradation.

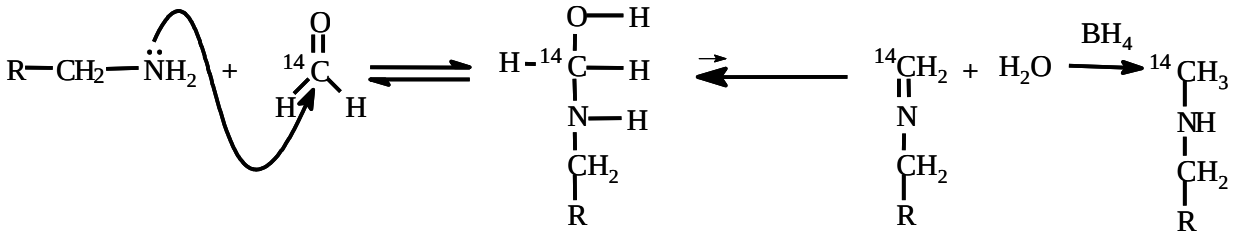

Figure 3. Reductive methylation reaction of amino groups in proteins using [^{14}C]formaldehyde
An amino group in the protein reacts with [^{14}C]formaldehyde to form a Schiff base. Addition of borohydride reduces the Schiff base to form a methyl derivative. This reaction can be repeated to form a dimethyl amino group [80].

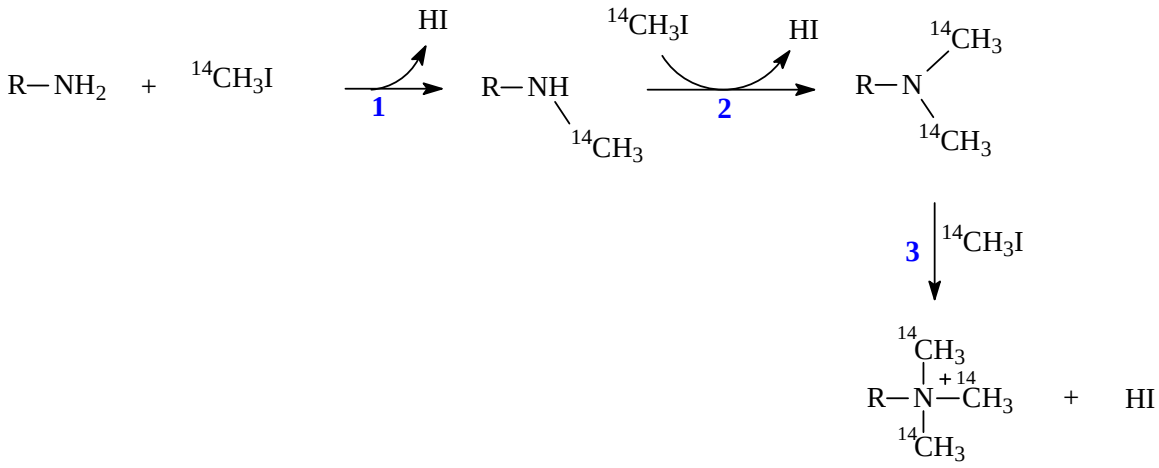

Figure 4. Trimethylation of amino groups on proteins using methyl iodide
An amino group in the protein reacts *in vacuo* with [^{14}C]methyl iodide to form a methyl derivative. This reaction is repeated to form a trimethyl derivative [81].

1-4 Objectives & rationale

Objective 1: Develop an appropriate neonate rat model to trace radiolabeled proteins. This study aims to investigate maternal influence on GItt in neonatal rats by developing a non-invasive gavage feeding method without the need for anesthetics. Therefore, 10 and 15 day old Sprague Dawley rats were gavage fed barium sulfate and their GItt was tracked using timed x-rays. The rationale was to design an effective rat model to determine if neonate rats can remain with their mothers for the duration of ADME studies.

Objective 2: Determine whether proteins can be labeled economically *in vacuo* with [^{14}C]methyl iodide to a sufficiently high specific radioactivity to be used in ADME studies. BSA and casein were used as test proteins to determine the efficacy of radiolabeling using the method described by Taralp and Kaplan [80].

Objective 3: Monitor the biodistribution of oro-gastric gavaged [^{14}C]CD14 through the gastrointestinal tract of neonate rats. Previous work has shown that CD14 was not found in the feces of breast fed infants, therefore the rationale for this experiment was to determine the fate of CD14 using a neonate rat model.

Objective 4: To determine if sCD14 would alter the production of cytokine by LPS-stimulated human peripheral blood mononuclear cells (PBMC). The rationale was to investigate if exogenous sources of CD14 (including human milk) would lessen the severity of an innate inflammatory response when monocytes are stimulated with LPS.

Chapter 2

Gastrointestinal transit in Sprague Dawley rats

2-1 Summary

The segmental and total gastrointestinal transit times (GItt) were measured in two different litters of 10 and 15 day old Sprague Dawley rat pups using barium sulfate. By tracking the leading front of the bolus on radiographs, the gastroduodenal and gastrocecal transit times in the pups were estimated. The gastroduodenal times for all pups (n = 21) were less than 0.17 hr. The gastrocecal times for 10 day old pups maintained with their dam (n = 5) ranged from 4 to 5 hr. When five pups from the same litter were removed from the dam, their gastrocecal times ranged from 2.5 to 5 hr. For the litter of 15 day old rat pups, when maintained with their dam (n = 6), the gastrocecal times ranged from 4 to 6 hr. 15 day old pups without their mother (n = 5) presented gastrocecal times ranging from 3.5 to 5 hr.

To measure the total gastrointestinal transit time, the duration from oro-gastric gavage until an observable defecation of the barium sulfate marker was recorded. Ten day old rat pups that remained with the dam had a total gastrointestinal transit time of 13.8 ± 0.9 hr. Those pups that were kept in the absence of the dam had a time of 9.3 ± 0.7 hr. This decrease (p<0.05) in total gastrointestinal transit time in the absence of the dam was age-dependent, as it was not observed (p>0.05) in the 15 day old rat pup litter. The GItt of 15 day old rats was significantly longer (p<0.05) than in 10 day old pups. The results provide a basis, for the design of future studies involving neonate rat metabolism, to include maternal presence and this information was used as a basis for determining experimental sampling times in all subsequent experiments described in Chapter 3.

2-2 Materials and methods

Materials

Liquid Polibar Plus barium sulfate suspension (53% w/v) was kindly supplied by the Children's Hospital of Eastern Ontario. Syringes (Becton Dickinson & Co, Franklin Lakes, USA) with polyethylene-10 tubing (Fisher Scientific, Ottawa, Canada) were used for oro-gastric gavage feeding. A Hitachi mobile x-ray unit (Model DGC-1010 set at 34 kv, 2mAs exposure) was used to capture images. Thermo Scientific Pierce CL-XPosure film was purchased from Fisher Scientific, Ottawa Canada. Normal saline (Baxter, Mississauga, Canada) was used for subcutaneous injections to keep the animals hydrated. Commercial, store purchased Enfamil A+ infant formula (Mead Johnson Nutritionals, Ottawa, Canada) was used to feed maternally deprived infant rats.

Gastrointestinal imaging

Studies were conducted in accordance with the University of Ottawa's Animal Care & Veterinary Service, approved by Ottawa Hospital Research Ethics Board, BMI-77. Ten day old (n = 10) and 15 day old (n = 11) Sprague Dawley rat pups (Charles River, St. Constant, Canada) weighing 19 - 28 g (10 day old rats, 21.51 ± 1.61 g; 15 day old rats, 27.40 ± 1.00 g) were placed into an Armstrong Envirocare Incubator (Model 190ASC) at 37ºC and fasted for 2 hr to empty the stomach cavity [60]. Selecting a 50% older rat litter with an average weight 27% greater than that of ten day old animals was used as a comparator. All pups were gavage fed 250µL of barium sulfate that was suspended in ddH_20 (1:1, v/v). Briefly, the barium sulfate suspension was loaded into a 1 mL syringe with needle and inserted in the end of a 20 cm length of polyethylene tubing. The length between the oral cavity and the

stomach of each rat was measured and used to mark the length of the tubing required to enter the stomach. The tubing was lubricated with mineral oil before insertion in the esophageal cavity. The tube was inserted until the tube marking was reached and a 250 µL bolus of barium sulfate suspension was administered into the stomach. Upon delivery of barium sulfate, the tube was gently removed and the pup was returned to its cage.

Rats were individually identified and divided into two groups: maintained in a cage with their mother, or placed in an incubator without the mother (substitution). For x-ray radiography, animals were placed into a cardboard holding grid with individual stalls to ensure serial tracking of bolus movement. X-ray radiographs were taken at 10, 20 and 30 min, followed by subsequent exposures every 30 min thereafter. At 4 hr, images were captured every hour for the duration of the experiment. The pups separated from their mother were handled at hourly intervals by weighing and feeding 1 mL of Enfamil A^+ infant formula to sustain their blood sugar levels between 2.8 and 7.4 mmol/L (OneTouch Ultra 2 blood glucose monitoring system, LifeScan Inc., Johnson & Johnson Inc., Milpitas, USA). In addition, to maintain the hydration status of pups, enough saline solution was injected subcutaneously to maintain weight throughout the course of the experiment.

For the present investigation, the gastroduodenal, gastrocecal and gastrointestinal transit times were defined as the duration for the leading edge of the barium sulfate to enter the duodenum, cecum and exit the anus, respectively. X-ray radiographic images were analyzed to determine these time points and representative examples of images depicting gastroduodenal, gastrocecal and gastrorectal times are presented in Figure 5. Gastroduodenal and gastrocecal times were reported as a range. Total gastrointestinal transit times were reported as the mean ± the standard error of the mean (SEM). Statistical analysis was

performed as a student *t*-test where $p<0.05$ was considered statistically significant.

(See Appendix A,B for all x-ray images from individual animals.)

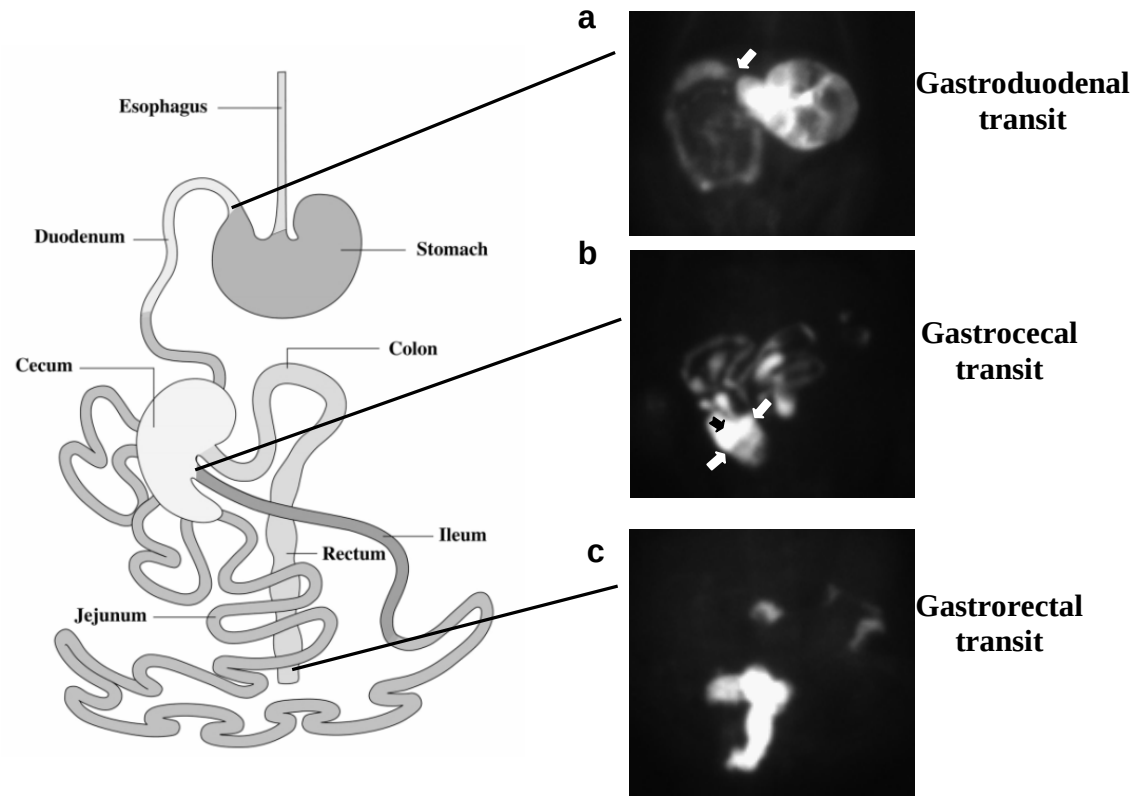

Figure 5. Barium sulfate radiocontrast imaging of the gastrointestinal tract in a 10 day old Sprague Dawley rat pup using x-radiography

a) The white arrow in the gastroduodenal transit image shows the leading edge of barium sulfate entering the duodenum from the stomach.

b) The black arrow in the gastrocecal transit image indicates the direction of barium sulfate movement as it entered the cecum; the two white arrows indicate the leading edge of barium sulfate.

c) The gastrorectal image shows the barium sulfate concentrated at the anal sphincter before being excreted by the rat. Anatomy of rat GI tract was adapted from DeSesso and Jacobson [81].

2-3 Results

Gastroduodenal and gastrocecal transit time

The gastroduodenal and gastrocecal transit times were recorded as ranges (Table 1). Given the logistics of handling and radiographing 21 rat pups, the first feasible time point to image the barium sulfate suspension was ten minutes into the experiment (0.17 hr). By that time, the leading edge of the bolus had entered the duodenum in all the animals, regardless of age or maternal presence. The gastrocecal time for 10 day old pups with their dam and without their dam was 4 – 5 hr and 2.5 – 5 hr, respectively. For 15 day old rats, the gastrocecal time with and without the dam was 4 – 6 hr and 3.5 – 5 hr, respectively.

Gastrointestinal transit time

The effect of age on GItt was determined by comparing the time from administration of barium sulfate into the stomach to the initial detectable excretion of barium sulfate from the anus between 10 and 15 day old rats. In the older Sprague Dawley pups, the transit times increased in both the maintenance ($p<0.05$) and deprivation groups ($p<0.05$) in comparison with those for 10 day old counterparts (Figure 6). In the presence of their mother, the mean total gastrointestinal transit time in 10 day old pups was 13.8 ± 0.9 hr compared with 17.3 ± 0.5 hr in 15 day old pups ($p<0.05$). In the absence of the dam, 10 day old rats had an average transit time of 9.3 ± 0.7 hr and this increased to 16.2 ± 0.6 hr in 15 day pups ($p<0.001$). Observable developmental changes in 15 day old rats in comparison to their 10 day old counterparts included additional body fur and increased palpebral fissuring (opening of eyelids). The body weight for 10 day old rats was 21.51 ± 1.61 g and for 15 day old rats was 27.40 ±1.00 g.

Table 1.
Range of gastroduodenal, gastrocecal and total transit times in 10 and 15 day rats

Parameter	Animals			
Rat age (days)	10		15	
Maternal presence[a]	M^+ (n = 5)	M^- (n = 5)	M^+ (n = 6)	M^- (n = 5)
Transit time (hr)[b]:				
Gastroduodenal	<0.17	<0.17	<0.17	<0.17
Gastrocecal	4 - 5	2.5 - 5	4 - 6	3.5 – 5
Total transit	9.5 - 17	7.8 - 12.8	16.2 - 18.2	14.4 - 17.4

[a] M^+ denotes pups remaining with the dam, M^- denotes rat pups that are separated from the dam.
[b] Gastroduodenal, gastrocecal and total transit times are defined as duration for the leading edge of oro-gastric gavaged barium sulfate to enter the duodenum, enter the cecum and exit the anus, respectively.

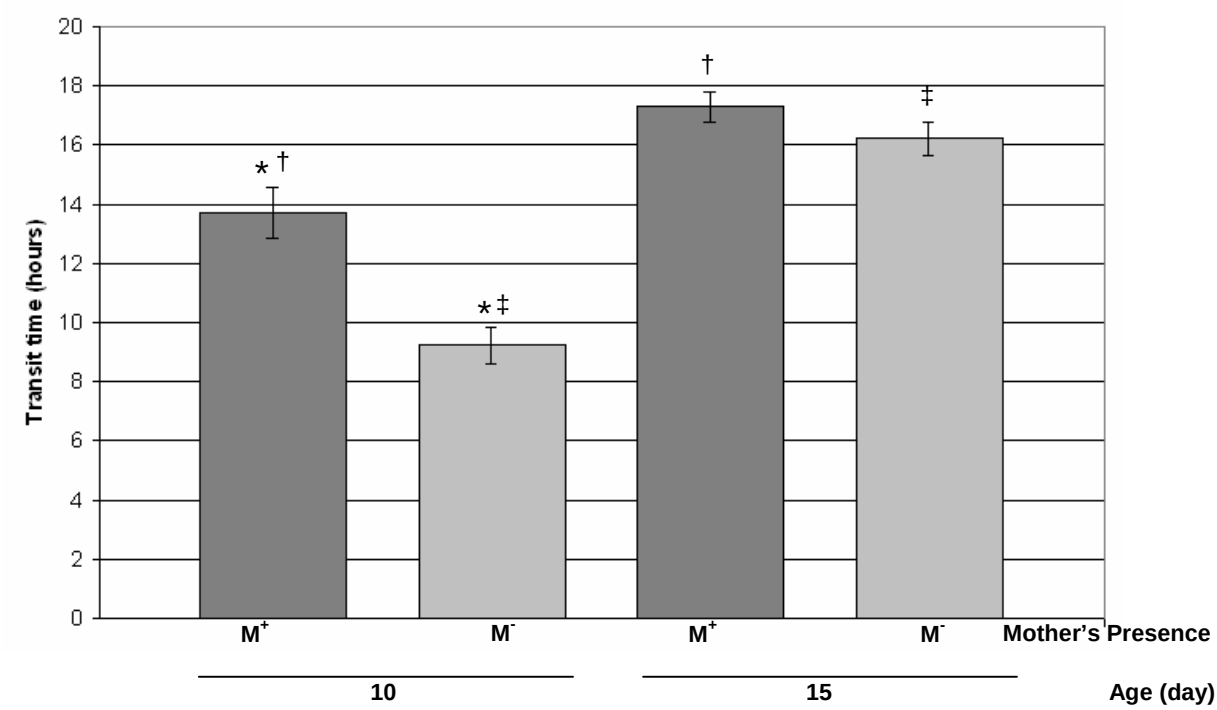

Figure 6. Gastrointestinal transit time in 10 and 15 day old rats in the presence (M^+) or absence (M^-) of their mothers

The total transit time was calculated as ($time_{barium\ sulfate\ observed\ in\ feces} - time_{barium\ sulfate\ ingested}$). The average transit time of a 10 day old pup was 13.8 hr ± 0.85 (SEM) with their mother and was 9.3 hr ± 0.66 (SEM) without the mother. The average transit time of a 15 day old pup was 17.3 hr ± 0.51 (SEM) with mother and was 16.2 hr ± 0.56 (SEM) without the mother.

* denotes a significant difference between the two groups ($p<0.001$).

†,‡ denote a significant difference between age groups ($p<0.05$). Data was analyzed with a student t-test for significance and $n = 5 – 6$.

The effect of maternal presence: Shorter gastrointestinal transit times in 10 day old pups without their mother were measured as compared to pups in their mother's presence ($p<0.001$) (Figure 6). In 15 day old rat pups, no significant difference ($p>0.05$) in GItt was observed between pups in the presence or absence of the mother.

2-4 Discussion

Transit times

The results of the present study show a gastroduodenal transit time of less than 0.17 hr in 10 and 15 day old pups (Table 1). For both the gastroduodenal and gastrocecal time points, no statistical analysis could be performed. Due to experimental and technical limitations, the frequency of radiographs and animal feeding times could not be performed simultaneously on all 21 animals. For this reason, the data were expressed as ranges. However, statistical analysis could be performed with total GI transit time, since it was possible to measure barium sulfate defecation using several stop watches.

In this investigation, the elimination of anesthesia removes the effects of this variable on GItt [82]. Invasive treatments such as indwelling gastric cannulae also modify GI motility and gut development [83, 84]. Total transit time was found to decrease for only the 10 day old rats in the absence of the mother because 15 day old rats demonstrated no significant difference. Considering that rats wean at 20 - 22 days of age, pups may start tolerating maternal absence as early as 15 days of age. However, the effect of infant formula and stress induced from subcutaneous saline injections must also be taken into account when considering such differences.

These findings may be compared to those of previous studies but direct comparisons are difficult to make due to lack of uniformity or standardized procedures. Different strains of rats, older age groups, or different markers and methods have been employed to estimate total transit time. For example, use of 1, 2 and 3 month old Wistar rats with ^{14}C-PEG (polyethylene glycol- 4000) as a non-absorbable tracer indicated a gastric emptying time of less than 30 min [67]. In a separate experiment, 49 - 112 day old Sprague Dawley rats were chemically restrained with a combination of 0.71 mg ketamine hydrochloride/g body weight and 0.5 mg of acetylpromazine maleate injected intramuscularly. Barium sulfate transit as determined by radiography revealed results similar to this study with a gastric emptying time of 11 min and a gastrocecal time of 5 hr [61].

In the present study, when 10 day old pups were compared to 15 day old pups, the total gastrointestinal transit time increased although there were no differences in gastroduodenal and gastrocecal transit times. This demonstrates that the effects of aging are related to transit times in the colonic segment specifically. As most nutrients and drugs are absorbed in the stomach and small intestine, this five day difference in rat age was shown to have no effect with regards to transit through the upper parts of the gastrointestinal tract.

In a somewhat different approach, a previous study investigated small and large bowel emptying times, by measuring the time for any given segment to empty 50% of its total contents. The small bowel emptying half-time was equivalent to 5 hr among 1, 2 and 3 month old rats. In contrast, the large bowel emptying half-times were 6, 12.5 and 13 hr for 1, 2 and 3 month old rats, respectively [67]. This suggests there was no difference in small intestinal transit time for different aged rats. It can be inferred that colonic transit time was

the reason for the increase in total transit time in older rats, as was also observed in the present investigation.

Maternal influence on GItt

Maternal separation may alter GItt in rat pups through a variety of factors including physiological stress, physical stress from needle injections, disruptive feeding schedule, diet and a lack of maternal stimuli. It was observed that pups that remained with their mother were exposed to a variety of stimuli in less stressful conditions throughout the course of the experiment. The mother provided on-demand feeding for her pups. The mother also performed anogenital licking which is thought to stimulate urine and feces elimination [85]. Others have observed that the synthesis of acetylcholine and the release of corticotropin-releasing factor were stimulated in young rats that were separated from their mother, leading to development of colonic epithelial dysfunction [86]. Such physiological and anatomical changes of the GI tract in rats, as they mature, may also alter gut transit times.

Temporal intervals between feeds, along with the specific diet provided during the experiment, may have impacted GItt. Rats maintained with their mothers continued to suckle rat milk as needed. Mammalian milk is known to be a rich source of lysozyme, lactoferrin, polymeric IgA, tumor necrosis factor (TNF) receptor, acetylhydrolase, IL-1 receptor antagonist, oligosaccharides and other bioactives [47]. The total milk fat solids content of Sprague Dawley rat milk is approximately 1.35 g/L [87], whereas the infant formula used in this study contained 3.6 g/L. In healthy men, it was observed that consumption of a fat emulsion (palm and oat oil) increased their orocecal time [88].

Therefore, the nutrient profile of rat milk is likely to influence gut motility because its composition facilitates metabolism, immune protection and promotes growth [89]. The pups that were separated from their mothers were provided with 1 mL of infant formula at regular one-hour intervals. This feeding process requiring human handling may have been an added source of stress for these animals [90] as well as the infant formula itself which is known to alter GI tract function and motility in comparison to mother's milk [91]. The differences between maternal milk and infant formula, which were not addressed in this work, point to a growing area of interest - that of the impact of neonatal nutrition on health status and the incidence of disease in later life [92]. According to the results in this study, it was demonstrated that the higher fat diet of infant formula did not increase transit time as was previously observed in humans [88]. Therefore, it can be inferred that the stress of maternal deprivation influenced the GItt far greater than the provided diet.

Knowing that maternal separation induces stress in neonate rats [86] and that it also influences GItt in the Wistar strains [53], one may infer that decreased GItt was a result of stress caused by maternal deprivation. It is possible that the differences between maternal and formula milk also played a role in altering GItt. The data suggest that future experiments monitoring absorption, digestion, metabolism and excretion (ADME) or pharmacokinetic studies using neonatal rats may be performed while maintaining them in the presence of their mothers. This may benefit the experimental outcome by reducing variation in transit time and lessening the impact on digestion and metabolism.

Chapter 3

Pharmacokinetic studies using radiolabeled ^{14}C protein

3-1 Summary

Historically radiolabeling proteins with ^{14}C has been performed using reductive methylation using [^{14}C]formaldehyde [93]. With significant advantages of a longer half-life and a smaller radiohazard, this simple procedure has been considered a good alternative to radioiodination. Using the method described by Taralp and Kaplan [80], *in vacuo* radiolabeling of proteins using [^{14}C]methyl iodide was attempted to achieve higher specific radioactivities in comparison with previously described methods. Bovine serum albumin (BSA) and casein were used as test proteins to determine the efficacy of radiolabeling. Finally, CD14 was radiolabeled to be tested in pharmacokinetic studies. Using this method, calculated specific radioactivities of 10 400, 10 800 and 163 000 dpm/μg were measured for [^{14}C]BSA, [^{14}C]casein and [^{14}C]CD14, respectively.

[^{14}C]BSA, [^{14}C]casein and [^{14}C]CD14 were fed to 10 day old Sprague Dawley rats. The proteins were radiolabeled to high enough specific radioactivity, that ^{14}C presence was detectable in the stomach, jejunum, duodenum, ileum, blood, liver, kidneys and spleen 480 min after feeding the animals [^{14}C]CD14. The method had a sensitivity of detecting the radioactivity of ^{14}C in an order of magnitude greater than background. The stomach had the highest ^{14}C radioactivity of all organs measured. The accumulation of ^{14}C-label in the organs of [^{14}C]CD14 fed rats, most notably the persistence of ^{14}C in the stomach 480 min post-gavage, is temporally and spatially distinct from [^{14}C]BSA and [^{14}C]casein fed rats.

3-2 Materials and methods

Materials

[^{14}C]Methyl iodide 2 mCi (52.9 mCi/mmol) was purchased from Perkin Elmer (Waltham, USA). Bovine serum albumin (A7906) and bovine milk casein (C7078) as lyophilized proteins were obtained from Sigma-Aldrich (Oakville, Canada), rhCD14 (383CD/CF - MW 35.8 kDa) from R&D Systems (Minneapolis, USA). Hydrogen peroxide 30% w/v (216763) and perchloric acid 70% (244252) were purchased from Sigma-Aldrich. Solvable^{TM} (6NE9100) and Internal Standard Kit ([^{14}C]W Standards) were obtained from Perkin Elmer, ScintiSafe^{TM} Plus 50% LSC-Cocktail (SX25-5) from Fisher Scientific (Ottawa, Canada), methylene blue (3-Q473) from Mallinckrodt Baker (Phillipsburg, USA) and Heparin sodium 1000 USP units/mL from Pharmaceutical Partners of Canada Inc (Richmond Hill, Canada).

^{14}C-Labeling of proteins

A protein solution (BSA or casein at 1 mg/mL and trehalose at 0.01 mg/mL) was adjusted to pH 10.5 with 1 N NaOH to enhance methylation of α- and ε-amino groups. α-Amino groups have pK_a values from 6.8 - 8.0, while ε-amino groups have values ranging from 10.4 - 11.1 [94]. An aliquot (500 µl) containing 500 µg of protein solution was lyophilized in an HP Agilent micro-insert test tube. *In vacuo* methylation with [^{14}C]methyl iodide (52.9 mCi/mmol) was performed according to the procedure described by Taralp and Kaplan [80] with the following modifications. The HP Agilent micro-insert containing lyophilized protein was placed into a larger test tube. A narrow constriction near the upper portion of the larger test tube was formed using a flame. An aliquot of the [^{14}C]methyl

iodide (40 µCi in 50 µl of toluene) was placed within the upper portion of the test tube, while the lower portion was placed within liquid nitrogen, causing the reagent to condense into the lower region of the test tube. The test tube remained submerged in a liquid nitrogen bath, while the test tube was evacuated and sealed under vacuum at 50 mTorr. The sealed tube was incubated at 85°C for 48 hr. Following the incubation, trace quantities of [^{14}C]methanol (a by-product from the reaction with trace amounts of water present) and any unreacted [^{14}C]methyl iodide were removed from the treated protein by liquid nitrogen trapping. After removal of the volatiles, labeled protein was resuspended in 500 µl of a 1% solution of NH_4HCO_3 and incubated at 37°C for 2 hr to hydrolyze methyl esters formed by reaction of the [^{14}C]methyl iodide with carboxylate groups on the protein. The sample was then lyophilized twice to remove any [^{14}C]methanol generated.

The CD14 protein (100 µg in 250 µl of water) was adjusted to pH 10 with 1 N NaOH and lyophilized. The *in vacuo* methylation was performed using the same radiolabeling protocol as with BSA and casein by the addition of 160 µCi [^{14}C]methyl iodide (52.9 mCi/mmol), in 40 µl of toluene as supplied by Perkin Elmer.

Animal model

Studies were conducted in accordance with the University of Ottawa's Animal Care & Veterinary Service, approved by Ottawa Hospital Research Ethics Board, BMI-77. Sprague Dawley rat pups (10 days old) weighing from 19 - 26 g were separated from their mother and placed into an incubator at 37ºC, while being fasted for 2 hr. The pups were returned to their mother and gavage fed either 6.25 µg of [^{14}C]BSA solution in 250 µL

(10 400 dpm/μg), 6.25 μg of [^{14}C]casein solution in 250 μL (10 800 dpm/μg) or 6.25 μg of [^{14}C]CD14 solution in 250 μL (163 000 dpm/μg).

Animals were anaesthetized with isoflurane at 20 min, 240 min and 480 min. Once the rats were nonresponsive, a cardiac puncture was performed to collect blood, followed by harvesting of the stomach, duodenum, jejunum, ileum, large intestine, liver, spleen, kidneys including isolation of small and large intestine luminal contents. The intestines were separated into the duodenum, jejunum, ileum and large intestine defined as 7%, 74%, 2% and 17% of total intestinal length, respectively [81].

Scintillation counting

A pre-weighed sample of homogenized organ tissue was placed into a 20 mL LSC vial and lyophilized. Perkin Elmer Solvable (1 mL) was added to each vial and incubated at 37°C for one week to fully solubilize the sample [95]. A 400 μL aliquot of a solution of 14% perchloric acid and 24% hydrogen peroxide was used to decolorize and further digest the samples [96]. Finally, LSC cocktail (15 mL) was added to each vial and radioactivity (cpm) was quantified by liquid scintillation counting (LKB Model 1214 Rackbeta).

3-3 Results

^{14}C-Labeling of proteins

As outlined in the materials and methods, proteins were radiolabeled with [^{14}C]methyl iodide *in vacuo*. The measured specific radioactivities were 10 400, 10 800 and 163 000 dpm/μg for BSA, casein and CD14, respectively (Table 2). A ten-fold increase in the specific radioactivity was achieved for [^{14}C]CD14 because a larger quantity of [^{14}C]methyl iodide per μg of protein was used. To determine LSC counting efficiency, a

Table 2.
Specific radioactivities (dpm/µg) of [^{14}C]BSA, [^{14}C]casein and [^{14}C]CD14

Sample	Specific Radioactivity (dpm/µg)
[^{14}C]BSA	10 400
[^{14}C]casein	10 800
[^{14}C]CD14	163 000

Five µL of the sample solutions (25 µg/mL) was dissolved using Solvable^{TM}, discolored using perchloric acid 70%: hydrogen peroxide 30% (1:4) followed by the addition of liquid scintillation cocktail. Counts were measured using a β counter (LKB Model 1214 Rackbeta Liquid Scintillation counter).

^{14}C-internal standard (100 300 dpm) was added into different organ samples covering a range of spectral quench parameter of the isotope (SQPI) values. The counting efficiency curve was fitted by nonlinear regression using GraphPad Prism version 5.03 for Windows (San Diego, USA). The following relationship was determined for calculating counting efficiency (Figure 7):

$y = \frac{9661x}{7332 + x} - 1.153x + 47.11$, where y = efficiency and x = SQPI

The efficiency calculated was used to convert counts per minute (cpm) to disintegrations per minute (dpm) for all organs measured (dpm = cpm/efficiency). It should be noted that the ^{14}C standards were shipped with a radioactivity of 100 300 dpm, however, considering radioisotope decay, a value of 100 296 dpm was used for calculations.

Pharmacokinetic studies using radiolabeled ^{14}C proteins

The *in vacuo* labeling method produced proteins of a sufficiently high specific radioactivity to quantify the ^{14}C-label in the organs of experimental animals fed radiolabeled proteins (Figure 8). At 480 min post-gavage the ^{14}C-radiolabel was detected in accessory organs such as blood, liver, kidney and spleen with a threshold of detection an order of magnitude or greater above background (Table 3). The method described demonstrated that concentrations of ^{14}C-label as high as 383 000 dpm/g were detectable. Other figures for [^{14}C]BSA, [^{14}C]casein and [^{14}C]CD14 at 20 min, 240 min and 480 min post-gavage are presented in Appendix C.

Following gavage feeding, the stomach was the initial reservoir for ^{14}C-label (Figure 9). As such, the stomach had the highest representative ^{14}C-concentration of all organs measured. [^{14}C]BSA and [^{14}C]casein followed a similar trend of decreasing ^{14}C counts over

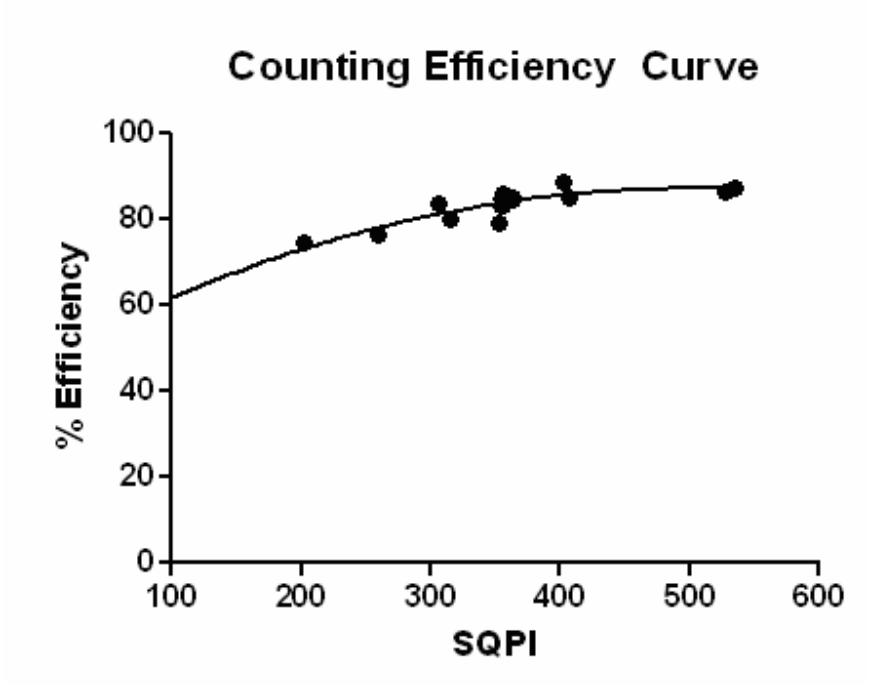

Figure 7. Counting efficiency curve for liquid scintillation counting
Random samples were selected over a range of (SQPI) values. Liquid scintillation counting of these samples occurred prior to and after the addition of a known ^{14}C standard (100 300 dpm). The percent efficiency was calculated [$(cpm_{added\ standard} - cpm_{original})/dpm_{standard}$] and was plotted against the original SQPI values to form an efficiency curve. A best fit line was plotted and the equation (y = efficiency and x = SQPI) was used to convert cpm to dpm in the remaining samples (dpm = cpm/efficiency). n = 19

$$y = \frac{9661x}{7332 + x} - 1.153x + 47.11$$

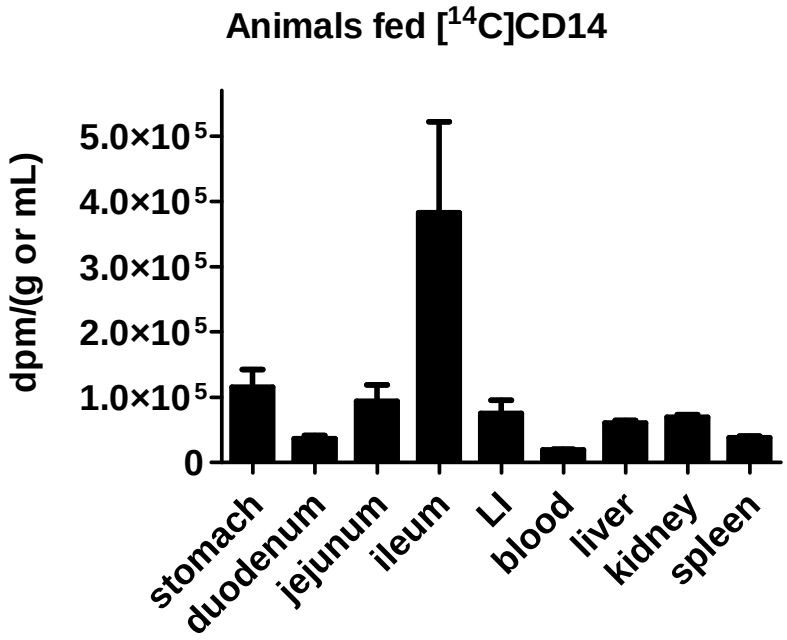

Figure 8. Representative graph of rats fed [^{14}C]CD14 and euthanized 480 min post-gavage

[^{14}C]CD14 (163 000 dpm/μg) was fed to 10 day old Sprague Dawley rats and they were sacrificed at 480 min. The stomach, duodenum, jejunum, ileum, large intestine (LI), blood, liver, kidneys and spleen were harvested and dissolved using Solvable. Solutions were decolorized using hydrogen peroxide and perchloric acid and subsequently mixed with liquid scintillation cocktail. Data were reported as dpm/(g or mL) and was expressed as mean ± SEM with an n = 2 - 4.

Table 3. Detectability of ^{14}C in Sprague Dawley rats 480 min post-gavage with [^{14}C]CD14 (1 020 000 dpm)

Organ	dpm/(g or mL)[a]	Fold over background[b]
Stomach	116 000	3270
Duodenum	37 000	55
Jejunum	93 900	8
Ileum	383 000	182
Large intestine	75 300	72
Blood	19 300	374
Liver	60 400	99
Kidney	69 700	28
Spleen	38 000	11

[a]Values are expressed as mean. Blood is the only value expressed as dpm/mL
[b]Background was an unfed control rat

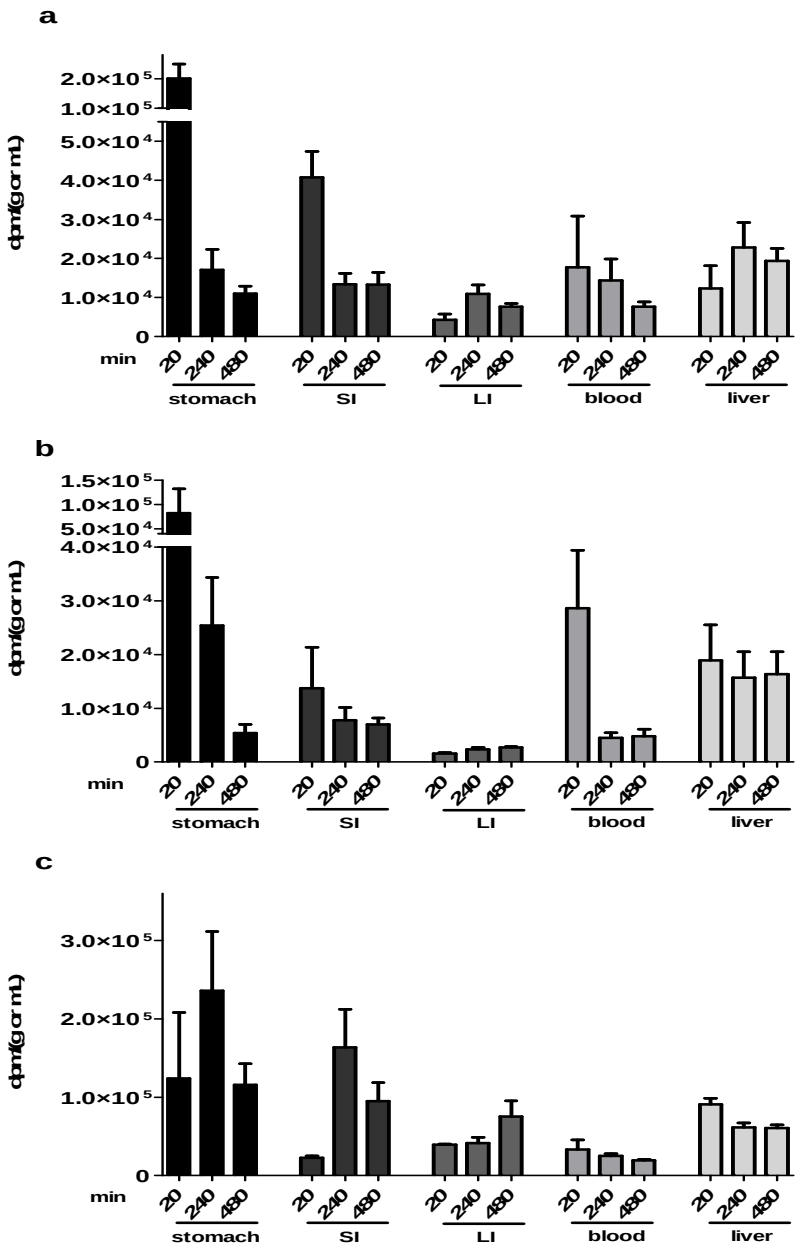

Figure 9. Distribution of ^{14}C in the organs of rats fed [^{14}C]BSA, [^{14}C]casein or [^{14}C]CD14

[^{14}C]BSA (10 400 dpm/µg), [^{14}C]casein (10 800 dpm/µg) or [^{14}C]CD14 (163 000 dpm/µg) were fed to 10 day old Sprague Dawley rats. They were euthanized at either 20, 240 or 480 min. The stomach, small intestine (SI), large intestine (LI), blood and liver were harvested and dissolved using Solvable^{TM}. Organs were decolorized using hydrogen peroxide and perchloric acid and subsequently mixed with a liquid scintillation cocktail. Data were reported as dpm/g and in the case of blood was reported as dpm/mL. Values were expressed as mean ± SEM with an n = 2 - 6.

time, consistent with normal stomach emptying. However, [^{14}C]CD14 did not follow this trend. Specifically, ^{14}C-concentrations nearly doubled in the stomach from 124 000 dpm/g at 20 min to 236 000 dpm/g by 240 min.

[^{14}C]BSA and [^{14}C]casein were detectable in the small intestine within 20 min and reached a steady state ^{14}C-concentration by 240 min (Figure 9 a,b). However, [^{14}C]CD14 entered the small intestine at a slower rate with a maximal accumulation of 164 000 dpm/g at 240 min (Figure 9 c). ^{14}C-label from BSA and casein fed animals was minimal in the large intestine. In rats fed [^{14}C]CD14, the increased ^{14}C-concentration in the large intestine after 480 min was consistent with decreased signal in the small intestine. Conversely, with [^{14}C]BSA and [^{14}C]casein, the radiolabel reached a steady state by 240 min in the small intestine with a further decrease in the large intestine suggesting that much of this label migrated elsewhere and did not reach the large intestine.

The luminal contents of the small intestine were also flushed out and collected for measurement of radiolabel content. [^{14}C]BSA and [^{14}C]casein followed a similar decreasing percent dose trend in the small intestinal lumen over time (Figure 10). The large intestinal lumen accumulated radiolabel at 480 min. Those animals fed [^{14}C]CD14 retained the radiolabel in the small and large intestinal lumens at 240 min. The signal in [^{14}C]CD14 fed rats indicated a percent dose in the lumen of the small intestine lower than that observed for [^{14}C]BSA and [^{14}C]casein fed rats. [^{14}C]CD14 also demonstrated a distinct trend of increasing percent dose in the small intestinal lumen over time, in comparison with [^{14}C]BSA and [^{14}C]casein which showed a decreasing percent dose.

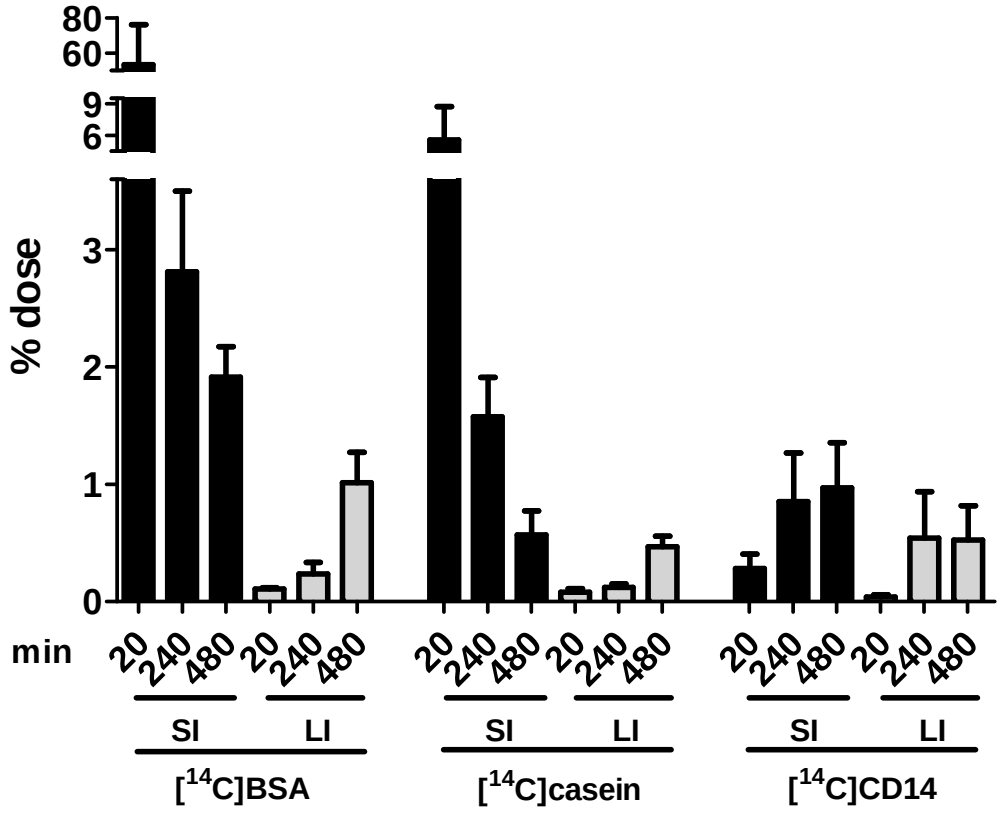

Figure 10. Distribution of percent dose fed in the intestinal lumen of rats fed [^{14}C]BSA, [^{14}C]casein or [^{14}C]CD14

[^{14}C]BSA (10 400 dpm/µg), [^{14}C]casein (10 800 dpm/µg) or [^{14}C]CD14 (163 000 dpm/µg) were fed to 10 day old Sprague Dawley rats. They were euthanized at either 20, 240 or 480 min. The small intestine (SI) and large intestine (LI) lumens were flushed using cold PBS. The intestinal contents were dissolved using Solvable, decolorized using hydrogen peroxide and perchloric acid and subsequently mixed with a liquid scintillation cocktail. Data were reported as the percentage of dose fed ((dpm_{sample} / dpm_{dose}) x 100%) and were expressed as mean ± SEM with an n = 2 - 6.

The ^{14}C-label for all fed proteins was rapidly detectable in the blood indicating direct absorption from the small intestine. In blood, the radiolabel was detectable at 20 min post-gavage followed by a decrease at 240 and 480 min. This suggests some level of transport to accessory digestive organs which may have diluted the available pool of ^{14}C in the blood. The ^{14}C-concentration from [^{14}C]CD14 fed rats in the blood was ten-fold lower in comparison to that observed for [^{14}C]BSA and [^{14}C]casein fed rats and suggests retention within the GI tract.

3-4 Discussion

^{14}C-Labeling of proteins

The results obtained demonstrate that proteins can be labeled with [^{14}C]methyl iodide by *in vacuo* methylation to a sufficiently high specific radioactivity for the quantification of the biodistribution of ^{14}C-label in organs after oral administration. Furthermore, the radiolabeled protein can be utilized for ADME studies requiring low-microgram quantities of protein fed to rat pups. Reaction of protein with [^{14}C]methyl iodide introduces covalent linkage of one to three $^{14}CH_3$ labels on the amino groups of the side-chain of lysine residues and the amino terminus, and one to two $^{14}CH_3$ labels on the imidazole side-chain of histidine residues [97]. Methyl iodide also reacts with carboxyl groups from aspartic and glutamic acid residues to form methyl esters. Unlike methylamino and methylimidazole groups, methyl esters are labile under alkaline conditions and would therefore be labile in the intestinal tract of animals. For this reason, the labeled protein was incubated at alkaline pH to hydrolyse the methyl esters and then lyophilized to remove [^{14}C]methanol.

The ^{14}C specific activity that can be achieved in labeling a pure protein by *in vacuo* methylation depends primarily on the specific radioactivity of the [^{14}C]methyl iodide reagent, the amount of reagent used and the number of lysine and histidine residues in the protein [80]. At the time of the protein ^{14}C-labeling, the specific radioactivity sufficient for ADME studies in rat pups was not known. As recombinant CD14 (rCD14) is an expensive protein to produce and BSA and casein are relatively inexpensive proteins, CD14 was labeled with a twenty-fold greater amount of [^{14}C]methyl iodide than that used for the labeling of BSA and casein. This was to ensure maximal incorporation of the label without having to rely on a second labeling reaction and without the use of additional protein. The specific activities obtained for the labeling of BSA and casein were 10 400 and 10 800 dpm/μg, respectively and this level was found to be adequate for quantification of ^{14}C in the organs of fed rats. In the case of CD14, the specific radioactivity achieved was more than an order of magnitude greater, namely, 163 000 dpm/μg. The results demonstrate that such a high level of specific radioactivity was not necessary. The CD14 could have been labeled to one-fifth of the specific radioactivity achieved in this study. Such a level would have been more than sufficient for the quantification of the ^{14}C distributed in the various organs.

A significant advantage of *in vacuo* labeling over aqueous-based labeling methodologies is that a high specific radioactivity can be achieved at a very low cost. The reason for the low cost was that there was no loss of ^{14}C label due to reaction with water and the vast majority of the label in the [^{14}C]methyl iodide was incorporated into the protein of interest. In the present study, the cost of the [^{14}C]methyl iodide used was $750 US/mCi. For the labeling of 100 μg of CD14 with 160 μCi of [^{14}C]methyl iodide, the cost was $1.20 US/μg

($17/μCi of labeled protein) and for the labeling of the 200 μg of BSA and casein, the cost was $0.06 US/μg ($13/μCi of labeled protein). The cost in the present study was under $20 US/μCi, where typically commercially produced ^{14}C-radiolabeled proteins are available at $200 - $300 US/μCi (e.g. Sigma-Aldrich albumin, ^{14}C methylated A4844-1UCI). It is possible that these costs could be further reduced by bulk purchase of the [^{14}C]methyl iodide.

Another significant advantage was that, unlike aqueous labeling procedures, the *in vacuo* ^{14}C-labeling of microgram quantities of protein can be performed just as efficiently as with large amounts of proteins. The reason was that the labeling was performed with lyophilized protein and the amount of label incorporated per unit of protein was therefore independent of the amount of protein present. This is especially important in cases where only small amounts of high cost protein are available, as in the case of CD14 used in this study.

Pharmacokinetic studies using radiolabeled ^{14}C proteins

The results obtained in this thesis are in good agreement with previous studies investigating the digestibility of BSA and casein. For example, after 10 min of *in vitro* incubation of BSA with either trypsin or chymotrypsin, intact native protein including proteolytic fragments were detectable [98]. However, 120 min after oral administration of BSA to mice, the protein was completely digested upon entry to the small intestine [98]. In the case of casein, it has been observed to be completely digested and yielding its greatest amino acid absorption in the ileum [99]. It is also known that native casein is completely degraded by the time it reaches the feces in rats [100] and is readily degraded by duodenal juices in infants [101, 102]. Also, rates of digestion were noted to be similar between

reductively methylated [^{14}C]casein and [^{14}C]BSA in comparison with their native forms [103]. This demonstrates that methylation does not significantly alter the digestive fate of these proteins.

The present results show similar ^{14}C-label accumulation in the organs for rats fed [^{14}C]BSA or [^{14}C]casein. For instance, in the stomach, ^{14}C was present at its highest concentration at 20 min for all fed proteins and decreased throughout the course of the experiment. This was consistent with normal gastrointestinal digestion. Furthermore, as these proteins move along the GI tract, they undergo further digestion by intestinal proteases and subsequent uptake by the intestinal microvilli. Even though this method only allows ^{14}C-label detection, the behavior of the signal reflects typical protein digestion. For example, 4 hr after human patients ingested BSA, small peptides and amino acids were recovered in their jejunum and ileum lumens [104]. In this current study, the signal observed in the luminal flushes of the small and large intestine corresponded to the values measured in the intestinal organs. Together, these data suggest ^{14}C-label was migrating from the lumen into the intestinal wall and subsequently into the blood and liver.

In contrast, the [^{14}C]CD14 fed rats showed a differing biodistribution of the ^{14}C-label amongst the organs from that of [^{14}C]BSA and [^{14}C]casein fed rats. Most notably, the ^{14}C-label did not accumulate to the same extent as that of [^{14}C]BSA and [^{14}C]casein in the large intestine lumen, which suggests CD14 transport or degradation. The ^{14}C signal persisted in the stomach and small intestine for up to 480 min post-gavage. If [^{14}C]CD14 was being readily degraded, the peptides and amino acid breakdown products would be rapidly translocated to the blood and other organs. The persistence of the ^{14}C-label

suggested the full length protein was being protected from degradation and further experimentation to determine the digestive fate of this protein is needed.

Chapter 4

Stimulation of human blood $CD14^+$ monocytes

4-1 Summary

$CD14^+$ monocytes were isolated from human peripheral blood mononuclear cells (PBMC). This subset of cells (10^5 cells/well) was either left untreated, stimulated with LPS (1 ng/mL), treated with rCD14 (15 µg/mL), preincubated with rCD14 (15 µg/mL) for 1 hr and subsequently stimulated with LPS (1 ng/mL) or treated with rCD14 (15 µg/mL). Protein production levels (pg/mL) and mRNA expression levels of the following cytokines were measured: TNF-α, IL-6, IL-8, IL-10 and IL-1β. The production of TNF-α, IL-6, IL-8 and IL-1β was highest when $CD14^+$ monocytes were stimulated with LPS alone. Monocytes stimulated with LPS and those challenged with rCD14 plus LPS showed a statistically significant difference ($p<0.05$) in TNF-α and IL-1β levels. For TNF-α, these results were confirmed using quantitative RT-PCR. A significant decrease in mRNA expression levels was observed with IL-6, IL-8 and IL-10 when LPS-challenged $CD14^+$ monocytes were preincubated with rCD14. The results demonstrate that an exogenous source of sCD14 may lessen the severity of cytokine production for TNF-α and IL-1β in response to LPS stimulation, suggesting that sCD14 may protect humans from excessive inflammation, thereby moderating adverse clinical symptoms such as sepsis.

4-2 Materials and methods

Reagents

Recombinant human CD14 (383-CD/CF) was obtained from R&D Systems and maintained in sterile magnesium-free D-PBS(-) (045-29795) from Wako Pure Chemical Industries Ltd (Osaka Japan) and 0.1% BSA (A9576) from Sigma-Aldrich Japan K.K. (Tokyo, Japan). LPS was isolated from *E. coli* 0111:B4 from Sigma-Aldrich. 2-Mercaptoethanol (135-07522) was obtained from WAKO and RPMI-1640 medium (R8758) was purchased from Sigma-Aldrich. HEPES (GIBCO 1M 15630) and PenStrep (GIBCO 15140; 10 000 units/mL penicillin, 10 000 µg/mL streptomycin) were purchased from Invitrogen (Tokyo, Japan). Fetal Bovine Serum (95300106) was from Moregate Biotech (Bulimba, Australia) RLT Lysis Buffer from Qiagen K.K. (Tokyo, Japan) and Lymphoprep (PoCAS 12B1S03) from Axis-Shield (Dundee, Scotland).

Peripheral blood mononuclear cell isolation

Blood samples were obtained from human subjects and experiments were approved by the institutional review board of Keio University School of Medicine. Approximately 30 mL of blood was diluted with D-PBS(-) and layered on Lymphoprep (Axis-Shield) before centrifuging at 200 revolutions per minute (rpm) for 20 min at room temperature. Viable peripheral blood mononuclear cells (PBMC) were recovered from the interface layer and diluted in MACS buffer (D-PBS(-), 0.5% BSA, 2mM EDTA).

$CD14^+$ monocyte isolation

A population of monocytes expressing CD14 was recovered from PBMC using MACS Cell Separation (Miltenyi Biotec) according to the manufacturer's instructions.

LPS and CD14 stimulation

$CD14^+$ monocytes were cultured in 96-well round-bottom tissue culture plates ($1x10^5$ cells/well) in RPMI 1640 medium (containing 10% fetal bovine serum, 100 units/mL PenStrep), 10 mM HEPES and 50 μM 2-mercaptoethanol. The cells were stimulated with either 1 ng/mL LPS, 15 μg/mL rCD14 or 15 μg/mL of rCD14 (preincubated for 1 hr) followed by 1 ng/mL LPS stimulation. Cells were incubated at 37ºC and 5% CO_2 for 6 hr. Cells were harvested for RNA isolation and culture supernatants were obtained and stored at -80ºC.

Cytokine bead assay

The human inflammatory cytokine bead array (CBA) kit by BD Biosciences (551811) was used to determine TNF-α, IL-6, IL-8, IL-10 and IL-1β concentrations. The analysis was performed according to manufacturer's protocol. Data was collected using FACSCalibur (Becton Dickinson Biosciences, FACStation version 2.0.1) with CellQuest software (BD Biosciences). Analysis was performed using GraphPad Prism.

RT-PCR

After six hours of stimulation, cells were lysed using RNA lysis buffer (containing 1% β-mercaptoethanol). RNA was extracted using RNeasy Micro kit (by Qiagen K.K.) and cDNA was synthesized using Quantitect RTkit (Qiagen K.K.). TaqMan Gene Expression Assay (Applied Biosystems) performed quantitative real-time polymerase chain reaction (RT-PCR) and was assessed using the DNA Engine Opticon 2 System (Bio-Rad), and analyzed with Opticon monitor software (MJ Research). The primers used were IL-6 (Hs00174131) IL-8 (Hs99999034), TNF-α (Hs00174128), IL-1β (Hs00155517),

β-actin (Hs99999903) (Applied Biosystems). RT-PCR results were normalized against β-actin control.

Statistical analysis

Student t-test was performed on cytokine and mRNA expression levels data and a difference of (p<0.05) was considered significant.

4-3 Results

Untreated $CD14^+$ monocytes (10^5 cells/well) isolated from PBMCs synthesized trace quantities of the measured cytokines (TNF-α, IL-6, IL-8, IL-1β, IL-10). Cytokine production of TNF-α, IL-6, IL-8 and IL-1β, is reported in Figure 11. The largest cytokine production quantities were observed when $CD14^+$ monocytes were stimulated with LPS (1 ng/mL). $CD14^+$ monocytes stimulated with LPS, those with rCD14 plus LPS and those with rCD14 alone, demonstrated a statistical difference amongst the groups (p<0.05) in TNF-α and IL-1β production. Whereas, IL-6 and IL-8 demonstrated a statistical increase in its production between $CD14^+$ monocytes challenged with LPS compared with rCD14 and those with rCD14 plus LPS and rCD14. Also, the production of IL-10 by $CD14^+$ monocytes showed a different trend when compared to the other measured cytokines. IL-10 production was highest in monocytes incubated with rCD14 plus LPS, which is a different observation compared to the other cytokines measured.

The basal mRNA for cytokines (TNF-α, IL-6, IL-8 or IL-10) are shown in Figure 12. The results were normalized to β-actin levels (in arbitrary units). mRNA levels for all cytokines were highest when $CD14^+$ monocytes were challenged with LPS (1 ng/mL). There

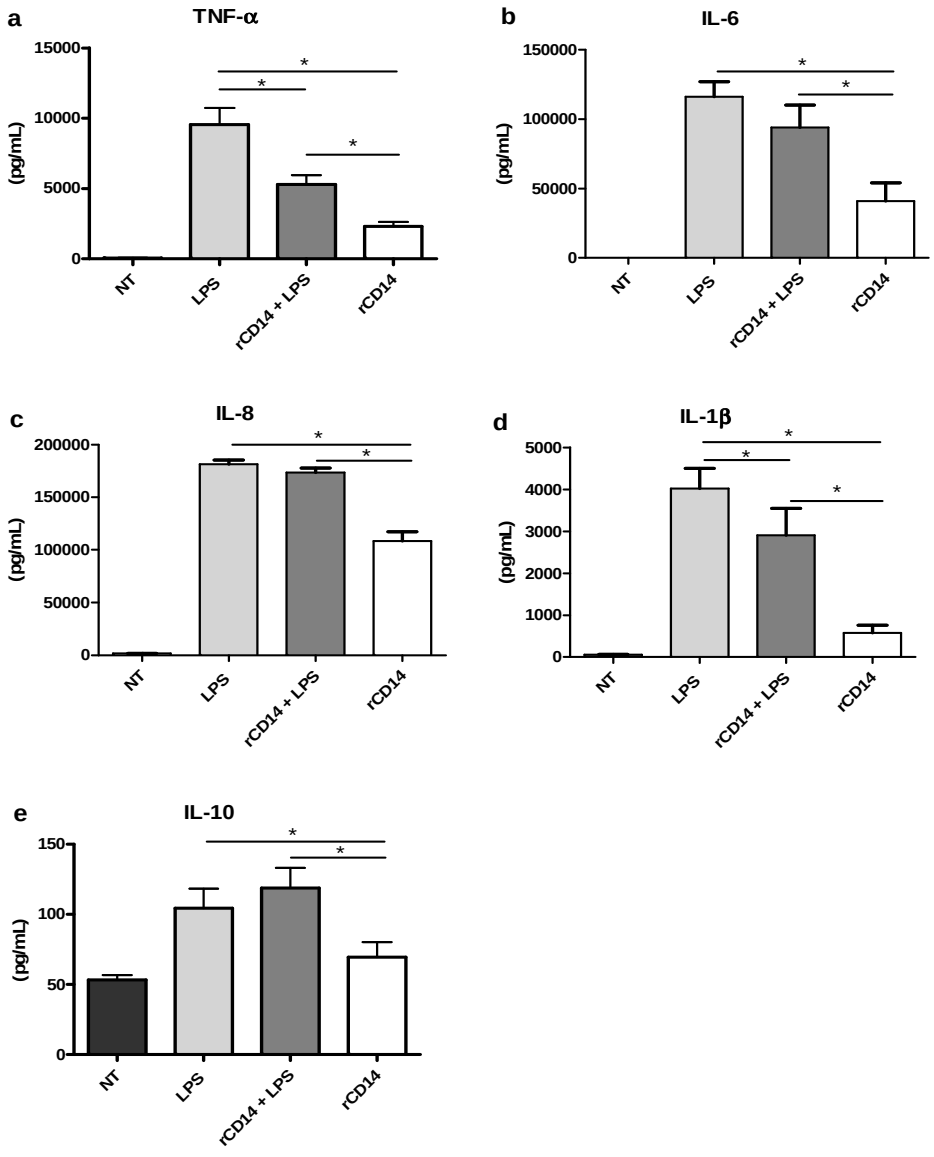

Figure 11. Influence of recombinant CD14 on cytokine production by LPS-stimulated $CD14^+$ monocytes

$CD14^+$ monocytes (10^5 cells/well) were: left untreated (NT), or stimulated with LPS (1 ng/mL) (LPS), or preincubated with rCD14 (15 µg/mL) for 1 hr and subsequently stimulated with LPS (1 ng/mL) (rCD14 + LPS), or treated with rCD14 (15 µg/mL) alone (rCD14).

All cells were treated for 6 hr at 37°C and 5% CO_2. Supernatants were collected and cells were treated with RNA Lysis Buffer and 1% 2-mercaptoethanol. A cytokine bead assay was performed to detect cytokine production of a) TNF-α, b) IL-6, c) IL-8, d) IL-1β, e) IL-10. Data were expressed as mean ± SEM from at least three independent experiments.

* $p<0.05$ was considered statistically significant.

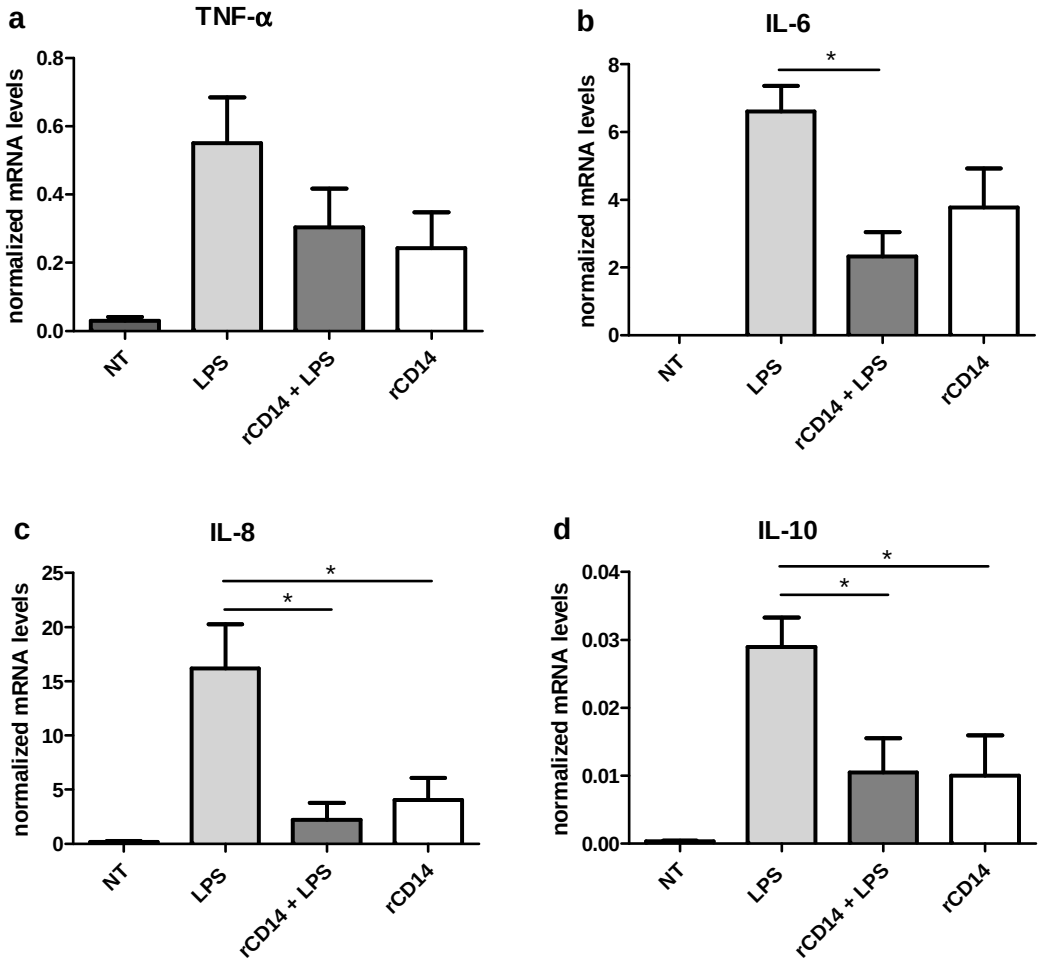

Figure 12. Quantitative RT-PCR of cytokine mRNA expression levels in isolated $CD14^+$ monocytes

TNF-α, IL-6, IL-8 or IL-10 mRNA levels were normalized to β-actin levels (in arbitrary units). $CD14^+$ monocytes (10^5 cells) were left untreated, stimulated with LPS (1 ng/mL), preincubated with rCD14 (15 µg/mL) for 1 hr and subsequently stimulated with LPS (1 ng/mL) or treated with rCD14 (15 µg/mL). Data expressed as mean ± SEM from at least three independent experiments.

* $p<0.05$ was considered statistically significant.

was a statistical decrease (p<0.05) in the mRNA expression levels of IL-6, IL-8 and IL-10 between $CD14^+$ monocytes stimulated with LPS and those cells preincubated with rCD14 (15 µg/mL) for 1 hr and subsequently incubated with LPS (1 ng/mL).

4-4 Discussion

The protective nature of exogenous sCD14 has been demonstrated in previous mouse [105, 106] and bovine [36] studies. It has been documented that overstimulation of TLRs by LPS may lead to uncontrolled inflammation, edema, systemic organ dysfunction and sepsis [107, 108]. To the author's knowledge, the present investigation is the first to show the behaviour of recombinant CD14 in human mononuclear cells. The objective of this study was to determine if rCD14 has any influence on the cytokine production of LPS stimulated PBMCs.

The results of the study showed a decrease (p<0.05) in cytokine production (TNF-α and IL-1β) when $CD14^+$ monocytes were pretreated with rCD14 prior to LPS stimulation in comparison with those challenged with only LPS. A similar trend was observed in the cytokine production of IL-6 and IL-8, however, the results were not statistically significant. A significant decrease was observed in the mRNA expression levels of IL-6, IL-8 and IL-10, when LPS-challenged $CD14^+$ monocytes were preincubated with rCD14. These results suggest that an exogenous source of sCD14 may regulate the downstream cytokine production when monocytes are challenged with LPS (Figure 1). The mRNA expression levels are consistent with the protein production levels of the cytokines examined with regards to LPS and LPS plus CD14 stimulation. The mechanism for this observation is still unknown, however, rCD14 may bind or outcompete with mCD14 expressed on the surface

of the monocytes [108], thereby reducing the interaction of LPS with the TLRs. Another possibility involves rCD14 itself binding to and rendering the LPS inactive. Although the mechanisms are unknown, it was observed in this study that $CD14^+$ monocytes that were not preincubated with rCD14 and instead challenged with a preformulated mixture of rCD14 and LPS, did not show a protective nature with regards to a decrease in cytokine production (data was not shown because $n = 1$). Therefore, rCD14 may interact with monocytes before LPS stimulation to produce a reduction in inflammation.

It was observed that rCD14 alone was able to induce cytokine production and mRNA expression levels. These were unexpected results, for which one possible explanation may include trace LPS contamination. In a similar study where an astrocytoma cell line U373 was stimulated with lower concentrations, 0.2 – 2 µg/mL of sCD14, it was observed that there was minimal IL-6 production [59]. In the present study, such potential trace LPS contamination was not observed in the no treatment group (NT in Figure 11, 12). Therefore, future studies should include a control for the CD14 solution containing PBS and the 'carrier', BSA. There is the possibility that a contamination occurred while preparing the CD14 solution in sterile magnesium-free D-PBS(-) with 0.1% BSA.

Previous investigations have examined the pathological and immunological impact of a recombinant source of CD14 when cell cultures or animals are subjected to an *E. coli* or LPS challenge. In *Bos taurus*, it has been observed that udders injected with recombinant bovine CD14 (rbosCD14) and stimulated with *E. coli* had reduced clinical symptoms, such as mammary swelling [105]. The cows also had a faster recruitment of neutrophils and lower TNF-α and IL-8 concentrations, in comparison with udders challenged with *E. coli* alone. *In vitro* experiments have shown that neutrophils release sCD14 in response to an LPS

challenge in a dose-dependent manner [36]. After an LPS challenge, it was also seen that sCD14 concentrations in bovine milk increased. The release of CD14 from bovine polymorphonuclear neutrophil leukocytes (PMN) is known to suppress secretion of IL-8 [109]. CD14's ability to reduce clinical inflammation was further observed in a mouse model where mice that were injected with either LPS or LPS plus rbosCD14 and had survival rates of 30% and 72%, respectively [106].

It is known that CD14 interacts with LPS, as well as LBP as seen in Figure 1. The quantities of LBP available in the culture media in this investigation were unknown. It has been shown that low concentrations of LBP can enhance the response of LPS bioactivity, while high concentrations of LBP can inhibit its activity which has been displayed *in vitro* and *in vivo* [31]. However, based on the results, it can be inferred that an exogenous source of sCD14 may be capable of reducing the production of proinflammatory cytokines when cells are challenged with a Gram negative infection. This is a beneficial observation, as excessive inflammatory response has adverse effects on the host, such as septic shock.

Chapter 5

Conclusions and future research

CD14 plays a key role in the innate immune system by recognizing PAMPs on the surface of invading microorganisms. Since it was found in high concentrations in human milk in comparison with serum, it has been suggested to aid in the innate immune system of breast feeding infants. However, in breast fed infants their urine and feces contained trace quantities of CD14, which renders an unknown fate within the digestive system.

The work in this thesis presents a newborn animal model to study fate and distribution of enterically administered proteins. The gastrointestinal transit time of 10 day old Sprague Dawley rats was determined and it was observed that pups that remained with their mothers throughout the course of the experiment, showed less signs of stress. Although previous literature describes the separation of rat pups from their mother's under similar experimental conditions, it was decided that the pup would show more natural gastrointestinal transit when they remain with their mothers.

The second focus of this thesis was to present a neonate model using rats to address the ongoing efforts of understanding CD14's fate upon ingestion. Firstly, a method described by Taralp and Kaplan [80] to radiolabel proteins *in vacuo* with [^{14}C]methyl iodide was utilized. BSA and casein were used as test proteins to investigate whether the proteins could be labeled to sufficiently high specific radioactivities to be used as tracers in the GI tract of

neonate rats upon consumption. Once it was determined that the methodology was effective at radiolabeling proteins to sufficiently high specific radioactivities, CD14 was labeled.

The third objective was to trace oro-gastric gavaged [^{14}C]CD14 through the gastrointestinal tract of neonate rats. It was observed that ^{14}C originating from [^{14}C]CD14 had different distribution patterns than those coming from fed [^{14}C]BSA and [^{14}C]casein. The integrity of CD14 as a protein or its recalcitrance to proteolysis was not determined in this thesis. The proteolytic digestion of CD14 could be investigated by various methods. The organs of rats fed [^{14}C]CD14 can be homogenized and the protein content can be isolated. The protein profile can be determined by sodium dodecyl sulfate (SDS) polyacrylamide gel electrophoresis. The radioactive ^{14}C can be identified by phosphorimaging. Another method to determine the rate of protein proteolysis in the organs is to separate full-length proteins from peptides and free amino acids using separation columns or filters. The eluted contents can be readily measured by liquid scintillation counting. Once the various CD14 peptides are obtained from the gastrointestinal lumen, intestinal epithelial cell (IEC) cultures can be used to determine binding efficiency to LPS, TLR4 and MD-2. IECs can also be used to examine if CD14 peptides can penetrate the intestinal barrier before being recognized by the immune system [110]. This will help to understand if gastrointestinal proteolysis affects innate immunity function.

The fourth objective explored the relationship between sCD14 and inflammatory response. It was investigated whether exogenous sCD14 (such as that found in human milk) could down-regulate the proinflammatory cytokine production in the GI tract. CD14^{+}

monocytes isolated from PBMC were used to probe this question *in vitro*. It was concluded that LPS-challenged $CD14^+$ monocytes that were pretreated with rCD14 had a reduced production in proinflammatory cytokines, TNF-α and IL-1β, and lowered mRNA expression levels with IL-6, IL-8 and IL-10. These results suggest that sCD14 may protect humans from excessive inflammation, which is known to have adverse clinical symptoms such as sepsis. The mechanism for this protective effect is still unknown, however, it can be speculated that rCD14 may bind or outcompete with mCD14 expressed on the surface of the monocytes [108], thereby reducing the interaction of LPS with the TLRs. These mechanisms can be further investigated by determining a dose-dependent relationship between rCD14 and LPS. Further cell culture work may also be employed in IECs by observing the influence of limiting the presence of MD-2 and LBP.

Modern gastroenterology, while challenged with severe chronic diseases such as IBD, still needs to progress in determining mechanisms of healthy gut function. It is in the author's hope that this thesis will contribute to these goals by providing insight into using better model animal studies and more refined and sensitive tracers for evaluating gut function.

References

[1] Brandtzaeg, P. 'ABC' of mucosal immunology. Nestlé Nutrition workshop series.Paediatric programme. 2009, 64.

[2] Takeuchi, K., Suzuki, S., Yagawa, M., Yuta, A., Majima, Y. A CD14 gene polymorphism is associated with the IgE level for dermatophagoides pteronyssinus. Acta Otolaryngol. 2005, 125:966-71.

[3] Dziarski, R. Recognition of bacterial peptidoglycan by the innate immune system. Cell Mol Life Sci. 2003, 60:1793-804.

[4] Gregory, C. D., Devitt, A. CD14 and apoptosis. Apoptosis. 1999, 4:11-20.

[5] Fitzgerald, K. A., Rowe, D. C., Golenbock, D. T. Endotoxin recognition and signal transduction by the TLR4/MD-2 complex. Microb Infect. 2004, 6:1361-7.

[6] Yu, B., Hailman, E., Wright, S. D. Lipopolysaccharide binding protein and soluble CD14 catalyze exchange of phospholipids. J Clin Invest. 1997, 99:315-24.

[7] Wang, P. Y., Kitchens, R. L., Munford, R. S. Phosphatidylinositides bind to plasma membrane CD14 and can prevent monocyte activation by bacterial lipopolysaccharide. J Biol Chem. 1998, 273:24309-13.

[8] Sugiyama, T., Wright, S. D. Soluble CD14 mediates efflux of phospholipids from cells. J Immunol. 2001, 166:826-31.

[9] Haziot, A., Chen, S., Ferrero, E., Low, M. G., Silber, R., Goyert, S. M. The monocyte differentiation antigen, CD14, is anchored to the cell membrane by a phosphatidylinositol linkage. J Immunol. 1988, 141:547-52.

[10] Setoguchi, M., Higuchi, Y., Yoshida, S., Nasu, N., Miyazaki, Y., Akizuki, S., Yamamoto, S. Insertional activation of N-myc by endogenous moloney-like murine retrovirus sequences in macrophage cell-lines derived from myeloma cell line-macrophage hybrids. Mol Cell Biol. 1989, 9:4515-22.

[11] Wright, S. D., Ramos, R. A., Tobias, P. S., Ulevitch, R. J., Mathison, J. C. CD14, a receptor for complexes of lipopolysaccharide (LPS) and LPS binding protein. Science. 1990, 249:1431-3.

[12] Ball, E. D., Graziano, R. F., Shen, L., Fanger, M. W. Monoclonal-antibodies to novel myeloid antigens reveal human neutrophil heterogeneity. P Natl Acad Sci -Biol. 1982, 79:5374-8.

[13] Ulevitch, R. J., Tobias, P. S. Receptor-dependent mechanisms of cell stimulation by bacterial-endotoxin. Annu Rev Immunol. 1995, 13:437-57.

[14] Hoshino, K., Takeuchi, O., Kawai, T., Sanjo, H., Ogawa, T., Takeda, Y., Takeda, K., Akira, S. Cutting edge: Toll-like receptor 4 (TLR4)-deficient mice are hyporesponsive to lipopolysaccharide: Evidence for TLR4 as the Lps gene product. J Immunol. 1999, 162:3749-52.

[15] Qureshi, S. T., Lariviere, L., Leveque, G., Clermont, S., Moore, K. J., Gros, P., Malo, D. Endotoxin-tolerant mice have mutations in toll-like receptor 4 (TLR4). J Exp Med. 1999, 189:615-25.

[16] Poltorak, A., He, X. L., Smirnova, I., Liu, M. Y., Van Huffel, C., Du, X., Birdwell, D., Alejos, E., Silva, M., Galanos, C., Freudenberg, M., Ricciardi-Castagnoli, P., Layton, B., Beutler, B. Defective LPS signaling in C3H/HeJ and C57BL/10ScCr mice: Mutations in Tlr4 gene. Science. 1998, 282:2085-8.

[17] Schumann, R. R., Leong, S. R., Flaggs, G. W., Gray, P. W., Wright, S. D., Mathison, J. C., Tobias, P. S., Ulevitch, R. J. Structure and function of lipopolysaccharide binding-protein. Science. 1990, 249:1429-31.

[18] Fujihara, M., Muroi, M., Tanamoto, K., Suzuki, T., Azuma, H., Ikeda, H. Molecular mechanisms of macrophage activation and deactivation by lipopolysaccharide: Roles of the receptor complex. Pharmacol Ther. 2003, 100:171-94.

[19] Miyake, K. Innate recognition of lipopolysaccharide by CD14 and toll-like receptor 4-MD-2: Unique roles for MD-2. Int Immunopharmacol. 2003, 3:119-28.

[20] Devitt, A., Parker, K. G., Ogden, C. A., Oldreive, C., Clay, M. F., Melville, L. A., Bellamy, C. O., Lacy-Hulbert, A., Gangloff, S. C., Goyert, S. M., Gregory, C. D. Persistence of apoptotic cells without autoimmune disease or inflammation in CD14-/- mice. J Cell Biol. 2004, 167:1161-70.

[21] Finlay, B. B., Hancock, R. E. W. Can innate immunity be enhanced to treat microbial infections? Nat Rev Microbiol. 2004, 2:497-504.

[22] Michie, H. R., Manogue, K. R., Spriggs, D. R., Revhaug, A., Odwyer, S., Dinarello, C. A., Cerami, A., Wolff, S. M., Wilmore, D. W. Detection of circulating tumor necrosis factor after endotoxin administration. N Engl J Med. 1988, 318:1481-6.

[23] Lee, J. D., Kato, K., Tobias, P. S., Kirkland, T. N., Ulevitch, R. J. Transfection of CD14 into 70Z/3 cells dramatically enhances the sensitivity to complexes of lipopolysaccharide (LPS) and LPS binding protein. J Exp Med. 1992, 175:1697-705.

[24] Jiang, Q., Akashi, S., Miyake, K., Petty, H. R. Lipopolysaccharide induces physical proximity between CD14 and toll-like receptor 4 (TLR4) prior to nuclear translocation of NF-kappa B. J Immunol. 2000, 165:3541-4.

[25] Akashi, S., Saitoh, S., Wakabayashi, Y., Kikuchi, T., Takamura, N., Nagai, Y., Kusumoto, Y., Fukase, K., Kusumoto, S., Adachi, Y., Kosugi, A., Miyake, K. Lipopolysaccharide interaction with cell surface toll-like receptor 4-MD-2: Higher affinity than that with MD-2 or CD14. J Exp Med. 2003, 198:1035-42.

[26] Ferrero, E., Jiao, D., Tsuberi, B. Z., Tesio, L., Rong, G. W., Haziot, A., Goyert, S. M. Transgenic mice expressing human CD14 are hypersensitive to lipopolysaccharide. Proc Natl Acad Sci U S A. 1993, 90:2380-4.

[27] Palsson-McDermott, E. M., O'Neill, L. A. Signal transduction by the lipopolysaccharide receptor, toll-like receptor-4. Immunology. 2004, 113:153-62.

[28] Moore, K. J., Andersson, L. P., Ingalls, R. R., Monks, B. G., Li, R., Arnaout, M. A., Golenbock, D. T., Freeman, M. W. Divergent response to LPS and bacteria in CD14-deficient murine macrophages. J Immunol. 2000, 165:4272-80.

[29] Haziot, A., Ferrero, E., Kontgen, F., Hijiya, N., Yamamoto, S., Silver, J., Stewart, C. L., Goyert, S. M. Resistance to endotoxin shock and reduced dissemination of Gram-negative bacteria in CD14-deficient mice. Immunity. 1996, 4:407-14.

[30] Shin, H. J., Lee, H., Park, J. D., Hyun, H. C., Sohn, H. O., Lee, D. W., Kim, Y. S. Kinetics of binding of LPS to recombinant CD14, TLR4, and MD-2 proteins. Mol Cell. 2007, 24:119-24.

[31] Kitchens, R. L., Thompson, P. A. Modulatory effects of sCD14 and LBP on LPS-host cell interactions. J Endotoxin Res. 2005, 11:225-9.

[32] Meng, J., Parroche, P., Golenbock, D. T., McKnight, C. J. The differential impact of disulfide bonds and N-linked glycosylation on the stability and function of CD14. J Biol Chem. 2007.

[33] Kim, J. I., Lee, C. J., Jin, M. S., Lee, C. H., Paik, S. G., Lee, H., Lee, J. O. Crystal structure of CD14 and its implications for lipopolysaccharide signaling. J Biol Chem. 2005, 280:11347-51.

[34] Pugin, J., Heumann, I. D., Tomasz, A., Kravchenko, V. V., Akamatsu, Y., Nishijima, M., Glauser, M. P., Tobias, P. S., Ulevitch, R. J. CD14 is a pattern recognition receptor. Immunity. 1994, 1:509-16.

[35] Blais, D. R., Harrold, J., Altosaar, I. Killing the messenger in the nick of time: Persistence of breast milk sCD14 in the neonatal gastrointestinal tract. Pediatr Res. 2006, 59:371-6.

[36] Lee, J. W., Paape, M. J., Elsasser, T. H., Zhao, X. Elevated milk soluble CD14 in bovine mammary glands challenged with *Escherichia coli* lipopolysaccharide. J Dairy Sci. 2003, 86:2382-9.

[37] Vaishnava, S., Behrendt, C. L., Ismail, A. S., Eckmann, L., Hooper, L. V. Paneth cells directly sense gut commensals and maintain homeostasis at the intestinal host-microbial interface. Proc Natl Acad Sci U S A. 2008, 105:20858-63.

[38] Newburg, D. S., Walker, W. A. Protection of the neonate by the innate immune system of developing gut and of human milk. Pediatr Res. 2007, 61:2-8.

[39] Salzman, N. H., Underwood, M. A., Bevins, C. L. Paneth cells, defensins, and the commensal microbiota: A hypothesis on intimate interplay at the intestinal mucosa. Semin Immunol. 2007, 19:70-83.

[40] Hooper, L. V. Bacterial contributions to mammalian gut development. Trends Microbiol. 2004, 12:129-34.

[41] Parkes, G. C., Sanderson, J. D., Whelan, K. The mechanisms and efficacy of probiotics in the prevention of Clostridium difficile-associated diarrhoea. Lancet Infect Dis. 2009, 9:237-44.

[42] Fung, W., Woo, Y., Wan-Abdullah, W., Ahmad, R., Easa, A. M., Liong, M. Benefits of probiotics: Beyond gastrointestinal health. Milchwissenschaft. 2009, 64:17-21.

[43] Cani, P. D., Delzenne, N. M. Gut microflora as a target for energy and metabolic homeostasis. Curr Opin Clin Nutr Metab Care. 2007, 10:729-34.

[44] Turnbaugh, P. J., Ley, R. E., Mahowald, M. A., Magrini, V., Mardis, E. R., Gordon, J. I. An obesity-associated gut microbiome with increased capacity for energy harvest. Nature. 2006, 444:1027-31.

[45] Forchielli, M. L., Walker, W. A. The effect of protective nutrients on mucosal defense in the immature intestine. Acta Paediatr. 2005, 94:74-83.

[46] Kamada, N., Hisamatsu, T., Okamoto, S., Chinen, H., Kobayashi, T., Sato, T., Sakuraba, A., Kitazume, M. T., Sugita, A., Koganei, K., Akagawa, K. S., Hibi, T. Unique CD14 intestinal macrophages contribute to the pathogenesis of Crohn disease via IL-23/IFN-gamma axis. J Clin Invest. 2008, 118:2269-80.

[47] Claud, E. C., Savidge, T., Walker, W. A. Modulation of human intestinal epithelial cell IL-8 secretion by human milk factors. Pediatr Res. 2003, 53:419-25.

[48] Sela, D. A., Chapman, J., Adeuya, A., Kim, J. H., Chen, F., Whitehead, T. R., Lapidus, A., Rokhsar, D. S., Lebrilla, C. B., German, J. B., Price, N. P., Richardson, P. M., Mills, D. A. The genome sequence of *Bifidobacterium longum* subsp *infantis* reveals adaptations for milk utilization within the infant microbiome. Proc Natl Acad Sci USA. 2008, 105:18964-9.

[49] Clark, J. A., Coopersmith, C. M. Intestinal crosstalk: A new paradigm for understanding the gut as the "motor" of critical illness. Shock. 2007, 28:384-93.

[50] Henare, S. J., Mellor, D. J., Lentle, R. G., Moughan, P. J. An appraisal of the strengths and weaknesses of newborn and juvenile rat models for researching gastrointestinal development. Lab Anim. 2008, 42:231-45.

[51] Harlow, H. F., Harlow, M. K., Dodsworth, R. O., Arling, G. L. Maternal behavior of rhesus monkeys deprived of mothering and peer associations in infancy. Proc Am Philos Soc. 1966, 110:58-66.

[52] Seay, B., Harlow, H. F. Maternal separation in the rhesus-monkey. J Nerv Ment Dis. 1965, 140:434-41.

[53] Enck, P., Merlin, V., Erckenbrecht, J. F., Wienbeck, M. Stress effects on gastrointestinal transit in the rat. Gut. 1989, 30:455-9.

[54] Smart, J. L., Stephens, D. N., Tonkiss, J., Auestad, N. S., Edmond, J. Growth and development of rats artificially reared on different milk-substitutes. Br J Nutr. 1984, 52:227-37.

[55] Tonkiss, J., Smart, J. L., Auestad, N. S., Edmond, J. Type of milk substitute influences growth of the gastrointestinal-tract in artificially reared rat pups. J Pediatr Gastroenterol Nutr. 1985, 4:818-25.

[56] Kanno, T., Koyanagi, N., Katoku, Y., Yonekubo, A., Yajima, T., Kuwata, T., Kitagawa, H., Harada, E. Simplified preparation of a refined milk formula comparable to rat's milk: Influence of the formula on development of the gut and brain in artificially reared rat pups. J Pediatr Gastroenterol Nutr. 1997, 24:242-52.

[57] Tuleu, C., Andrieux, C., Boy, P., Chaumeil, J. C. Gastrointestinal transit of pellets in rats: Effect of size and density. Int J Pharm. 1999, 180:123-31.

[58] Blais, D. R., Altosaar, I. Humanizing infant milk formula to decrease postnatal HIV transmission. Trends Biotechnol. 2007, 25:376-84.

[59] Labeta, M. O., Vidal, K., Nores, J. E., Arias, M., Vita, N., Morgan, B. P., Guillemot, J. C., Loyaux, D., Ferrara, P., Schmid, D., Affolter, M., Borysiewicz, L. K., Donnet-Hughes, A., Schiffrin, E. J. Innate recognition of bacteria in human milk is mediated by a milk-derived highly expressed pattern recognition receptor, soluble CD14. J Exp Med. 2000, 191:1807-12.

[60] Miller, D. L. Rat small intestine - development, composition and effects of perfusion. Am J Dig Dis. 1971, 16:247-54.

[61] Perry, R. L., Carrig, C. B., Williams, J. F., Johnson, C. A., Kaneene, J. B. Anatomic features and radiographic observations of gastric emptying and small intestinal motility in the rat. Lab Anim Sci. 1993, 43:586-93.

[62] Turan, C., Ozdemir, M. The effect of intestinal plication on intestinal transit time in rats. Pediatr Surg Int. 2004, 20:425-8.

[63] Munakata, A., Iwane, S., Todate, M., Nakaji, S., Sugawara, K. Effects of dietary fiber on gastrointestinal transit time, fecal properties and fat absorption in rats. Tohoku J Exp Med. 1995, 176:227-38.

[64] Loiseau, G., Millischer, R., Donadieu, A. M., Marquet, J. P. Gastrointestinal prokinetic and antiemetic effects of a new substituted pyrimidine, O 6553 (2-methylamino-4-N-methylpiperazino-5-thiomethyl-6-chloropyrimidine hydrochloride). Arzneim -Forsch. 1977, 27:606-11.

[65] Krueger, D., Grossklaus, R., Herold, M., Lorenz, S., Klingebiel, L. Gastrointestinal transit and digestibility of maltitol, sucrose and sorbitol in rats: A multicompartmental model and recovery study. Experientia. 1992, 48:733-40.

[66] Shinohara, H., Williams, C. S., McWilliam, D. L., Koldovsky, O., Philipps, A. F., Dvorak, B. Transforming growth factor-alpha delays gastric emptying and small intestinal transit in suckling rats. Scand J Gastroenterol. 2001, 36:356-60.

[67] Dameto, M. C., Rayo, J. M., Esteban, S., Planas, B., Tur, J. A. Effect of cafeteria diet on the gastrointestinal transit and emptying in the rat. Comp Biochem Physiol A Comp Physiol. 1991, 99:651-5.

[68] Harmatz, P. R., Carrington, P. W., Giovinobarry, V., Hatz, R. A., Bloch, K. J. Intestinal adaptation during lactation in the mouse II. Altered intestinal processing of a dietary-protein. Am J Physiol. 1993, 264:G1126-32.

[69] Abia, R., Fry, S. C. Degradation and metabolism of C-14-labelled proanthocyanidins from carob (*Ceratonia siliqua*) pods in the gastrointestinal tract of the rat. J Sci Food Agric. 2001, 81:1156-65.

[70] Yadav, H., Jain, S., Sinha, P. R. The effect of probiotic dahi containing *Lactobacillus acidophilus* and *Lactobacillus casei* on gastropathic consequences in diabetic rats. J Med Food. 2008, 11:62-8.

[71] Mittelstadt, S. W., Hemenway, C. L., Spruell, R. D. Effects of fasting on evaluation of gastrointestinal transit with charcoal meal. J Pharmacol Toxicol Methods. 2005, 52:154-8.

[72] Conover, C. D., Lejeune, L., Shum, K., Shorr, R. G. L. The influence of polyethylene glycol conjugation on bovine hemoglobin's intrinsic effect on the gastrointestinal system of the rat. Life Sci. 1996, 59:1861-9.

[73] Chang, F. Y., Lee, S. D., Yeh, G. H., Wang, P. S. The motor actions of natural neurokinins and their specific agonists on the gastrointestinal tract of the rat. Chin J Physiol (Taipei). 1992, 35:337-48.

[74] Bianchi, G., Ferretti, P., Recchia, M., Rocchetti, M., Tavani, A., Manara, L. Morphine tissue levels and reduction of gastrointestinal transit in rats. Correlation supports primary action site in the gut. Gastroenterology. 1983, 85:852-8.

[75] Vaught, J. L., Cowan, A., Gmerek, D. E. A species difference in the slowing effect of intrathecal morphine on gastrointestinal transit. Eur J Pharmacol. 1983, 94:181-4.

[76] Torjman, M. C., Joseph, J. I., Munsick, C., Morishita, M., Grunwald, Z. Effects of isoflurane on gastrointestinal motility after brief exposure in rats. Int J Pharm. 2005, 294:65-71.

[77] Miller-Gilbert, A. L., Dubuque, S. H., Dvorak, B., Williams, C. S., Grille, J. G., Woodward, S. S., Koldovsky, O., Kling, P. J. Enteral absorption of erythropoietin in the suckling rat. Pediatr Res. 2001, 50:261-7.

[78] Tack, B. F., Dean, J., Eilat, D., Lorenz, P. E., Schechter, A. N. Tritium labeling of proteins to high specific radioactivity by reductive methylation. J Biol Chem. 1980, 255:8842-7.

[79] Jentoft, N., Dearborn, D. G. Labeling of proteins by reductive methylation using sodium cyanoborohydride. J Biol Chem. 1979, 254:4359-65.

[80] Taralp, A., Kaplan, H. Chemical modification of lyophilized proteins in nonaqueous environments. J Protein Chem. 1997, 16:183-93.

[81] DeSesso, J. M., Jacobson, C. F. Anatomical and physiological parameters affecting gastrointestinal absorption in humans and rats. Food Chem Toxicol. 2001, 39:209-28.

[82] Murphy, D. B., Sutton, J. A., Prescott, L. F., Murphy, M. B. Opioid-induced delay in gastric emptying - a peripheral mechanism in humans. Anesthesiology. 1997, 87:765-70.

[83] Soulsby, C. T., Khela, M., Yazaki, E., Evans, D. F., Hennessy, E., Powell-Tuck, J. Measurements of gastric emptying during continuous nasogastric infusion of liquid feed: Electric impedance tomography versus gamma scintigraphy. Clin Nutr. 2006, 25:671-80.

[84] Sangild, P. T., Fowden, A. L., Trahair, J. F. How does the foetal gastrointestinal tract develop in preparation for enteral nutrition after birth? Livest Prod Sci. 2000, 66:141-50.
[85] Moore, C. L., Chadwickdias, A. M. Behavioral-responses of infant rats to maternal licking - variations with age and sex. Dev Psychobiol. 1986, 19:427-38.

[86] Gareau, M. G., Jury, J., Perdue, M. H. Neonatal maternal separation of rat pups results in abnormal cholinergic regulation of epithelial permeability. Am J Physiol -Gastr L. 2007, 293:G198-203.

[87] Del Prado, M., Delgado, G., Villalpando, S. Maternal lipid intake during pregnancy and lactation alters milk composition and production and litter growth in rats. J Nutr. 1997, 127:458-62.

[88] Haenni, A., Sundberg, B., Yazdanpandah, N., Viberg, A., Olsson, J. Effect of fat emulsion (fabuless) on orocecal transit time in healthy men. Scand J Gastroenterol. 2009, 44:1186-90.

[89] Severin, S., Xia, W. S. Milk biologically active components as nutraceuticals: Review. Crit Rev Food Sci Nutr. 2005, 45:645-56.

[90] Daskalakis, N. P., Kaperoni, M., Koros, C., de Kloet, E. R., Kitraki, E. Environmental and tactile stimulation modulates the neonatal handling effect on adult rat spatial memory. Int J Dev Neurosci. 2009, 27:747-55.

[91] Tooley, K. L., Howarth, G. S., Butler, R. N., Lymn, K. A., Penttila, I. A. The effects of formula feeding on physiological and immunological parameters in the gut of neonatal rats. Dig Dis Sci. 2009, 54:1432-9.

[92] Puiman, P., Stoll, B. Animal models to study neonatal nutrition in humans. Curr Opin Clin Nutr Metab Care. 2008, 11:601-6.

[93] Means, G. E., Feeney, R. E. Chemical modifications of proteins: A review. J Food Biochem. 1998, 22:399-426.

[94] Vakos, H. T., Kaplan, H., Black, B., Dawson, B., Hefford, M. A. Use of the pH memory effect in lyophilized proteins to achieve preferential methylation of alpha-amino groups. J Protein Chem. 2000, 19:231-7.

[95] Ballatori, N., Fang, F., Christian, W. V., Li, N., Hammond, C. L. Ost alpha-ost beta is required for bile acid and conjugated steroid disposition in the intestine, kidney, and liver. Am J Physiol -Gastr L. 2008, 295:G179-86.

[96] Rencova, J., Vlkova, A., Curik, R., Holusa, R., Vesela, G. Influence of heavy metals upon the retention and mobilization of polonium-210 in rats. Int J Radiat Biol. 2004, 80:769-76.

[97] Vakos, H. T., Black, B., Dawson, B., Hefford, M. A., Kaplan, H. In vacuo esterification of carboxyl groups in lyophilized proteins. J Protein Chem. 2001, 20:521-31.

[98] Yamada, C., Yamashita, Y., Seki, R., Izumi, H., Matsuda, T., Kato, Y. Digestion and gastrointestinal absorption of the 14-16-kDa rice allergens. Biosci Biotechnol Biochem. 2006, 70:1890-7.

[99] Darcy-Vrillon, B., Souffrant, W. B., Laplace, J. P., Rerat, A., Corring, T., Vaugelade, P., Gebhardt, G., Koehler, R. Exogenous and endogenous contributions to nitrogen fluxes in the digestive tract of pigs fed a casein diet. II. Ileal and faecal digestibilities and absorption of amino acids. Reprod Nutr Dev. 1991, 31:561-73.

[100] Corpet, D. E., Bellier, R., Petrowitsch, S., Vigouroux, Y. Digestion and fermentation of proteins in rats fed keratin, albumin, cooked casein and antibiotics. Reprod Nutr Dev. 1994, 34:57-64.

[101] Lindberg, T., Engberg, S., Sjoberg, L. B., Lonnerdal, B. In vitro digestion of proteins in human milk fortifiers and in preterm formula. J Pediatr Gastroenterol Nutr. 1998, 27:30-6.

[102] Jakobsson, I., Lindberg, T., Benediktsson, B. In vitro digestion of cows milk-proteins by duodenal juice from infants with various gastrointestinal disorders. J Pediatr Gastroenterol Nutr. 1982, 1:183-91.

[103] Wallace, R. J. Hydrolysis of 14C-labelled proteins by rumen micro-organisms and by proteolytic enzymes prepared from rumen bacteria. Br J Nutr. 1983, 50:345-55.

[104] Adibi, S. A., Mercer, D. W. Protein digestion in human intestine as reflected in luminal, mucosal, and plasma amino-acid concentrations after meals. J Clin Invest. 1973, 52:1586-94.

[105] Lee, J. W., Paape, M. J., Elsasser, T. H., Zhao, X. Recombinant soluble CD14 reduces severity of intramammary infection by *Escherichia coli* . Infect Immun. 2003, 71:4034-9.

[106] Lee, J. W., Paape, M. J., Zhao, X. Recombinant bovine soluble CD14 reduces severity of experimental *Escherichia coli* mastitis in mice. Vet Res. 2003, 34:307-16.

[107] Gross, P., Brandl, K., Dierkes, C., Schoelmerich, J., Salzberger, B., Glueck, T., Falk, W. Lipopolysaccharide-trap-fc, a multifunctional agent to battle Gram-negative bacteria. Infect Immun. 2009, 77:2925-31.

[108] Wall, R., Powell, A., Sohn, E., Foster-Frey, J., Bannerman, D., Paape, M. Enhanced host immune recognition of mastitis causing *Escherichia coli* in CD-14 transgenic mice. Anim Biotechnol. 2009, 20:1-14.

[109] Sohn, E. J., Paape, M. J., Bannerman, D. D., Connor, E. E., Fetterer, R. H., Peters, R. R. Shedding of sCD14 by bovine neutrophils following activation with bacterial lipopolysaccharide results in down-regulation of IL-8. Vet Res. 2007, 38:95-108.

[110] Heyman, M. Symposium on 'dietary influences on mucosal immunity': How dietary antigens access the mucosal immune system. Proc Nutr Soc. 2001, 60:419-26.

Contributions of Collaborators

The following people have contributed to the recruitment of patients, sample collections and experimental work in this thesis:

Chapters 2

Dr. David Mack, Chief of Gastroenterology, Hepatology & Nutrition, Department of Pediatrics at the Children's Hospital of Eastern Ontario, helped analyze x-rays to determine gastrointestinal transit time.

Chapter 3

Dr. William Spencer, Postdoctoral Fellow and Tonya Ward, graduate student in the Department of Biochemistry, Microbiology & Immunology, Faculty of Medicine, University of Ottawa, assisted with animal experiments.

Dr. Van Thong Pham and Professor Harvey Kaplan helped with ^{14}C-radiolabeling of proteins.

Appendices

Appendix A

Ten animals, numbered Rat 1 to Rat 10
X-ray images of barium sulfate from gavage fed 10 day old Sprague Dawley rats

Rat 1

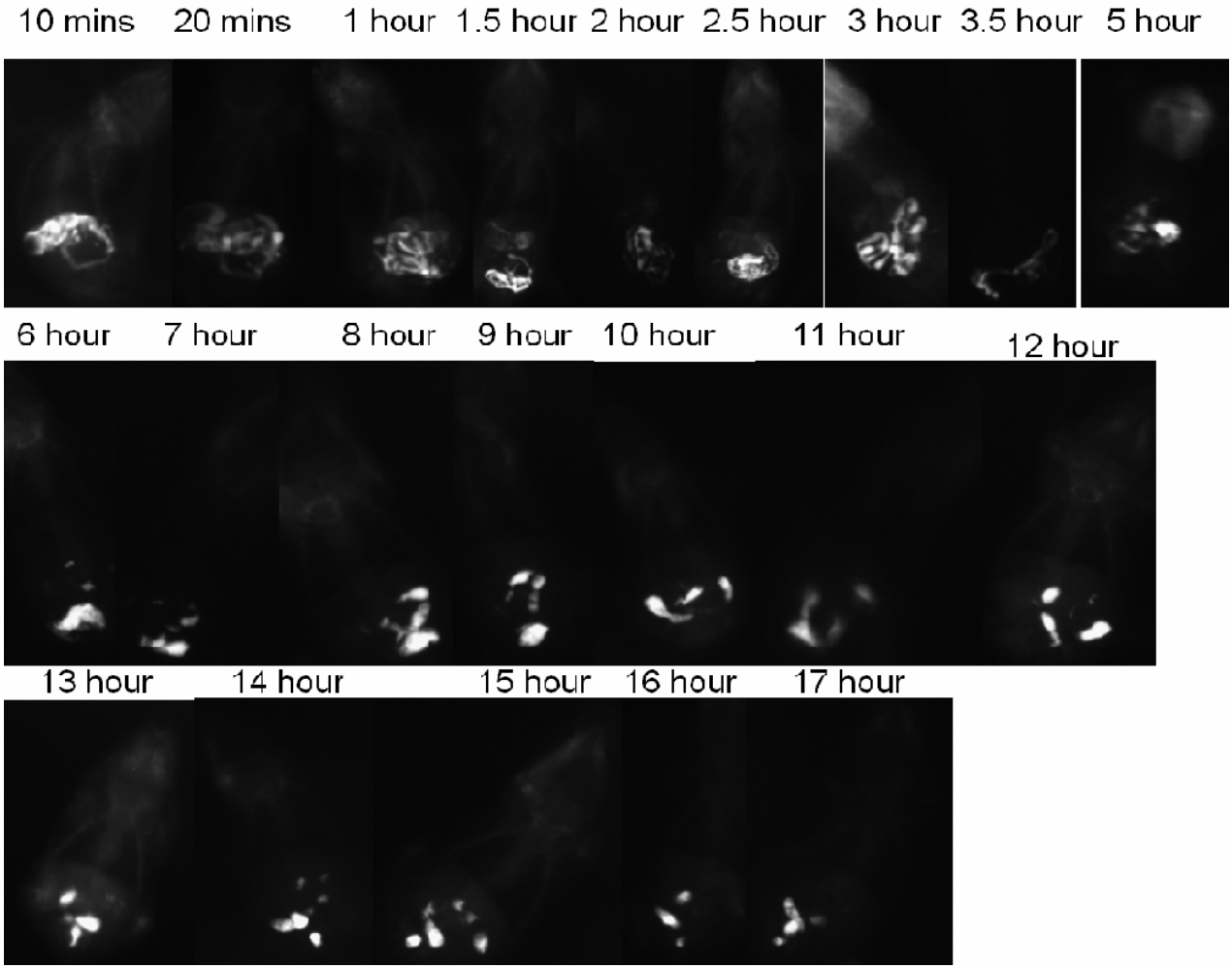

Rat 2

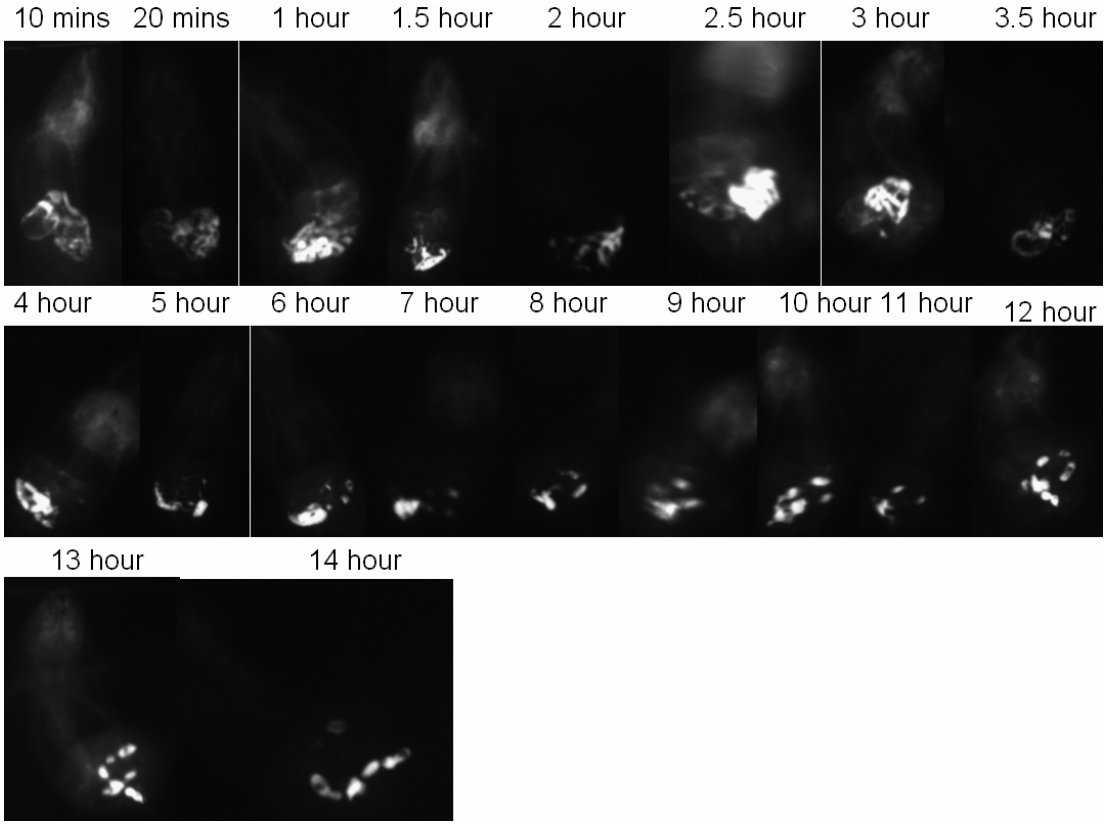
10 mins
20 mins
1 hour
1.5 hour
2 hour
2.5 hour
3 hour
3.5 hour
4 hour
5 hour
6 hour
7 hour
8 hour
9 hour
10 hour
11 hour
12 hour
13 hour
14 hour

Rat 3

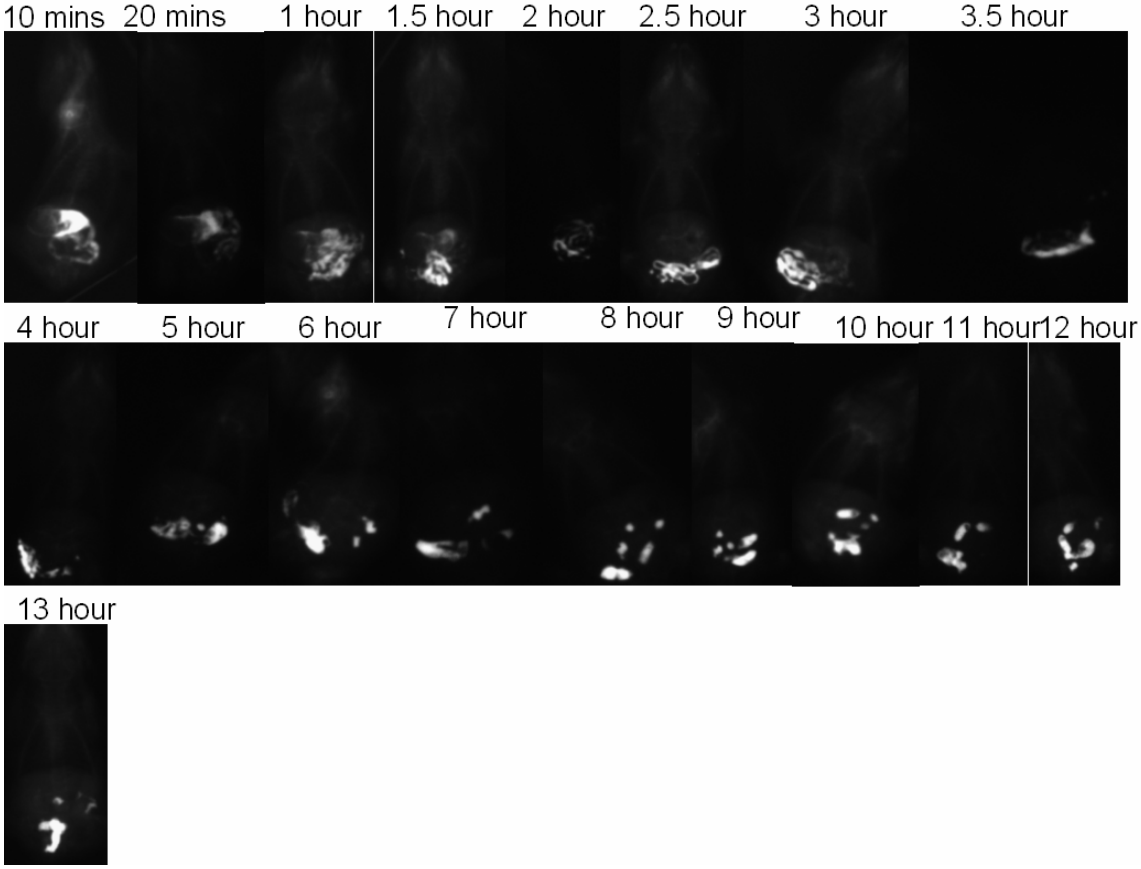
10 mins
20 mins
1 hour
1.5 hour
2 hour
2.5 hour
3 hour
3.5 hour
4 hour
5 hour
6 hour
7 hour
8 hour
9 hour
10 hour
11 hour
12 hour
13 hour

Rat 4

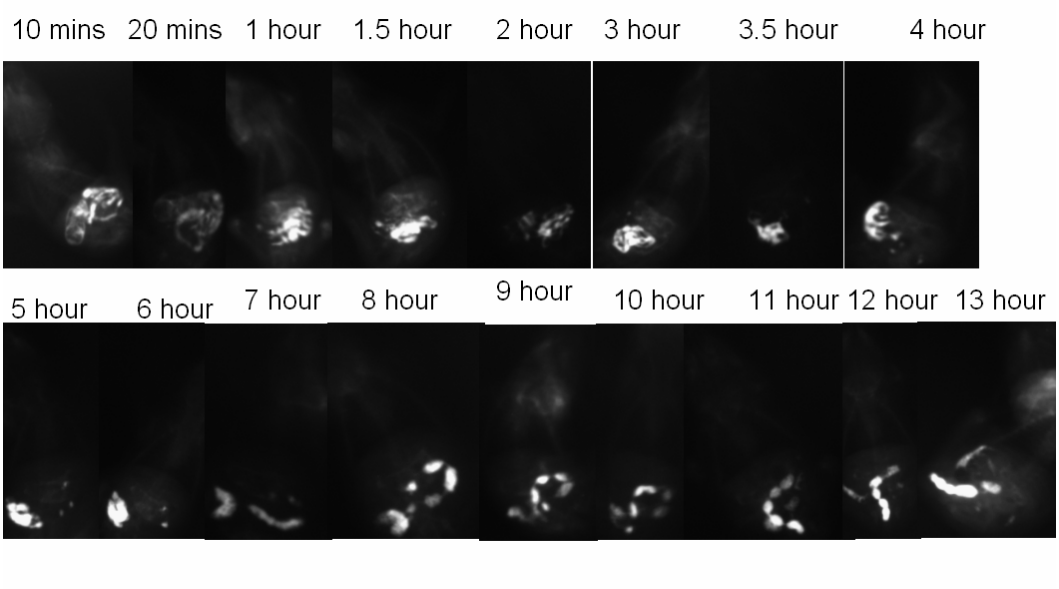
10 mins
20 mins
1 hour
1.5 hour
2 hour
3 hour
3.5 hour
4 hour
5 hour
6 hour
7 hour
8 hour
9 hour
10 hour
11 hour
12 hour
13 hour

Rat 5

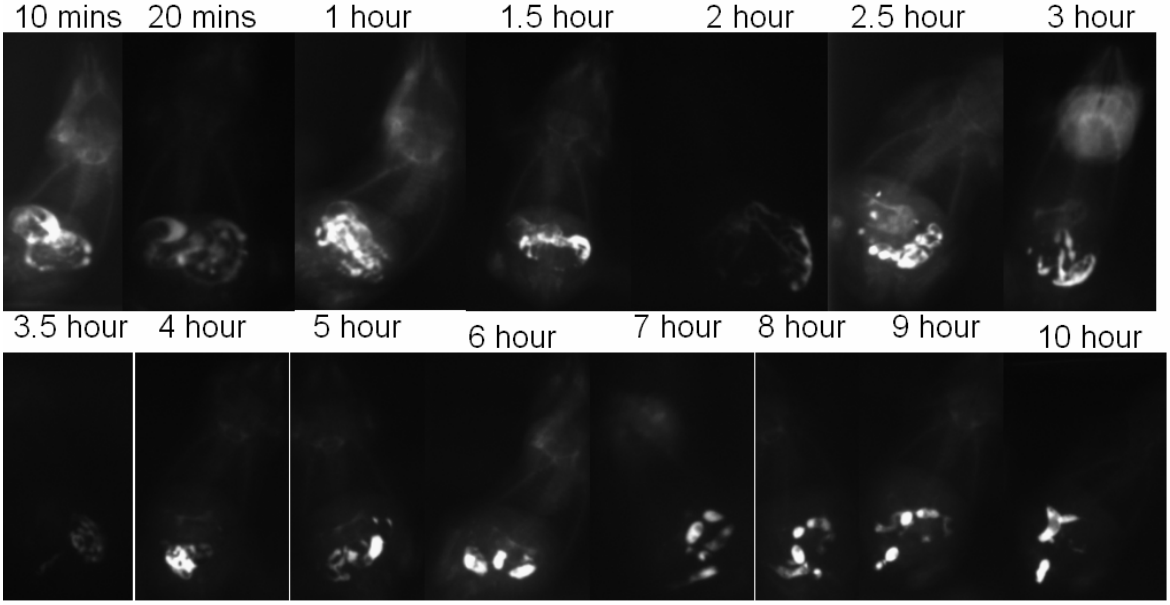
10 mins
20 mins
1 hour
1.5 hour
2 hour
2.5 hour
3 hour
3.5 hour
4 hour
5 hour
6 hour
7 hour
8 hour
9 hour
10 hour

Rat 6

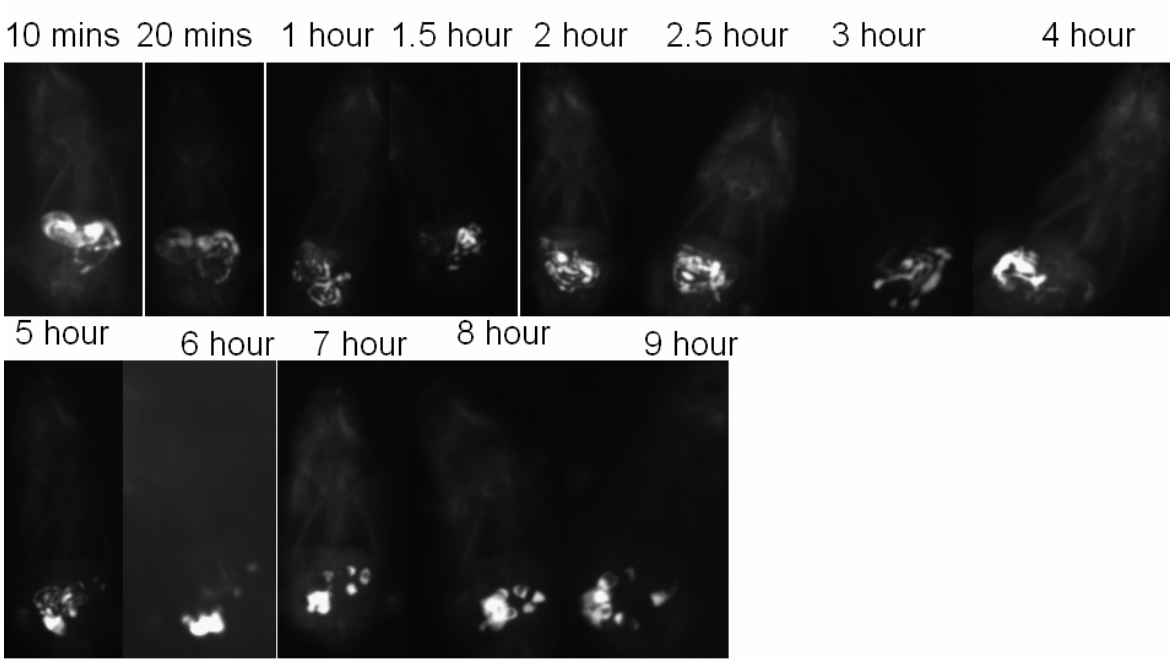
10 mins
20 mins
1 hour
1.5 hour
2 hour
2.5 hour
3 hour
4 hour
5 hour
6 hour
7 hour
8 hour
9 hour

Rat 7

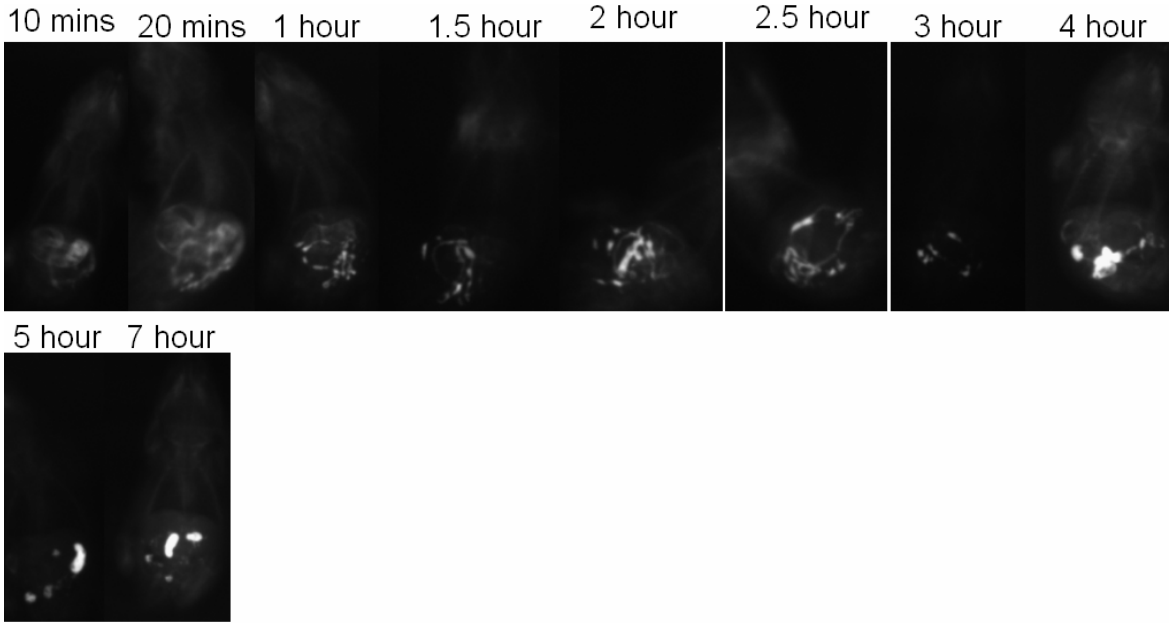
10 mins
20 mins
1 hour
1.5 hour
2 hour
2.5 hour
3 hour
4 hour
5 hour
7 hour

Rat 8

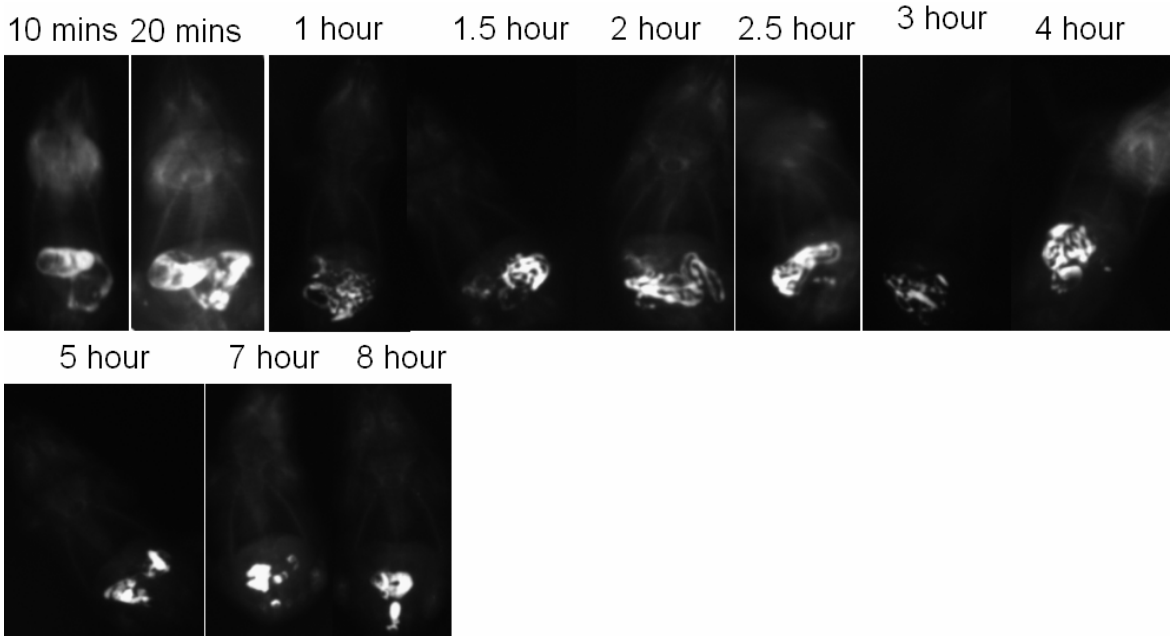
10 mins
20 mins
1 hour
1.5 hour
2 hour
2.5 hour
3 hour
4 hour
5 hour
7 hour
8 hour

Rat 9

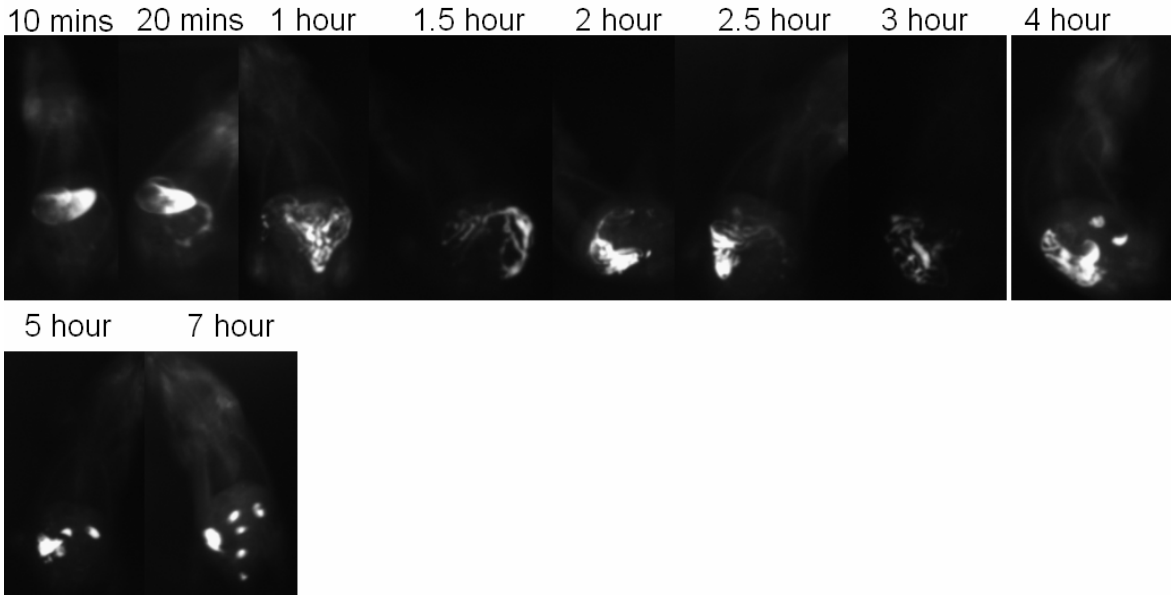
10 mins
20 mins
1 hour
1.5 hour
2 hour
2.5 hour
3 hour
4 hour
5 hour
7 hour

Rat 10

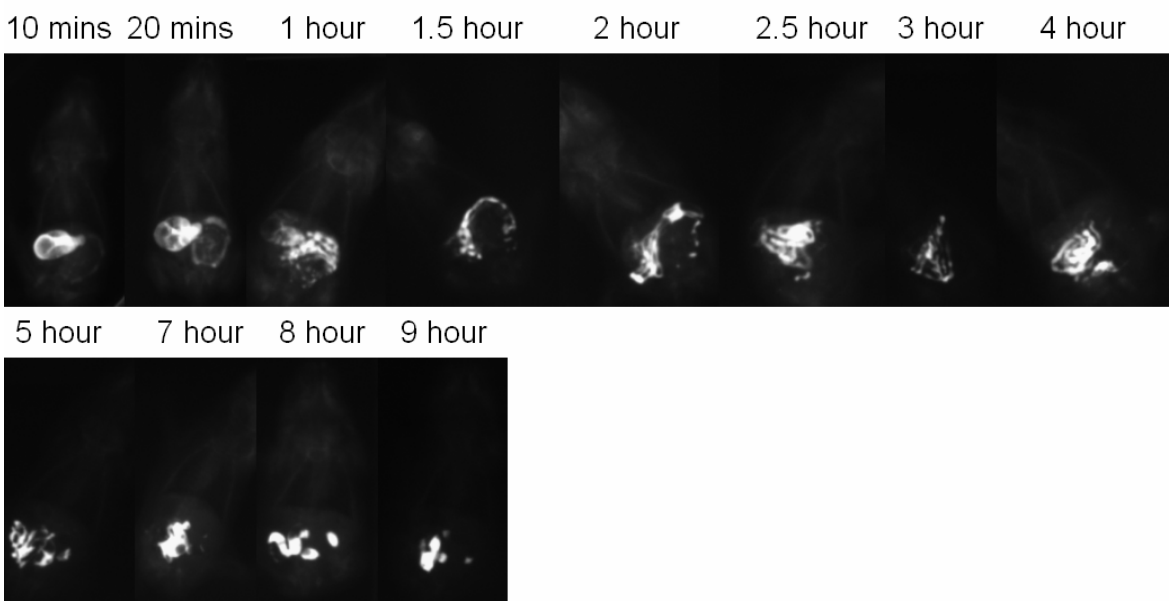
10 mins
20 mins
1 hour
1.5 hour
2 hour
2.5 hour
3 hour
4 hour
5 hour
7 hour
8 hour
9 hour

Appendix B

Eleven animals, numbered Rat 11 to Rat 21
X-ray images of barium sulfate from gavage fed 15 day old Sprague Dawley rats

Rat 11

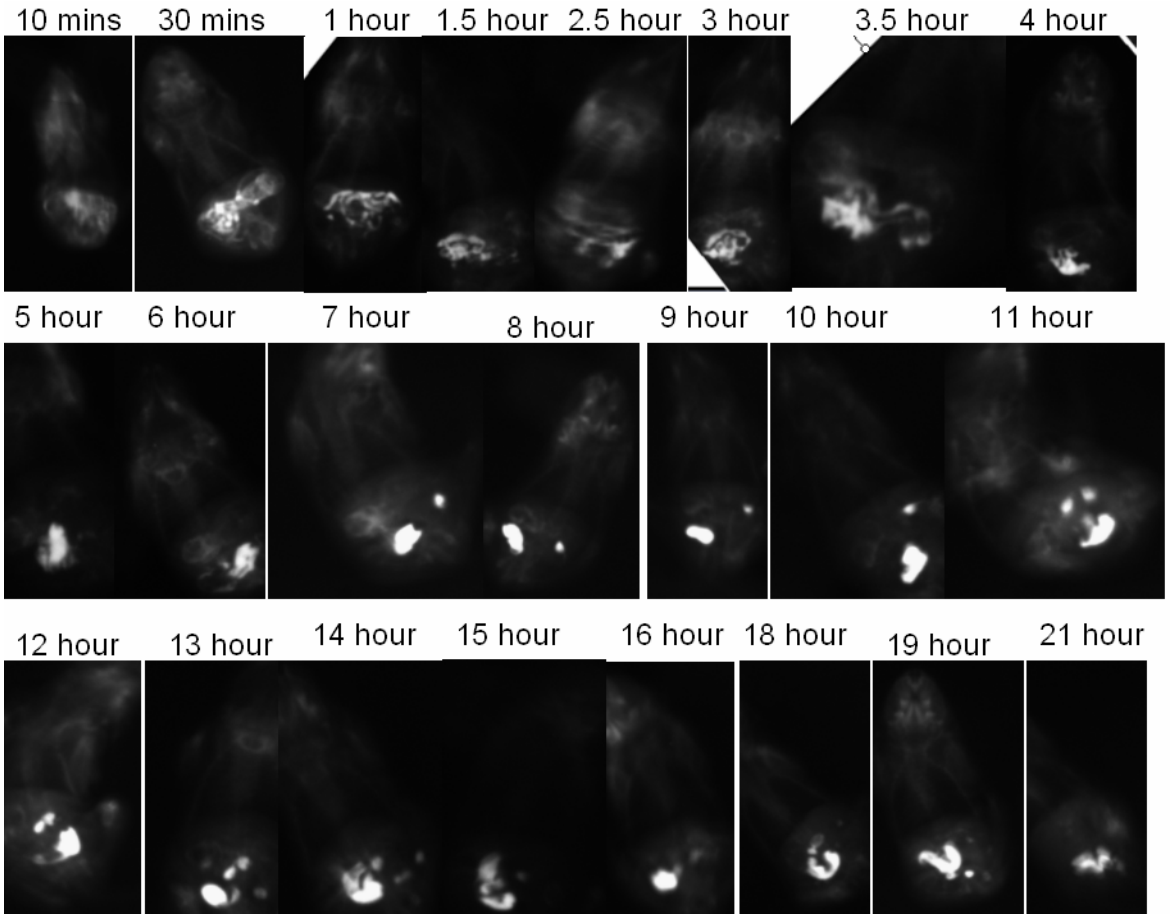

Rat 12

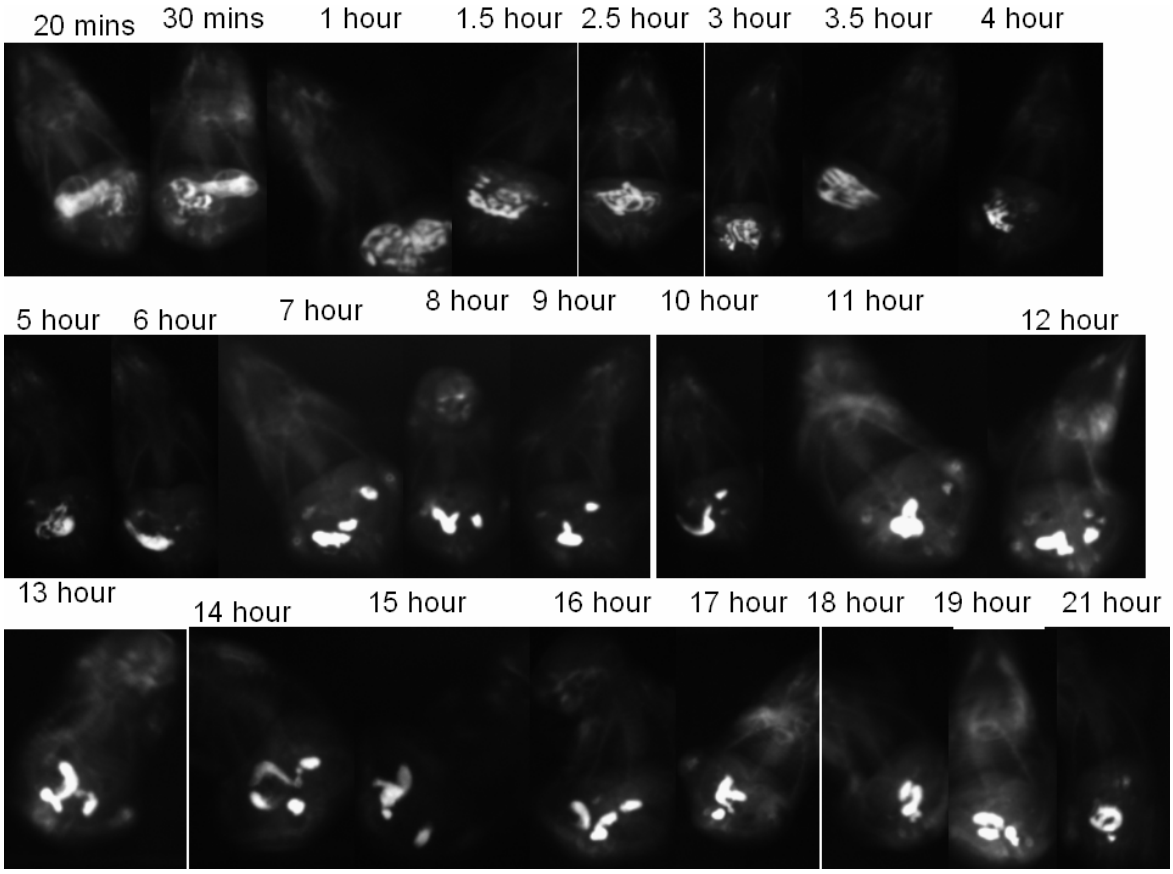
20 mins
30 mins
1 hour
1.5 hour
2.5 hour
3 hour
3.5 hour
4 hour
5 hour
6 hour
7 hour
8 hour
9 hour
10 hour
11 hour
12 hour
13 hour
14 hour
15 hour
16 hour
17 hour
18 hour
19 hour
21 hour

Rat 13

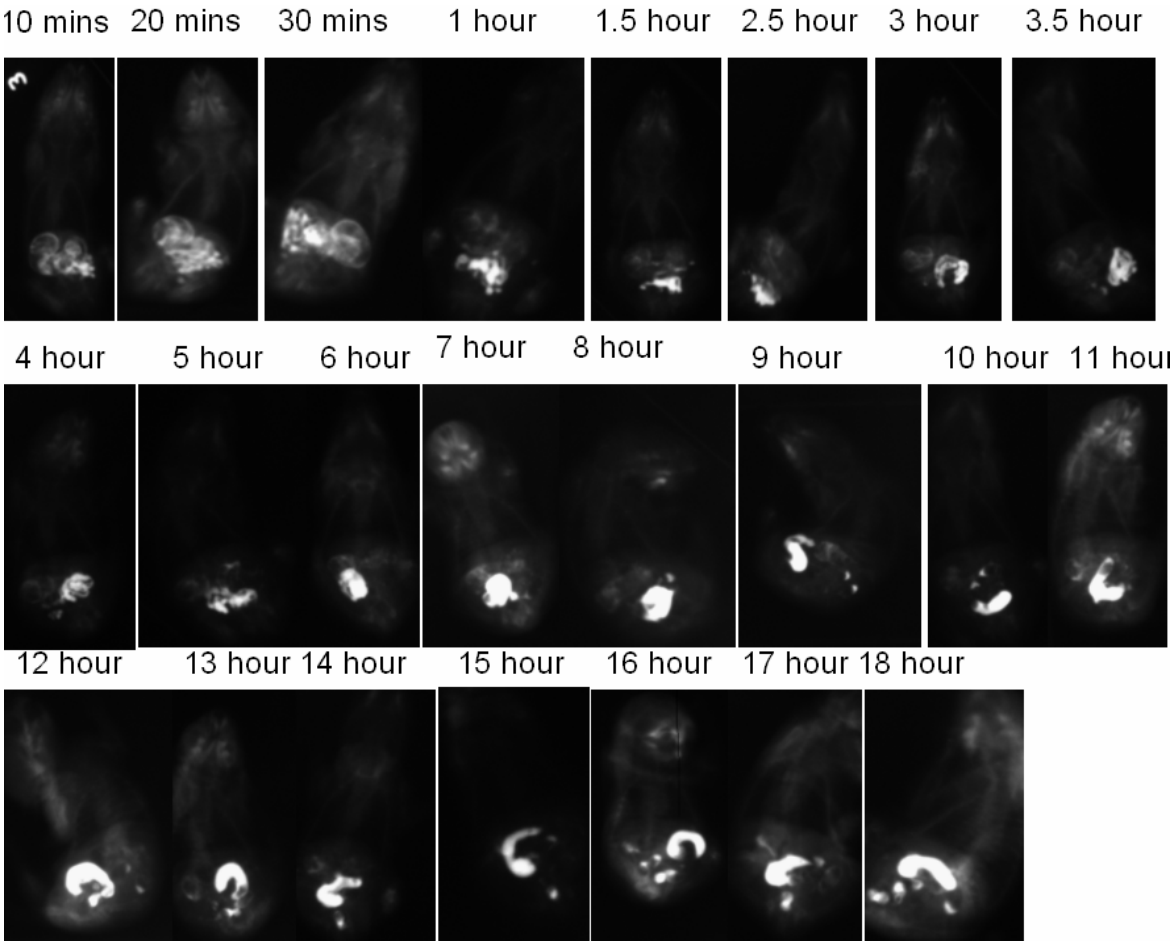
10 mins
20 mins
30 mins
1 hour
1.5 hour
2.5 hour
3 hour
3.5 hour
4 hour
5 hour
6 hour
7 hour
8 hour
9 hour
10 hour
11 hour
12 hour
13 hour
14 hour
15 hour
16 hour
17 hour
18 hour

Rat 14

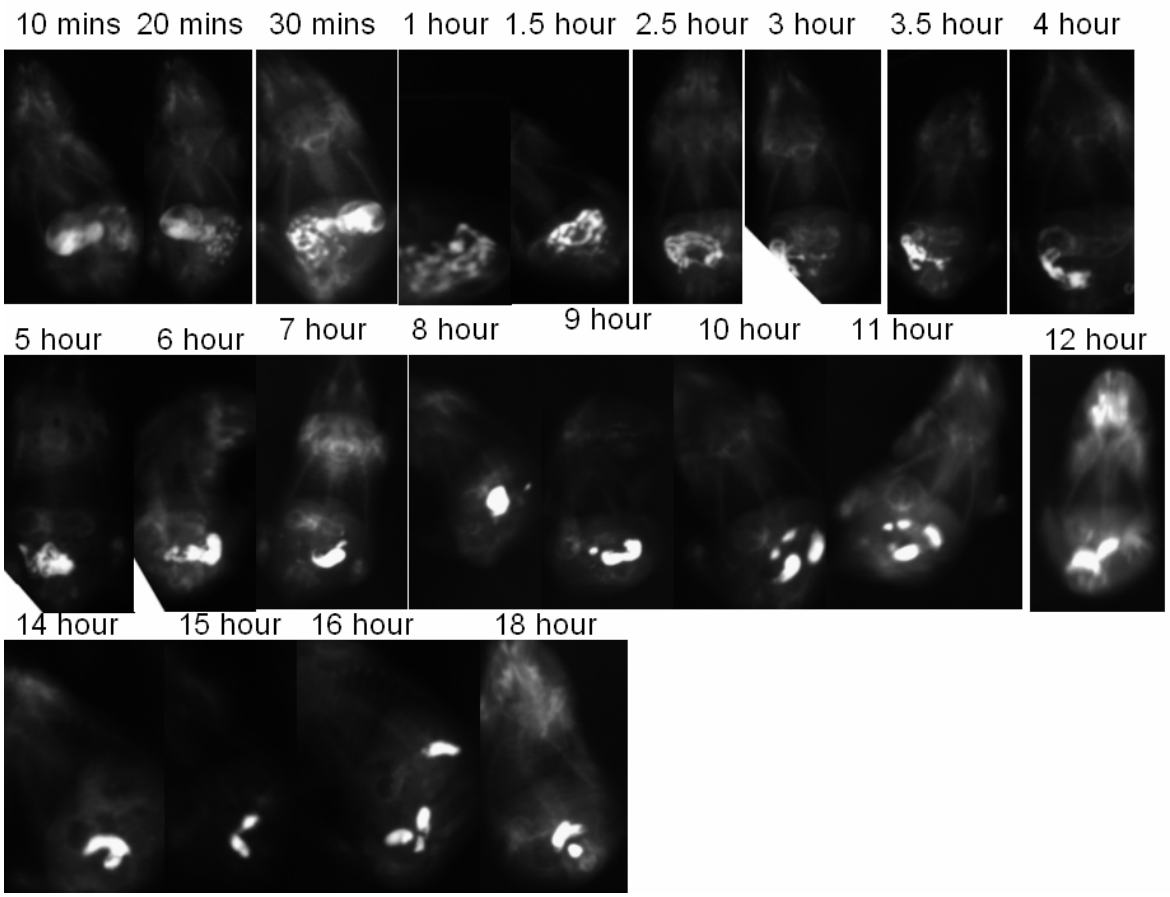
10 mins
20 mins
30 mins
1 hour
1.5 hour
2.5 hour
3 hour
3.5 hour
4 hour
5 hour
6 hour
7 hour
8 hour
9 hour
10 hour
11 hour
12 hour
14 hour
15 hour
16 hour
18 hour

Rat 15

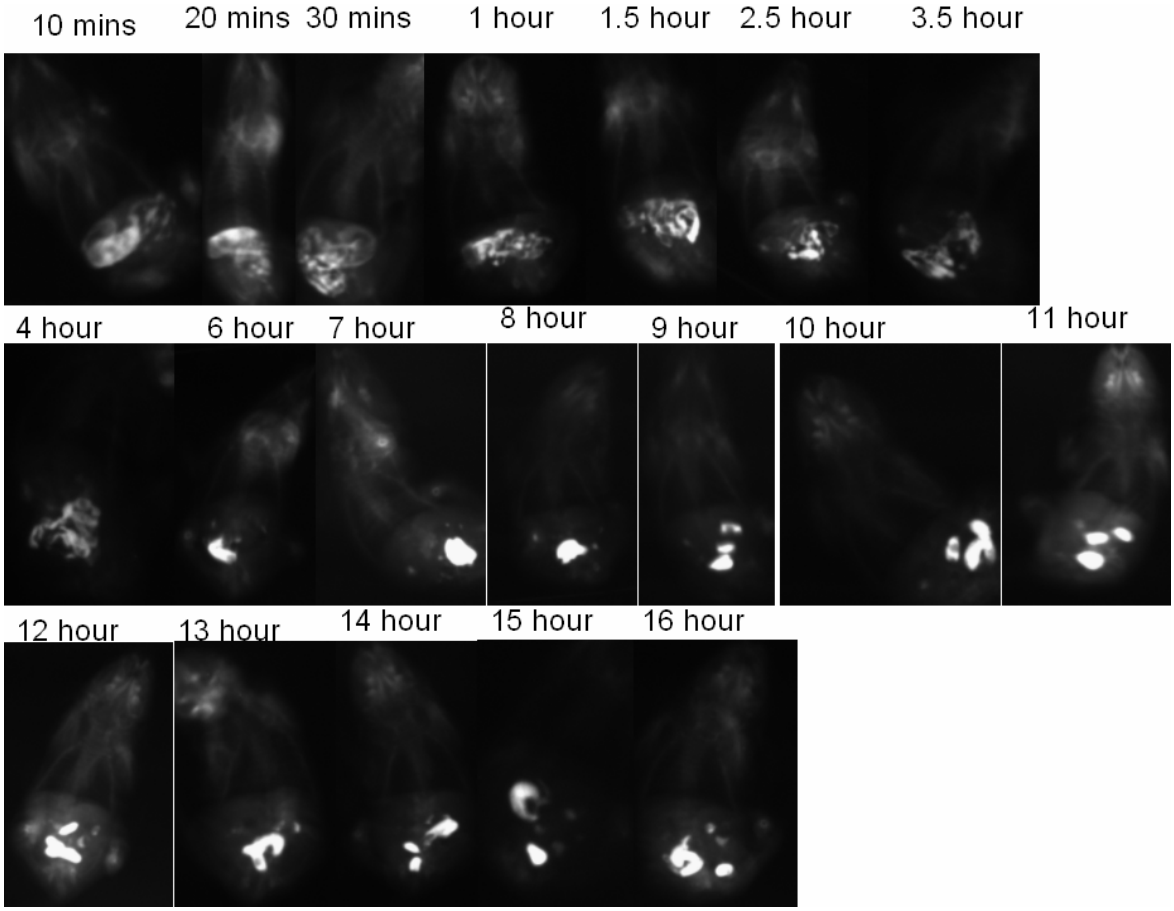
10 mins
20 mins
30 mins
1 hour
1.5 hour
2.5 hour
3.5 hour
4 hour
6 hour
7 hour
8 hour
9 hour
10 hour
11 hour
12 hour
13 hour
14 hour
15 hour
16 hour

Rat 16

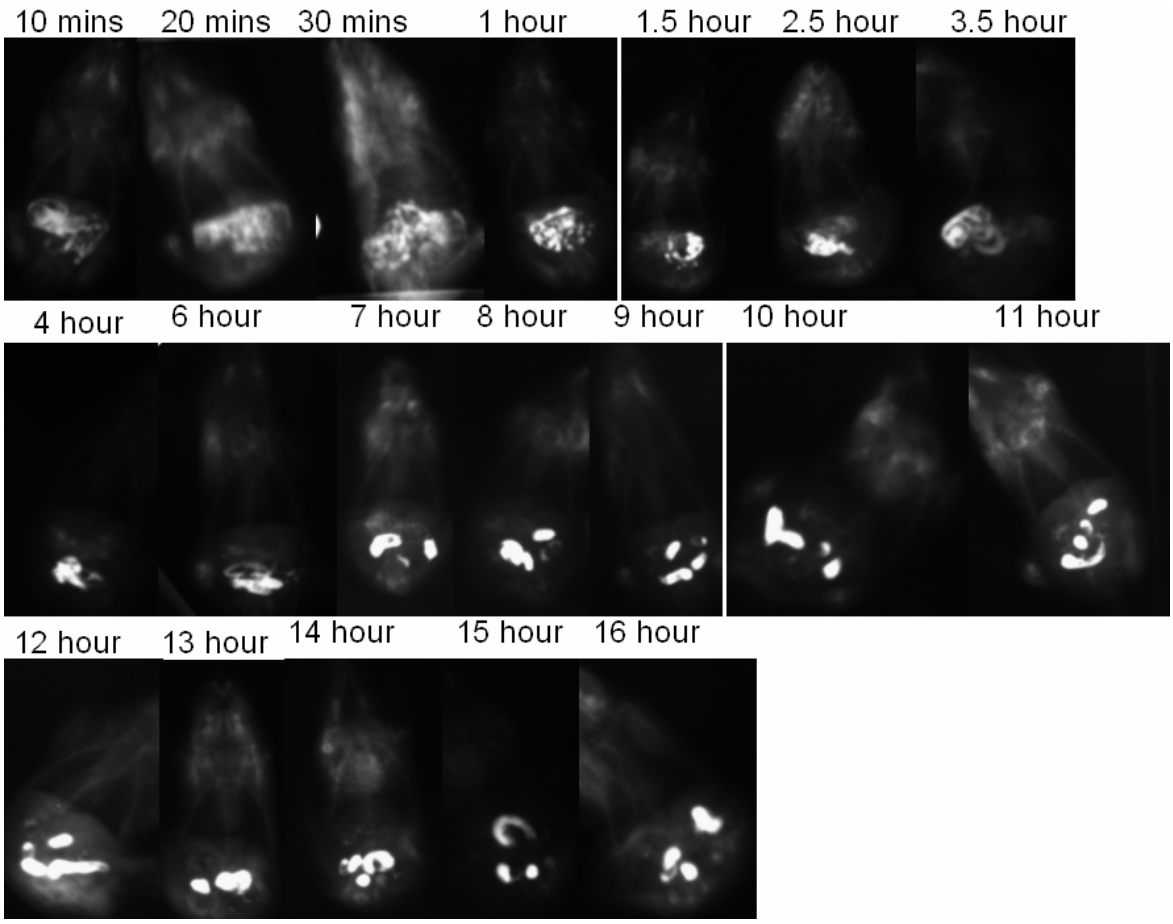
10 mins
20 mins
30 mins
1 hour
1.5 hour
2.5 hour
3.5 hour
4 hour
6 hour
7 hour
8 hour
9 hour
10 hour
11 hour
12 hour
13 hour
14 hour
15 hour
16 hour

Rat 17

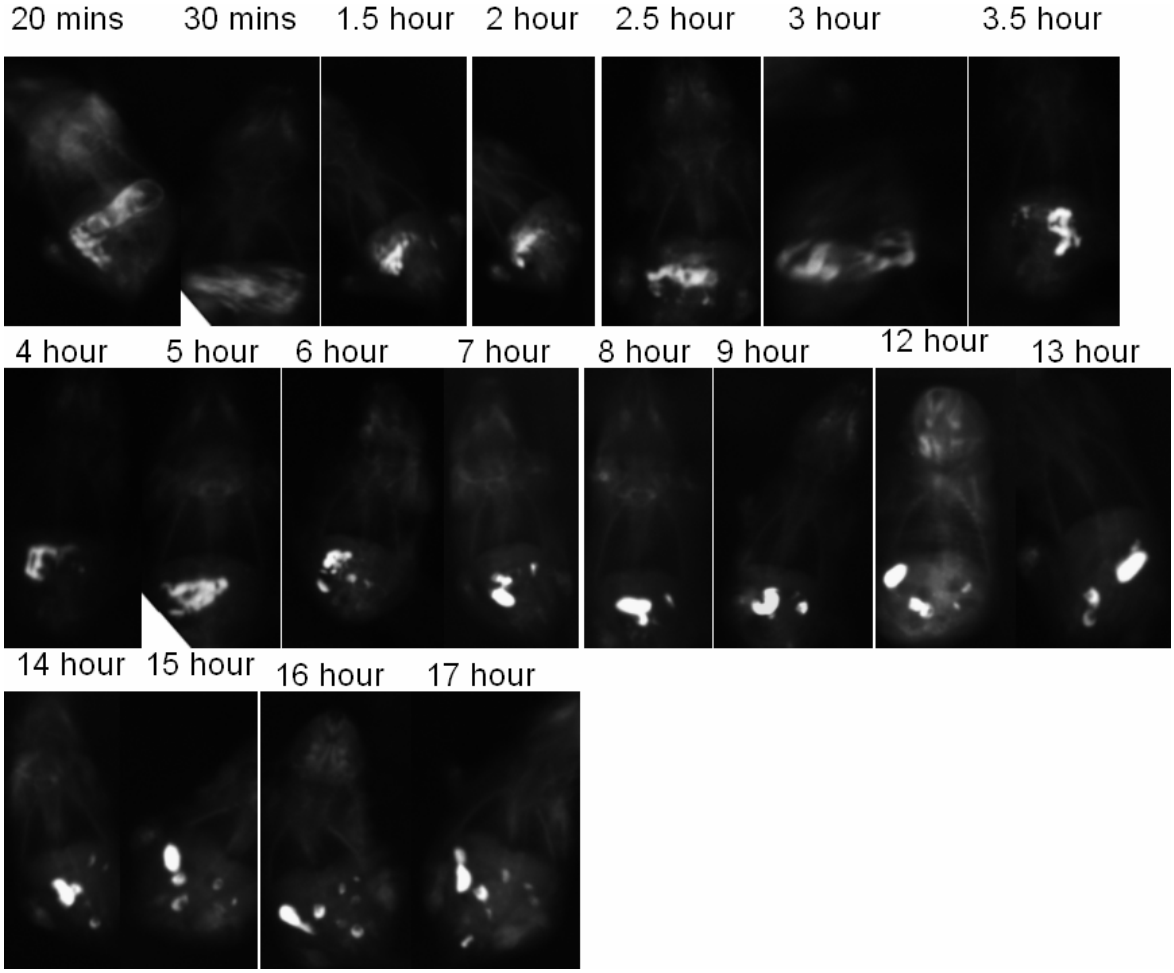
20 mins
30 mins
1.5 hour
2 hour
2.5 hour
3 hour
3.5 hour
4 hour
5 hour
6 hour
7 hour
8 hour
9 hour
12 hour
13 hour
14 hour
15 hour
16 hour
17 hour

Rat 18

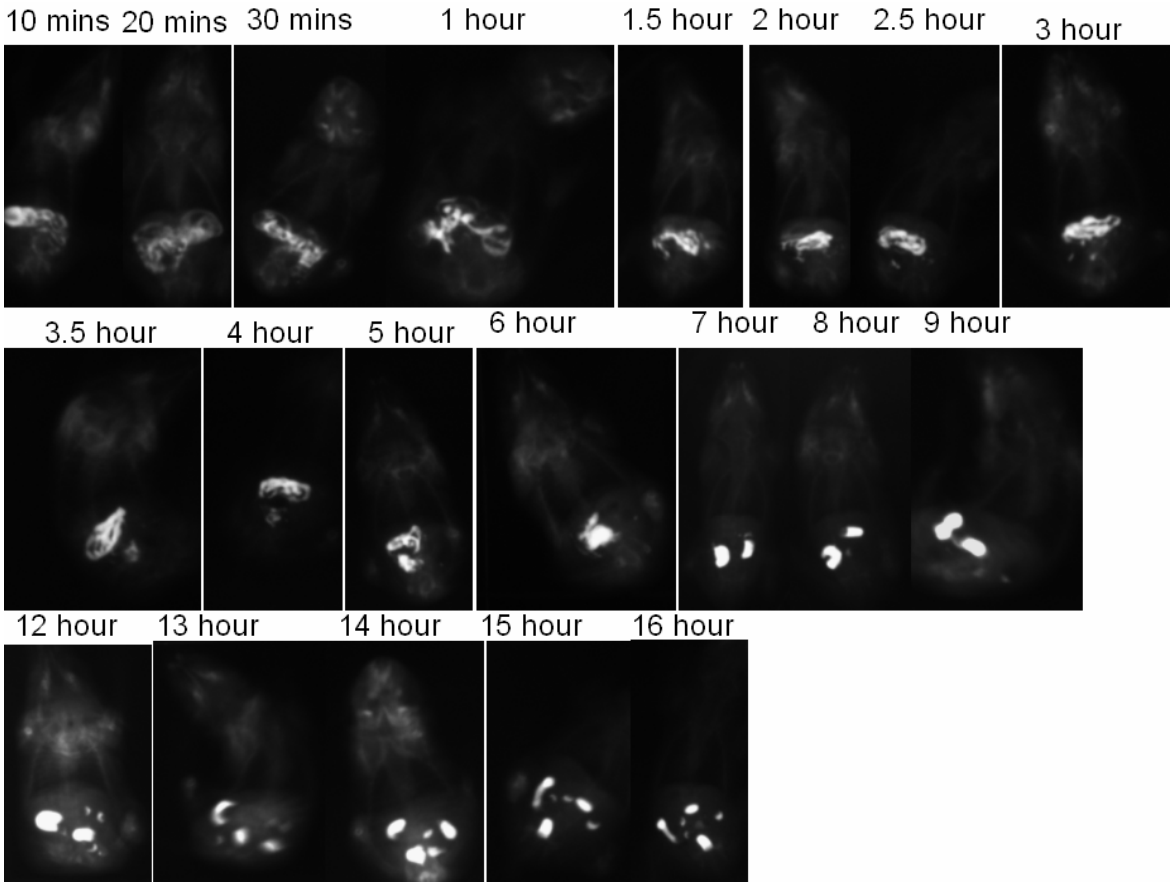
10 mins
20 mins
30 mins
1 hour
1.5 hour
2 hour
2.5 hour
3 hour
3.5 hour
4 hour
5 hour
6 hour
7 hour
8 hour
9 hour
12 hour
13 hour
14 hour
15 hour
16 hour

Rat 19

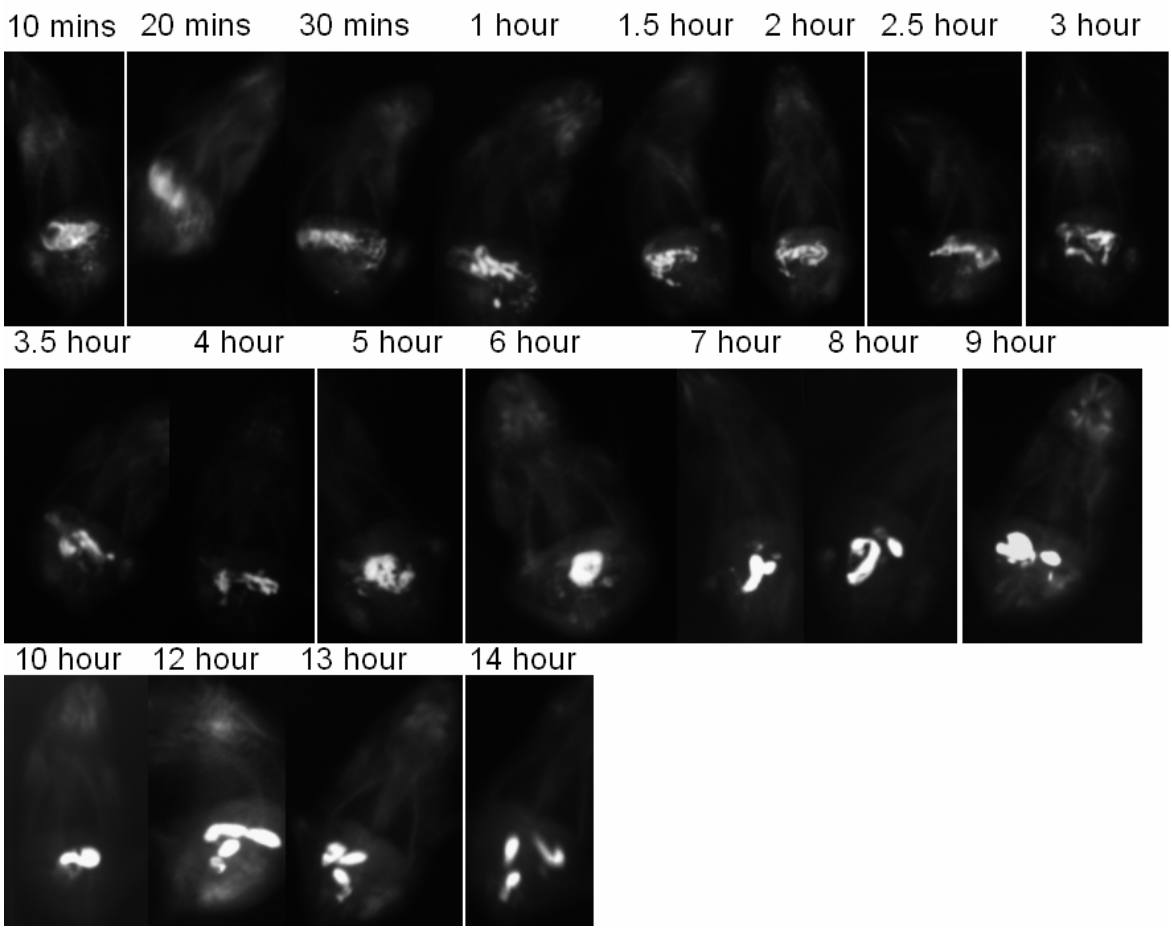
10 mins
20 mins
30 mins
1 hour
1.5 hour
2 hour
2.5 hour
3 hour
3.5 hour
4 hour
5 hour
6 hour
7 hour
8 hour
9 hour
10 hour
12 hour
13 hour
14 hour

Rat 20

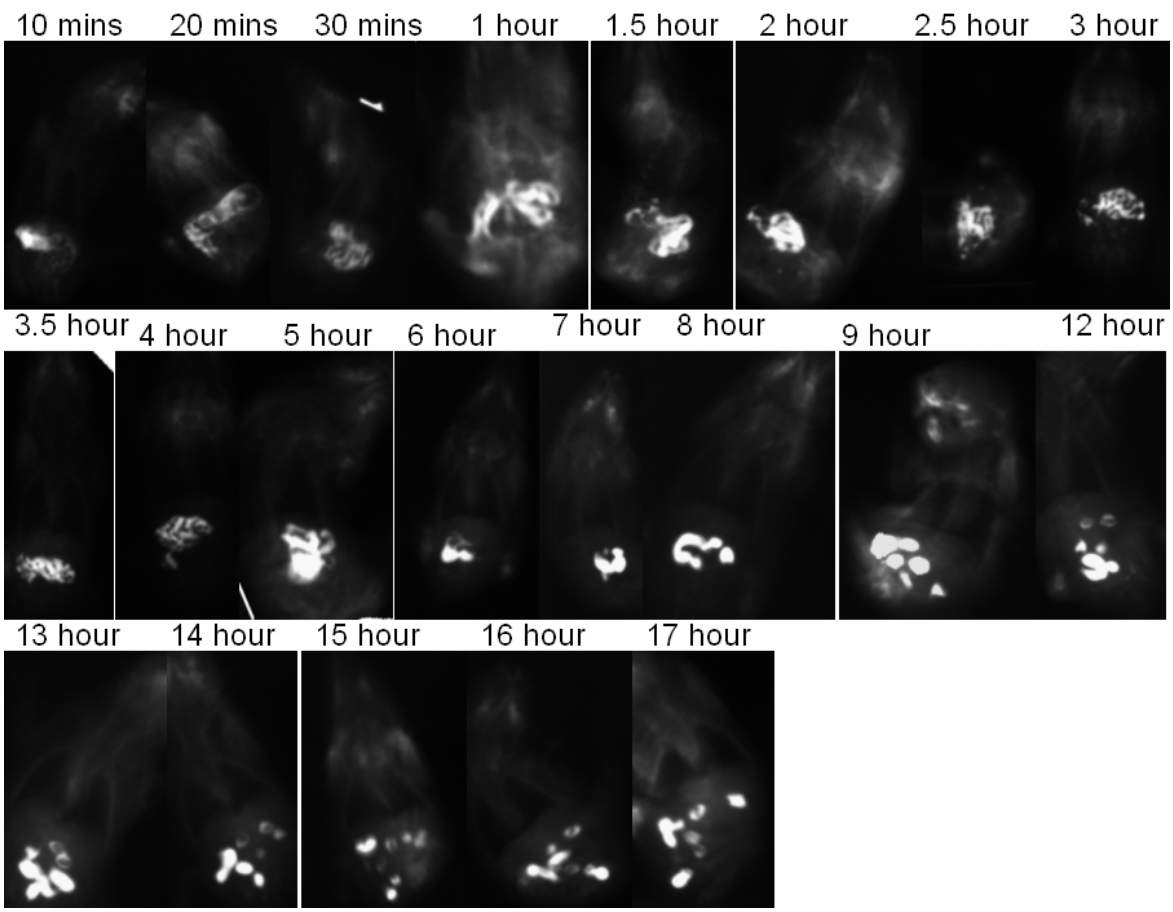
10 mins
20 mins
30 mins
1 hour
1.5 hour
2 hour
2.5 hour
3 hour
3.5 hour
4 hour
5 hour
6 hour
7 hour
8 hour
9 hour
12 hour
13 hour
14 hour
15 hour
16 hour
17 hour

Rat 21

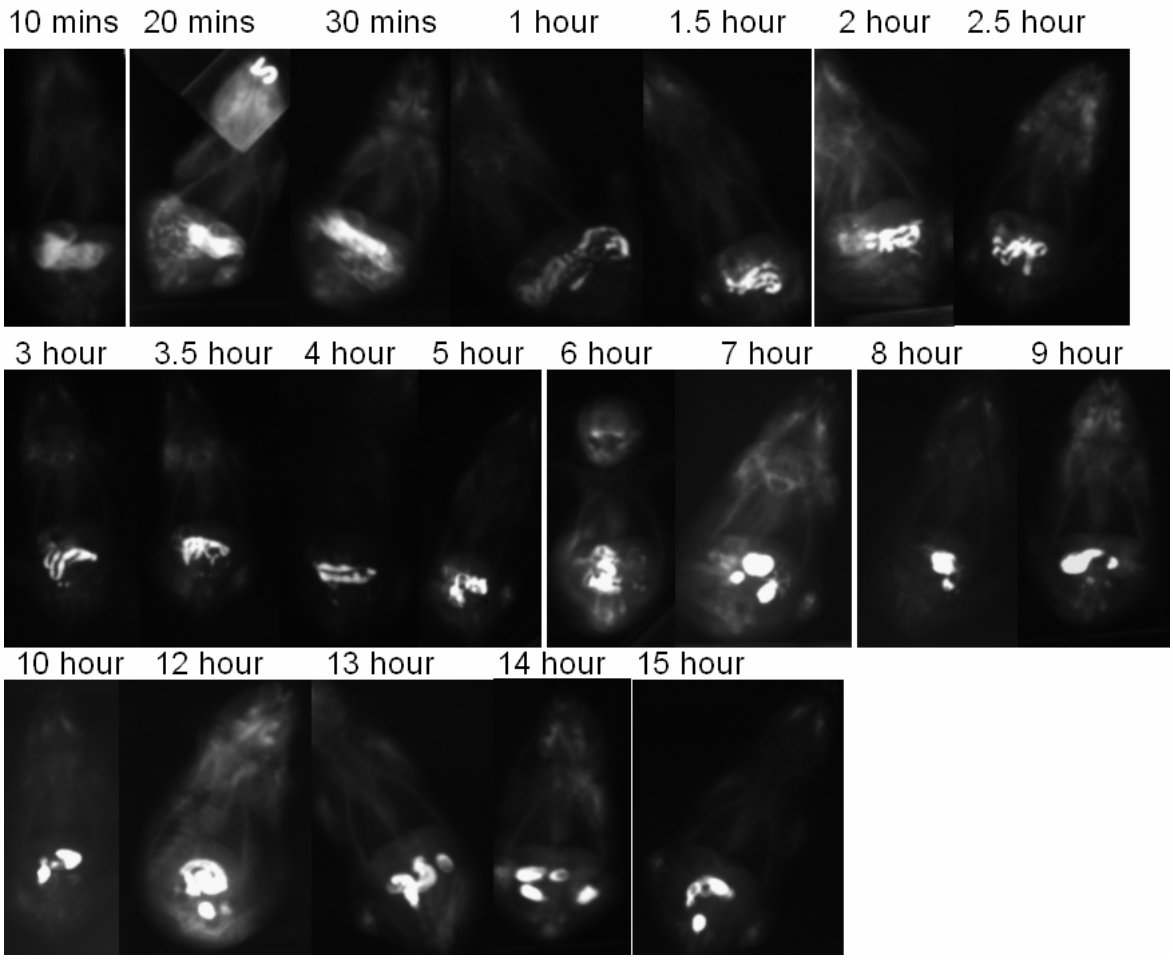
10 mins
20 mins
30 mins
1 hour
1.5 hour
2 hour
2.5 hour
3 hour
3.5 hour
4 hour
5 hour
6 hour
7 hour
8 hour
9 hour
10 hour
12 hour
13 hour
14 hour
15 hour

Appendix C

Graphs of the biodistribution of ^{14}C-radiolabel in organs excised from rats fed [^{14}C]BSA, [^{14}C]casein and [^{14}C]CD14 and euthanized at 20, 240 and 480 min post-gavage.

The stomach, duodenum, jejunum, ileum, large intestine (LI), blood, liver, kidneys and spleen were harvested and dissolved using Solvable^{TM}. Solutions were decolorized using hydrogen peroxide and perchloric acid and subsequently mixed with liquid scintillation cocktail. Data were reported as dpm/(g or mL) and expressed as mean ± SEM, n = 2 - 4.

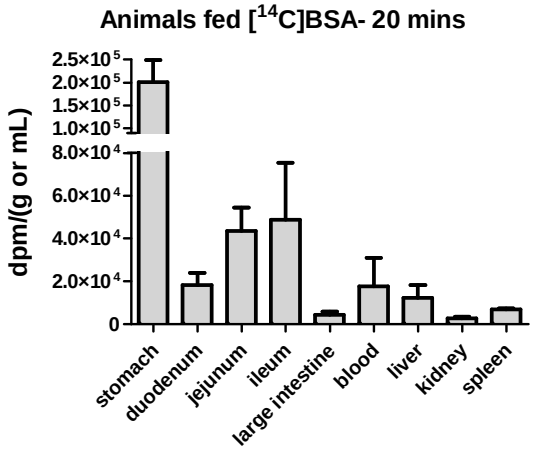

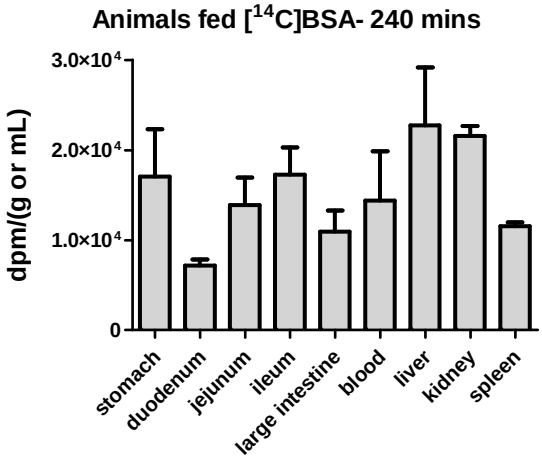

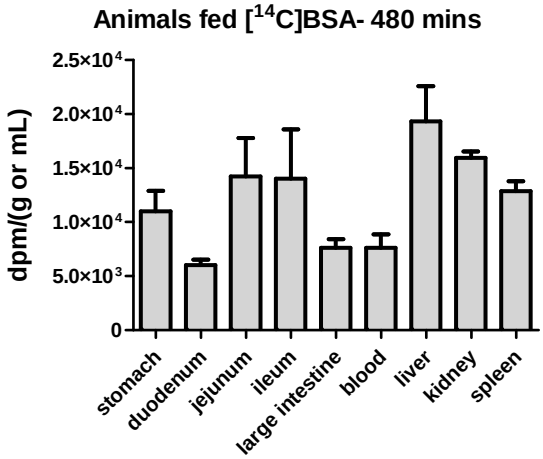

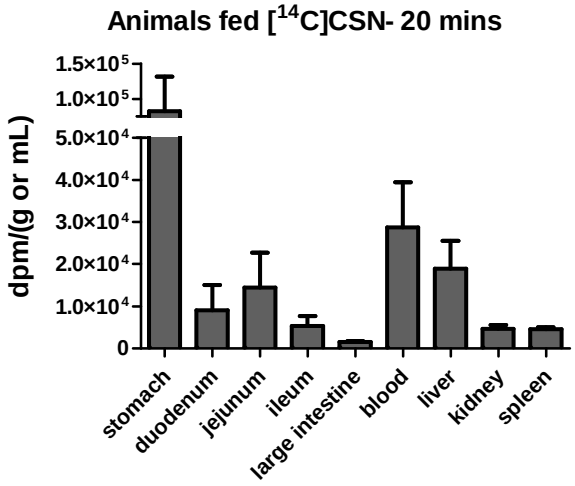
Animals fed [14C]CSN- 20 mins
dpm/(g or mL)
1.5×10^5
1.0×10^5
5.0×10^4
4.0×10^4
3.0×10^4
2.0×10^4
1.0×10^4
0
stomach
duodenum
jejunum
ileum
large intestine
blood
liver
kidney
spleen

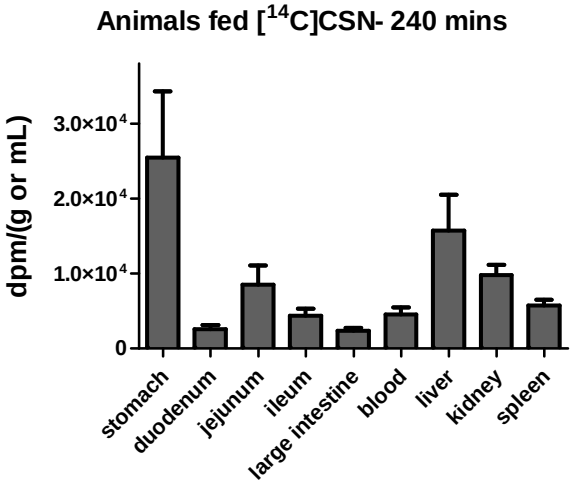
Animals fed [14C]CSN- 240 mins
dpm/(g or mL)
3.0×10^4
2.0×10^4
1.0×10^4
0
stomach
duodenum
jejunum
ileum
large intestine
blood
liver
kidney
spleen

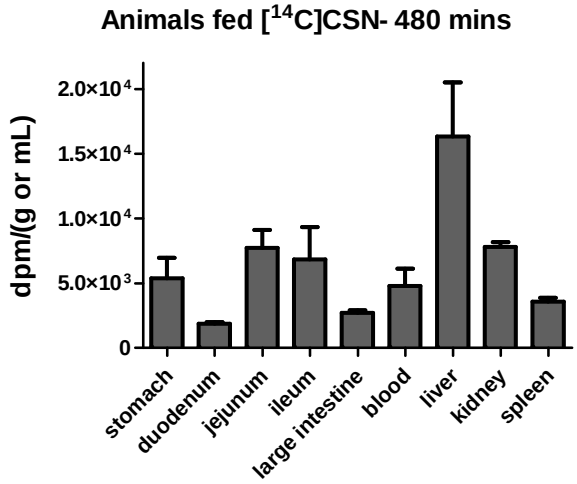
Animals fed [14C]CSN- 480 mins
dpm/(g or mL)
2.0×10^4
1.5×10^4
1.0×10^4
5.0×10^3
0
stomach
duodenum
jejunum
ileum
large intestine
blood
liver
kidney
spleen

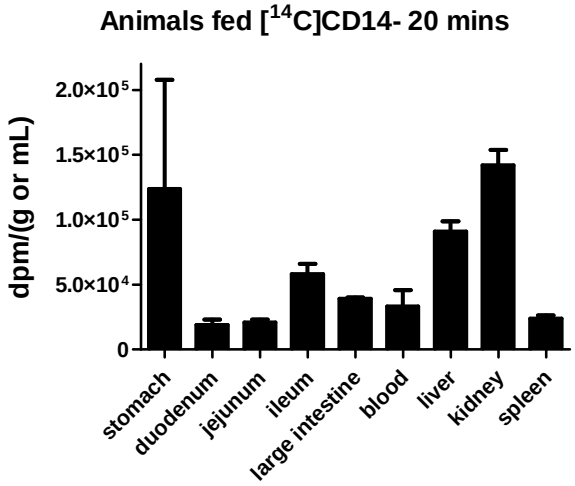
Animals fed [14C]CD14- 20 mins
dpm/(g or mL)
2.0×10^5
1.5×10^5
1.0×10^5
5.0×10^4
0
stomach
duodenum
jejunum
ileum
large intestine
blood
liver
kidney
spleen

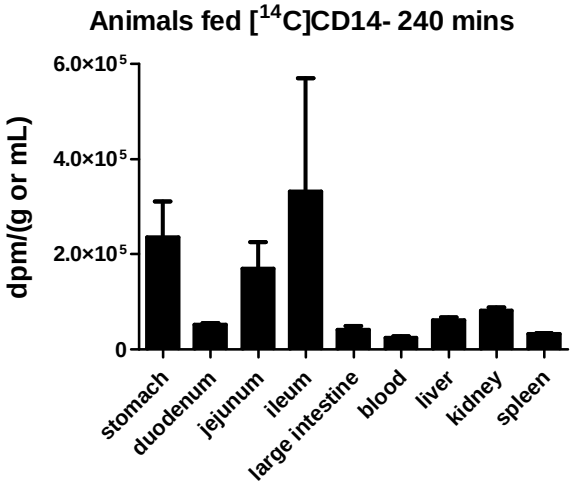
Animals fed [14C]CD14- 240 mins
dpm/(g or mL)
6.0×10^5
4.0×10^5
2.0×10^5
0
stomach
duodenum
jejunum
ileum
large intestine
blood
liver
kidney
spleen

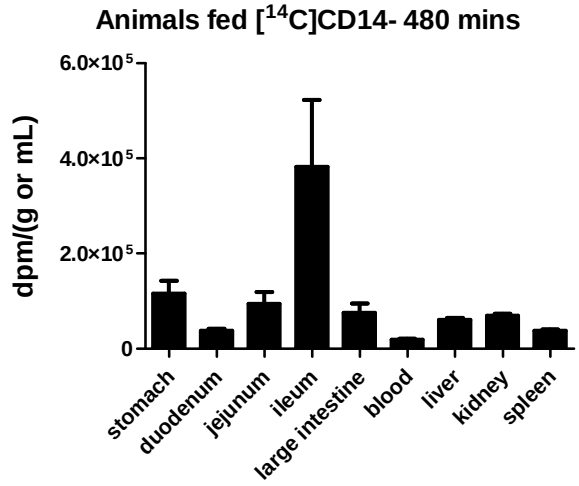
Animals fed [14C]CD14- 480 mins
dpm/(g or mL)
6.0×10^5
4.0×10^5
2.0×10^5
0
stomach
duodenum
jejunum
ileum
large intestine
blood
liver
kidney
spleen

Curriculum Vitae

Laura Davis

EDUCATION

Sept 2010- April 2012 — **2012 MBA candidate**, Schulich School of Business
- Recipient of prestigious Seymour Schulich entrance scholarship $22,000
- Recipient of Ontario Graduate Scholarship (OGS) $15,000

Jan 2008- April 2010 — **MSc. in Biochemistry**, University of Ottawa, Ontario
Biodistribution of ^{14}C in the digestive organs of rats fed [^{14}C]CD14 protein

June 2009- August 2009 — **Visiting Researcher**, Keio University, Tokyo, Japan
Cytokine production of stimulated human blood $CD14^{+}$ monocytes

Sept 2002- April 2006 — **BSc.Hon,** University of Guelph, Ontario
Major: Food Science

WORK EXPERIENCE

May 2010- Present — **Research Assistant**, *Schulich School of Business*, York University
- Explore the challenges facing Canadian nonprofit boards

May 2007- Dec 2007 — **Research Assistant,** *Nestlé Research Center*, Switzerland
- Managed and successfully delivered on a research project to develop a prototype ingredient for Casa Buitoni pasta in Italy, while leading technicians in the pilot plant
- Presented R&D project achievements to Nestlé senior management resulting in additional funding
- Because of project's success, was offered an opportunity to complete an industry-based PhD with Nestlé

Sept 2006- Feb 2007 — **Food Safety Microbiologist,** *Nestlé Product Technology Centre*, Germany
- Developed a novel natural food preservative and proved its efficacy through designing methodology and conducting research
- Successfully translated research into food products by collaborating with a team of international chefs in Nestlé's test kitchen
- Was promoted to Research Assistant in Switzerland

April 2004- August 2004 — **Quality Assurance Assistant,** *Nestlé Canada Inc*., Toronto
- Ensured product quality to maximize consumer demand by performing audits and releasing products based on sensory statistics
- Solved manufacturing issue that was reducing production and output

SCHOLARSHIPS

2010	• **Seymour Schulich MBA entrance scholarship** ($22,000)
2010	• **Ontario Graduate Scholarship** ($15,000)
2008-2010	• **Alexander Graham Bell Scholarship** NSERC CGS M ($17,500)
2009	• **Japan Society for the Promotion of Sciences Fellowship** at Keio University, Tokyo, Japan
2008-2010	• Recipient of the University of Ottawa **Excellence Scholarship & Admission Scholarship**
2002-2006	• Recipient of **Fermenich Millenium Scholarship, Greig Muir Memorial Scholarship, Aiming for the Top Scholarship, Univeristy of Guelph Entrance Scholarship, Nealanders International Award**

TEACHING & VOLUNTEER EXPERIENCES

Sept 2009- Dec 2009 **Marker/Proctor,** BCH 4130 Normal Human Nutrition
- Guest lecturer for two lectures on the water soluble vitamins unit

April 2008- April 2010 **Science Educator**, 'Let's Talk Science' & 'Science Travels', Ottawa
- Traveled to Nunavut to teach nutrition and science to Inuit communities
- Demonstrated science experiments to Ottawa and Northern Ontario students ages 6- 17 years to foster their interest in science

Jan 2008- May 2008 **Technology Venture Challenge**, Eastern Ontario Universities
- Competed in challenge to develop a technology-based business proposal with Ottawa's leading technology entrepreneurs, investors and business professionals
- Advanced to the semi-finals along with the mentorship of an Ottawa CEO

Jan 2008- April 2008 **Mentor,** *Sanofi-Aventis Biotalent Challenge,* University of Ottawa
- Mentored three high school students in effective experiment design and research resulting in all students achieving university scholarships

POSTER PRESENTATIONS

May 2009 13th Annual Breastfeeding Conference, Ottawa Valley Lactation Consultants, Ottawa, Canada

June 2009 Japan Society for the Promotion of Sciences Summer Program, Sokendai University, Japan

SCIENTIFIC CONFERENCES

May 2009 13th Annual Breastfeeding Conference, Ottawa Valley Lactation Consultants, Ottawa, Canada

July 2009 9th World Congress on Inflammation, Tokyo, Japan